Bond Behavior of Reinforcing Steel in Ultra-High Performance Concrete

October 2014

FHWA Publication No. FHWA-HRT-14-090

U.S. Department of Transportation
Federal Highway Administration

FOREWORD

With the ever increasing congestion and deterioration of our nation's highway system, a need exists to develop highly durable and rapidly constructed infrastructure systems. Durable bridge structures that would require less intrusive maintenance and would exhibit longer life spans thus maximizing the use of the facility are highly desirable. Expediting bridge construction can minimize traffic flow disruptions. Ultra-high performance concrete (UHPC) is an advanced construction material which affords new opportunities to envision the future of the highway infrastructure. The Federal Highway Administration has been engaged in research on the optimal uses of UHPC in the highway bridge infrastructure since 2001 through its Bridge of the Future initiative. This report presents results of a study aimed at assessing the potential of using UHPC-class materials to anchor or lap splice deformed reinforcing bars in field-cast connections. This concept could potentially allow for the simplification of connection details in some prefabricated bridge systems, and may also allow for the development and deployment of expedited construction techniques.

This report corresponds to the TechBrief titled "Bond Behavior of Reinforcing Steel in Ultra-High Performance Concrete" (FHWA-HRT-089). This report is being distributed through the National Technical Information Service for informational purposes. The content in this report is being distributed "as is" and may contain editorial or grammatical errors.

TECHNICAL REPORT DOCUMENTATION PAGE

1. Report No. FHWA-HRT-14-090	2. Government Accession No.	3. Recipient's Catalog No.
4. Title and Subtitle Bond Behavior of Reinforcing Steel in Ultra-High Performance Concrete		5. Report Date October 2014 6. Performing Organization Code:
7. Author(s) Jiqiu Yuan and Benjamin A. Graybeal		8. Performing Organization Report No.
9. Performing Organization Name and Address Office of Infrastructure Research & Development Federal Highway Administration 6300 Georgetown Pike McLean, VA 22101-2296		10. Work Unit No. 11. Contract or Grant No.
12. Sponsoring Agency Name and Address Office of Infrastructure Research & Development Federal Highway Administration 6300 Georgetown Pike McLean, VA 22101-2296		13. Type of Report and Period Covered March 2013 – March 2014 14. Sponsoring Agency Code HRDI-40

15. Supplementary Notes

This document was developed by research staff at the Turner-Fairbank Highway Research Center. Portions of the work were completed by PSI, Inc. under contract DTFH61-10-D-00017. Jiqiu Yuan of PSI, Inc. is a contract researcher on FHWA's structural concrete research efforts and Ben Graybeal of FHWA both manages the FHWA Structural Concrete Research Program and leads the Bridge and Foundation Engineering Research team.

16. Abstract

Ultra-High Performance Concrete (UHPC) is a relatively new class of advanced cementitious composite materials, which exhibits high compressive [above 21.7 ksi (150 MPa)] and tensile [above 0.72 ksi (5 MPa)] strengths. The discrete steel fiber reinforcement included in UHPC allows the concrete to maintain tensile capacity beyond cracking of the cementitious matrix. The combination of the matrix and fiber performance allow for a reduction on the development length of reinforcing bar, thus providing the potential for a redesign of some structural systems such as field–cast connections between prefabricated bridge elements. The bond behavior of deformed reinforcing bar in UHPC is investigated in this study by conducting direct tension pullout tests. Over 200 tests were completed and the effect of embedment length, concrete cover, bar spacing, concrete strength, bar size and type on bond strength were investigated. It was found that the development length of embedded reinforcement in UHPC can be significantly reduced. Guidance on the embedment of deformed reinforcing bars into UHPC is provided.

This report corresponds to the TechBrief titled "Bond Behavior of Reinforcing Steel in Ultra-High Performance Concrete" (FHWA-HRT-089).

17. Key Words Ultra-high performance concrete, UHPC, fiber-reinforced concrete, reinforcing bar, bond strength, anchorage, development length, splice length	18. Distribution Statement No restrictions. This document is available through the National Technical Information Service, Springfield, VA 22161.

19. Security Classif. (of this report) Unclassified	20. Security Classif. (of this page) Unclassified	21. No. of Pages 78	22. Price N/A

Form DOT F 1700.7 (8-72) Reproduction of completed page authorized

SI* (MODERN METRIC) CONVERSION FACTORS

APPROXIMATE CONVERSIONS TO SI UNITS

Symbol	When You Know	Multiply By	To Find	Symbol
		LENGTH		
in	inches	25.4	millimeters	mm
ft	feet	0.305	meters	m
yd	yards	0.914	meters	m
mi	miles	1.61	kilometers	km
		AREA		
in^2	square inches	645.2	square millimeters	mm^2
ft^2	square feet	0.093	square meters	m^2
yd^2	square yard	0.836	square meters	m^2
ac	acres	0.405	hectares	ha
mi^2	square miles	2.59	square kilometers	km^2
		VOLUME		
fl oz	fluid ounces	29.57	milliliters	mL
gal	gallons	3.785	liters	L
ft^3	cubic feet	0.028	cubic meters	m^3
yd^3	cubic yards	0.765	cubic meters	m^3
	NOTE: volumes greater than 1000 L shall be shown in m^3			
		MASS		
oz	ounces	28.35	grams	g
lb	pounds	0.454	kilograms	kg
T	short tons (2000 lb)	0.907	megagrams (or "metric ton")	Mg (or "t")
		TEMPERATURE (exact degrees)		
^oF	Fahrenheit	5 (F-32)/9 or (F-32)/1.8	Celsius	^oC
		ILLUMINATION		
fc	foot-candles	10.76	lux	lx
fl	foot-Lamberts	3.426	$candela/m^2$	cd/m^2
		FORCE and PRESSURE or STRESS		
lbf	poundforce	4.45	newtons	N
lbf/in^2	poundforce per square inch	6.89	kilopascals	kPa

APPROXIMATE CONVERSIONS FROM SI UNITS

Symbol	When You Know	Multiply By	To Find	Symbol
		LENGTH		
mm	millimeters	0.039	inches	in
m	meters	3.28	feet	ft
m	meters	1.09	yards	yd
km	kilometers	0.621	miles	mi
		AREA		
mm^2	square millimeters	0.0016	square inches	in^2
m^2	square meters	10.764	square feet	ft^2
m^2	square meters	1.195	square yards	yd^2
ha	hectares	2.47	acres	ac
km^2	square kilometers	0.386	square miles	mi^2
		VOLUME		
mL	milliliters	0.034	fluid ounces	fl oz
L	liters	0.264	gallons	gal
m^3	cubic meters	35.314	cubic feet	ft^3
m^3	cubic meters	1.307	cubic yards	yd^3
		MASS		
g	grams	0.035	ounces	oz
kg	kilograms	2.202	pounds	lb
Mg (or "t")	megagrams (or "metric ton")	1.103	short tons (2000 lb)	T
		TEMPERATURE (exact degrees)		
^oC	Celsius	1.8C+32	Fahrenheit	^oF
		ILLUMINATION		
lx	lux	0.0929	foot-candles	fc
cd/m^2	$candela/m^2$	0.2919	foot-Lamberts	fl
		FORCE and PRESSURE or STRESS		
N	newtons	0.225	poundforce	lbf
kPa	kilopascals	0.145	poundforce per square inch	lbf/in^2

*SI is the symbol for the International System of Units. Appropriate rounding should be made to comply with Section 4 of ASTM E380.
(Revised March 2003)

TABLE OF CONTENTS

CHAPTER 1. INTRODUCTION 9

GENERAL 9
ULTRA-HIGH PERFORMANCE CONCRETE 10
LITERATURE REVIEW ON BOND STRENGTH BETWEEN DEFORMED REINFORCING STEEL AND UHPC 10
OBJECTIVE 11
OUTLINE OF REPORT 12

CHAPTER 2. EXPERIMENTAL INVESTIGATION 13

INTRODUCTION 13
UHPC FORMULATION 13
UHPC COMPRESSIVE STRENGTH 14
REINFORCING STEEL 14
TEST SETUP AND PROCEDURES 17
SPECIMEN PREPARATION 20
TEST MATRIX 22

CHAPTER 3. PULLOUT TESTS RESULTS 23

INTRODUCTION 23
TERMINOLOGY AND SPECIMEN NOTATION 23
CRACKING AND DAMAGE MECHANISM 25
FACTORS AFFECTING BOND 29
Casting Orientation *29*
Effect of Embedment Length *31*
Side Cover *34*
Bar Spacing *39*
UHPC Compressive Strength *46*
Reinforcing Bar Size *52*
Reinforcing Bar Type and Yielding Strength *54*

CHAPTER 4. DESIGN RECOMMENDATIONS FOR REINFORCING BAR EMBEDDED IN UHPC 59

MINIMUM BAR STRESS OF LESSER OF YIELD OR 75 **KSI** (517 MPA) 59
MINIMUM BAR STRESS OF LESSER OF YIELD OR 75 **KSI** (517 MPA) – ALTERNATIVE 63
BAR STRESS ABOVE 75 **KSI** (517 MPA) OR BAR RUPTURE BEFORE BOND FAILURE 67

CHAPTER 5. CONCLUSIONS 69

INTRODUCTION 69
CONCLUSIONS 69
RECOMMENDED DESIGN 70
FUTURE RESEARCH 71

ACKNOWLEDGMENTS 73

REFERENCES 74

LIST OF FIGURES

Figure 1. Graph. Tensile stress strain response of reinforcing bars. 15
Figure 2. Photo. Reinforcing bar rib pattern. 17
Figure 3. Illustration. Overall configuration of test specimens. 18
Figure 4. Illustration. Pullout test specimens layout. 18
Figure 5. Illustration. Loading setup. 19
Figure 6. Photograph. Loading setup. 20
Figure 7. Photograph. Displacement measurement via three LVDTs. 20
Figure 8. Photograph. UHPC strip casting setup and orientation: (a) side pour setup; (b) side pour casting; (c) upright pour setup; and (d) upright pour casting. 21
Figure 9. Illustration. Conceptual bar stress versus slip response 24
Figure 10. Equation. Average bond stress in reinforcing bar. 24
Figure 11. Illustration. Pullout tests: (a) forces on bars; and (b) crack patterns. 26
Figure 12. Photo. Crack patterns: (a) longitudinal splitting cracks to adjacent No. 8 bars; (b) splitting cracks to side face; (c) splitting cracks to side face and adjacent No. 8 bars; and (d) UHPC tensile failure with opened diagonal cracks. 27
Figure 13. Photo. Diagonal crack observation: (a) visual inspection; and (b) crack inspection with denatured alcohol. 28
Figure 14. Photo. Conical surface failure: (a) conical surface around the bar; and (b) conical surface extended to the side face. 28
Figure 15. Graph. Effect of embedment length: $f_{s,max}$ versus embedment length l_d. 34
Figure 16. Illustration. Bond splitting cracks: (a) $c_{si} > c_{so}$; and (b) $c_{si} < c_{so}$. 35
Figure 17. Graph. Effect of side cover: bond strength μ_{TEST} versus side cover for specimens in Sets 1, 2 and 3. The c_{si} is constant. 38
Figure 18. Graph. Effect of side cover: bond strength μ_{TEST} versus side cover for specimens in Sets 4 and 5. The c_{si} is constant. 39
Figure 19. Graph. Effect of bar spacing: bond strength μ_{TEST} versus $2c_{si}$ for specimens in Set 1. The c_{so} is constant. 42
Figure 20. Illustration. Geometrical demonstration of $l_s tan(\theta)$ and $2c_{si}$. 43
Figure 21. Graph. Effect of bar spacing: bond strength μ_{TEST} versus $2c_{si}$ for specimens in Set 2. The c_{so} is constant. 44
Figure 22. Graph. Effect of bar spacing: bond strength μ_{TEST} versus $2c_{si}$ for specimens in Set 3. The c_{so} is constant. 44
Figure 23. Graph. Effect of bar spacing: bond strength μ_{TEST} versus $2c_{si}$ for specimens in Set 4. The c_{so} is constant. 45
Figure 24. Graph. Effect of UHPC compressive strength: bond (a) u_{TEST} versus f'_c and (b) u_{TEST} versus $f'^{1/2}_c$ for specimens in Set 1. 49
Figure 25. Graph. Effect of UHPC compressive strength: *(a)* u_{TEST} versus f'_c and (b) u_{TEST} versus $f'^{1/2}_c$ for specimens in Set 2. 50
Figure 26. Graph. Effect of UHPC compressive strength: *(a)* u_{TEST} versus f'_c and (b) u_{TEST} versus $f'^{1/2}_c$ for specimens in Set 3. 51

Figure 27. Chart. Bond strength versus bar size. 54
Figure 28. Chart. Average bar stress at bond failure for different types of reinforcing bar. 55
Figure 29. Graph. Bar stress at bond failure versus embedment length for all tests with A1035 No. 5 bars. 60
Figure 30. Graph. Bar stress at bond failure versus embedment length for all tests with A1035 No. 5 bars and with a side cover $\geq 2.7d_b$. 61
Figure 31. Graph. Bar stress at bond failure versus embedment length for tests with A1035 No. 7 bars and epoxy coated No.8 bars. 63
Figure 32. Chart. Bar stress at bond failure for all A1035 No.5 bars with different design details. All specimens had a bar clear spacing between $2d_b$ and $l_s tan(\theta)$. 65
Figure 33. Chart. Bar stress at bond failure for all epoxy coated and uncoated No.5 bars with different design details. All specimens had a bar clear spacing between $2d_b$ and $l_s tan(\theta)$. 66
Figure 34. Chart. Bar stress at bond failure for all A1035 No. 4 and No.7 bars and epoxy coated No. 8 bar with different design details. All specimens had a bar clear spacing between $2d_b$ and $l_s tan(\theta)$. 67

LIST OF TABLES

Table 1. Typical field-cast UHPC material properties. 11
Table 2. UHPC mix design. 13
Table 3. Properties of Reinforcing Steel 16
Table 4. Test Specimens – Effect of Casting Orientation. 30
Table 5. Test specimens – effect of embedment length. 32
Table 6. Test specimens – effect of side cover. 36
Table 7. Test specimens – effect of bar spacing 40
Table 8. Bond strength reduction for bar clear spacing out of the range of $2d_b < 2c_{si} < l_s tan(\theta)$. 45
Table 9. Test specimens – effect of UHPC compressive strength. 47
Table 10. Test specimens – effect of bar size. 53
Table 11. Test specimens – effect of bar type. 56
Table 12. Bond stress reduction between different types of reinforcing bar. 58

LIST OF ABBREVIATIONS AND NOTATION

ABBREVIATIONS

ABC	Accelerated Bridge Construction
ASTM	American Society For Testing and Materials
DOT	Departments Of Transportation
FHWA	Federal Highway Administration
LVDT	Linear Variable Differential Transformer
PBES	Prefabricated Bridge Elements And Systems
UHPC	Ultra-High Performance Concrete

NOTATION

c_{so}	= side concrete cover for reinforcing bar
c_{si}	= one-half of the bar clear spacing
d_b	= reinforcing bar diameter
f'_c	= concrete compressive strength
$f_{s,crack}$	= bar stress at first observed crack
$f_{s,max}$	= maximum bar stress at bond failure
l_d	= embedment length
l_s	= lap spliced length
s_1	= bar slip at bond failure
μ_{TEST}	= average bond strength at bond failure
θ	= angle between the diagonal cracks and testing bar

CHAPTER 1. INTRODUCTION

GENERAL

The use of accelerated bridge construction (ABC) techniques continues to grow as owners across the country look for construction solutions that reduce impacts on the users of the infrastructure. In ABC construction, one common technique used is prefabricated bridge elements and systems (PBES). In this practice, bridge elements are prefabricated offsite, then assembled and connected onsite during an expedited construction timeframe. The use of prefabricated bridge elements necessitates the use of field-applied connections between these elements. Field-cast concrete or other cementitious material connections have been deployed for decades by State departments of transportation (DOTs). However, decades of experience has led to the recognition that the field-cast connections often prove to be susceptible to degradation that can lead to substandard performance of the overall bridge system.

Connection systems for PBES are selected based on a variety of considerations. Critical properties of connection systems can include the rate of mechanical property development within the connection, the dimensional stability of the field-cast material, the durability of the field-cast material, and the ease of construction of the overall system.[1] This document reports on research conducted through the Structural Concrete Research Program at the Federal Highway Administration Turner-Fairbank Highway Research Center. In this research project, connection details using different grout materials, including traditional non-shrinkage grout, epoxy grout, Ultra-High Performance Concrete (UHPC), and magnesium grout, are being evaluated. This report mainly focuses UHPC materials.

UHPC is a relatively new class of cementitious composite materials. Since 2000, when UHPC became commercially available in the United States, a series of research projects has demonstrated the capabilities of the material. A handful of State DOTs have deployed UHPC components within their infrastructure, and many more are actively considering the use of UHPC. Many State DOTs, bridge design firms, and construction firms have expressed their interest of using UHPC in bridge construction, especially for field-cast connections deployed in the construction of PBES structures. As late 2013, 32 bridges in the United States have been constructed using field-cast UHPC connections.[2]

As opposed to conventional grouted connections which frequently contain complex reinforcement configurations, UHPC connections often involve much simpler reinforcement configurations such as the lap splicing of straight lengths of reinforcement. A few specific connection details, such as those discussed in *Behavior of Field-Cast Ultra-High Performance Concrete Bridge Deck Connections Under Cyclic and Static Structural Loading* and *Development of a Field-Cast Ultra-High Performance Concrete Composite Connection Detail for Precast Concrete Bridge Decks*, have been rigorously tested at service and ultimate performance limits.[3,4] The advanced material properties of UHPC provide a potential to develop a simple and robust connection system for prefabricated bridge elements. The research

project discussed in this document investigated the bond performance between deformed reinforcing bar and UHPC. One objective of the research is to facilitate the development of design guidelines for using field-cast UHPC in innovative connection details.

ULTRA-HIGH PERFORMANCE CONCRETE

Advances in the science of concrete materials have led to the development of a new class of advanced cementitious materials, namely UHPC. These concretes tend to contain high cementitious materials contents and very low water-to-cementitious materials ratio, and to exhibit high compressive and tensile strengths. The discrete steel fiber reinforcement included in UHPC allows the concrete to maintain tensile capacity beyond cracking of the cementitious matrix. UHPC has been defined as follows:

> *UHPC is a cementitious composite material composed of an optimized gradation of granular constituents, a water-to-cementitious materials ratio less than 0.25, and a high percentage of discontinuous internal fiber reinforcement. The mechanical properties of UHPC include compressive strength greater than 21.7 ksi (150 MPa) and sustained post-cracking tensile strength greater than 0.72 ksi (5 MPa). UHPC has a discontinuous pore structure that reduces liquid ingress, significantly enhancing durability compared to conventional concrete.*[2,5]

A typical field-cast UHPC material properties are presented in Table 1, which represents average values for a number of test parameters relevant to the use of UHPC as obtained from independent testing of a commercially available product.[6] This research published by the Federal Highway Administration in 2006 investigated a number of material properties of UHPC. The research analyzed both mechanical- and durability-based behaviors of UHPC to assess its potential for use in future highway and bridge construction projects. It should be noted that the UHPC investigated in that study was designed for precast applications with accelerated curing and thus exhibited a reduced compressive strength under field casting and curing applications as compared to current UHPC products.

LITERATURE REVIEW ON BOND STRENGTH BETWEEN DEFORMED REINFORCING STEEL AND UHPC

Limited research has investigated the bond performance of deformed reinforcing bar in UHPC. New York State Department of Transportation performed pullout tests on reinforcing bar embedded in 15.7 in. (400 mm) diameter UHPC cylinders.[5] The No. 4, 5, and 6 bars were embedded 2.9, 3.9, and 4.9 inches (75, 100, and 125 mm) into the UHPC, respectively, and all fractured before bond failure.

Fehling et al. [7] performed pullout tests on 0.47 in. (12 mm) diameter bars with varied concrete cover and embedment length in UHPC. Their test results indicated that increasing concrete cover and increasing embedment length each resulted in an increase on the bond strength. For

specimens with a concrete cover of 1.5d_s (d_s: diameter of reinforcing steel), an embedded length of 8d_s would yield the bar with a yield strength of approximately 80 ksi (551 MPa). For specimens with a concrete cover of 2.5d_s, an embedded length of 5d_s would yield the bar.

Table 1. Typical field-cast UHPC material properties.

Material Characteristic	Average Result
Density	2,480 kg/m^3 (155 lb/ft^3)
Compressive Strength (ASTM C39; 28-day strength)	126 MPa (18.3 ksi)
Modulus of Elasticity (ASTM C469; 28-day modulus)	42.7 GPa (6200 ksi)
Split Cylinder Cracking Strength (ASTM C496)	9.0 MPa (1.3 ksi)
Prism Flexure Cracking Strength (ASTM C1018; 305-mm (12-in.) span)	9.0 MPa (1.3 ksi)
Mortar Briquette Cracking Strength (AASHTO T132)	6.2 MPa (0.9 ksi)
Direct Tension Cracking Strength (Axial tensile load)	5.5–6.9 MPa (0.8–1.0 ksi)
Prism Flexural Tensile Toughness (ASTM C1018; 305-mm (12-in.) span)	I_{30} = 48
Long-Term Creep Coefficient (ASTM C512; 77 MPa (11.2 ksi) load)	0.78
Long-Term Shrinkage (ASTM C157; initial reading after set)	555 microstrain
Total Shrinkage (Embedded vibrating wire gage)	790 microstrain
Coefficient of Thermal Expansion (AASHTO TP60–00)	14.7 x10^{-6} mm/mm/ºC (8.2 x10^{-6} in./in./ºF)
Chloride Ion Penetrability (ASTM C1202; 28-day test)	360 coulombs
Chloride Ion Permeability (AASHTO T259; 12.7-mm (0.5-in.) depth)	< 0.06 kg/m^3 (< 0.10 lb/yd^3)
Scaling Resistance (ASTM C672)	No Scaling
Abrasion Resistance (ASTM C944 2x weight; ground surface)	0.73 grams lost (0.026 oz. lost)
Freeze-Thaw Resistance (ASTM C666A; 600 cycles)	RDM = 112%
Alkali-Silica Reaction (ASTM C1260; tested for 28 days)	Innocuous

Graybeal and Swenty [8] conducted pullout tests on No.4 reinforcing steel embedded into 6 in. (152 mm) cubes. Two types of UHPC were tested, with the test configuration including a 3 in. (76 mm) debond length and a 3 in. (76 mm) bond length along the centerline of the cube. One UHPC formulation resulted in bar yield before the ultimate pullout failure. The other UHPC formulation resulted in bar rupture before bond failure.

Pullout tests were also performed by Holschemacher et al. [9,10] and they observed that the bond strength and stiffness increases with testing ages.

OBJECTIVE

The objective of this research is to extensively evaluate the factors that affect bond strength between deformed reinforcing bar and UHPC and make recommendations for designs using reinforcing steel in UHPC.

OUTLINE OF REPORT

The research discussed herein investigated the parameters that could affect bond strength between deformed bar and UHPC. Direct tension pullout tests were conducted and more than 200 tests were included in this report. The parameters, including the structural characteristics like the embedment length, concrete side cover, bar spacing, bar size, and bar type and the materials properties like UHPC compressive strength and bar yielding strength, were considered in the study.

This report is divided into five chapters. Chapter 1 provides the introduction and the objective of the research. The background information about UHPC materials and the previous research on bond strength between deformed bar and UHPC are also included in Chapter 1. Then the experimental tests setup and the tests results are presented in Chapter 2 and Chapter 3, respectively. Design recommendations for using reinforcing steel in UHPC are presented in Chapter 4. At the end, Chapter 5 summarizes the conclusions based on this research.

CHAPTER 2. EXPERIMENTAL INVESTIGATION

INTRODUCTION

The research discussed herein focuses on the assessment of bond performance of deformed bar in field-cast grout. This is an ongoing research program at the FHWA Turner-Fairbank Highway Research Center as part of a larger effort focused on developing innovative connection details for prefabricated bridge components. This report mainly presents the results of the bond behavior between deformed bar and UHPC. Direct tension pullout tests were conducted. The experimental setup is presented in this chapter.

Details of the UHPC formulation investigated in this study, included the proportioning of the UHPC material and its compressive strength properties, are presented first. Then the deformed steel bar properties are reported. Both normal strength Grade 60 bar, including uncoated and epoxy coated, and high strength Grade 120 uncoated bar were used in the study and their yield strength, tensile strength, and deformation properties are reported. Next, the details of the specimen preparation and the pullout tests configuration are presented. Finally, the design philosophy of the test matrix is introduced.

UHPC FORMULATION

The UHPC used for this research is a product produced by Lafarge North America. The specific product tested is Ductal JS1212 and mix proportions are shown in Table 2.

Table 2. UHPC mix design.

Material	Amount (lb/yd^3 (kg/m^3))
Premix Powder	3700 (2195)
Water	219 (130)
Premia 150[*]	30 (18)
Optima 100[**]	20 (12)
Turbocast 650A[†]	39 (23)
Steel Fibers (2%[4])[‡]	263 (156)

[*] A modified phosphonate plasticizer; [**] A modified polycarboxylate high-range water-reducing admixture; [†] A non-chloride accelerator [‡] Steel fibers content of 2% by volume.

As shown in Table 2, this UHPC formulation contains premix power, water, Premia 150 (a modified phosphonate plasticizer), Optima 100 (a modified polycarboxylate high-range water-reducing admixture), Turbocast 650A (a non-chloride accelerator), and steel fibers. The steel fibers included in this mix design were nondeformed, cylindrical, high-tensile strength steel. They have a diameter of 0.008 in. (0.2 mm) with a length of 0.5 in. (12.7 mm). The steel tensile strength is specified to be greater than 290 ksi (2000 MPa). The steel fibers have a thin brass

coating which provides lubrication during the drawing process and provides corrosion resistance for the raw fibers. A constant steel fiber content of two percent by volume was used in this study.

UHPC COMPRESSIVE STRENGTH

Alongside each batch of pullout test specimens, a set of three compression test cylinders were cast. All cylinders were 3 in. (76.2 mm) nominal diameter with approximately 6 in. (152.4 mm) lengths. These cylinders were cast at the same time as the pullout test specimens. After each cylinder mold was filled, the cylinder was briefly vibrated on a vibrating table to assist in the release of entrapped air. The cylinders were then finished with a magnesium hand float and covered in plastic. The cylinders were cured alongside the pullout test specimens in the ambient laboratory environment.

The compressive mechanical testing was completed through modified version of the ASTM C39 Standard Test Method for Compressive Strength of Cylindrical Concrete Specimens.[11] The employed test method has been engaged multiple times in the past.[6,12,13] From the standpoint of the ASTM C39 test method, the load rate was increased from 35 psi/second (0.24 MPa/second) to 150 psi/second (1.0 MPa/second) due to the high compressive strength of UHPC and the duration of test that would result from the slower load rate.

The compressive strength for each of UHPC batch is reported in Chapter 3, alongside the pullout test results. The UHPC used in this study had an average compressive strength of 13.5 ksi (93 MPa) at one day, with a minimum of 11.7 ksi (81 MPa) and a maximum of 14.2 (98 MPa) for 33 specimens tested in 11 batches. It had an average compressive strength of 19.4 ksi (133 MPa) at seven days, with a minimum of 18.5 ksi (128 MPa) and a maximum of 20.5 (141 MPa) for 21 specimens tested in 7 batches. It had an average compressive strength of 21.3 ksi (147 MPa) at 14 days, with a minimum of 20.3 ksi (140 MPa) and a maximum of 22.2 (153 MPa) for six specimens tested in two batches. The majority of the tests in this study were conducted at one day or seven days after casting.

REINFORCING STEEL

The properties of reinforcing steel used in this study are reported in this section. The bar type and size used in the study are presented first, then the yield strength and tensile strength for each bar are reported. The deformation properties and rib pattern of the reinforcing bar are also included in this section.

Three types of reinforcing bar were tested in this study, including normal strength Grade 60 uncoated and epoxy coated bar and high strength Grade 120 uncoated bar. All the Grade 60 uncoated and epoxy coated bar meet the specification of ASTM A615[14], and will be referred to as uncoated and epoxy coated bar, respectively; all the high strength Grade 120 uncoated bar meets the specification of ASTM A1035[15], and will be referred to as A1035 bar in later discussions. The Grade 120 high strength bar is manufactured by MMFX Technologies Corporation. The bar sizes tested in the study include uncoated bar No.5, epoxy coated bar No.5 and No.8, and A1035 bar No.4, No.5, and No.7. The steel bar mechanical properties were tested

following ASTM A370[16]. Two bars were tested for each nominal size used in the pull out specimens. Strain was measured with an 8 in. (203 mm) extensometer. The tests were conducted under displacement control. For the Grade 60 bars, the free-running rate of separation of the crosshead was adjusted to have a loading speed of 0.003 in. per min per inch until the strain in the extensometer reached 0.1%; then speed was adjusted to 0.002 in. per min per inch and the specimen was loaded until the strain reached 1%, and at the this point, the extensometer was removed; the test was then continued at a speed of 0.03 in. per min per inch until the bar fractured. For the Grade 120 bars, the free-running rate of separation of the crosshead was adjusted to have a loading speed of 0.006 in. per min per inch until the strain in the extensometer reached 0.5%; then speed was adjusted to 0.003 in. per min per inch and the specimen was loaded until the strain reached 2.5%, and at the this point, the extensometer was removed; the test was then continued at a speed of 0.03 in. per min per inch until the bar fractured. The yield strength was determined using the 0.2% offset method. The tensile stress versus strain curve for each type and size reinforcing bar is presented in Figure 1, and the yield and tensile strengths are listed in Table 3. In general, as shown in Figure 1 and Table 3, the uncoated has a yield strength of approximately 75 ksi (517 MPa) and tensile strength of 118 ksi (814 MPa) while the yield and tensile strength of epoxy coated bar are 70 and 108 ksi (483 and 745 MPa), respectively. The A1035 bar has a yield strength (0.2% offset method) of approximately 130 ksi (896 MPa) and tensile strength of 170 ksi (1172 MPa). All of the bar tested in this study exhibited nearly identical stress-strain response from the initiation of loading through the attainment of a tensile stress of 68 ksi (469 MPa).

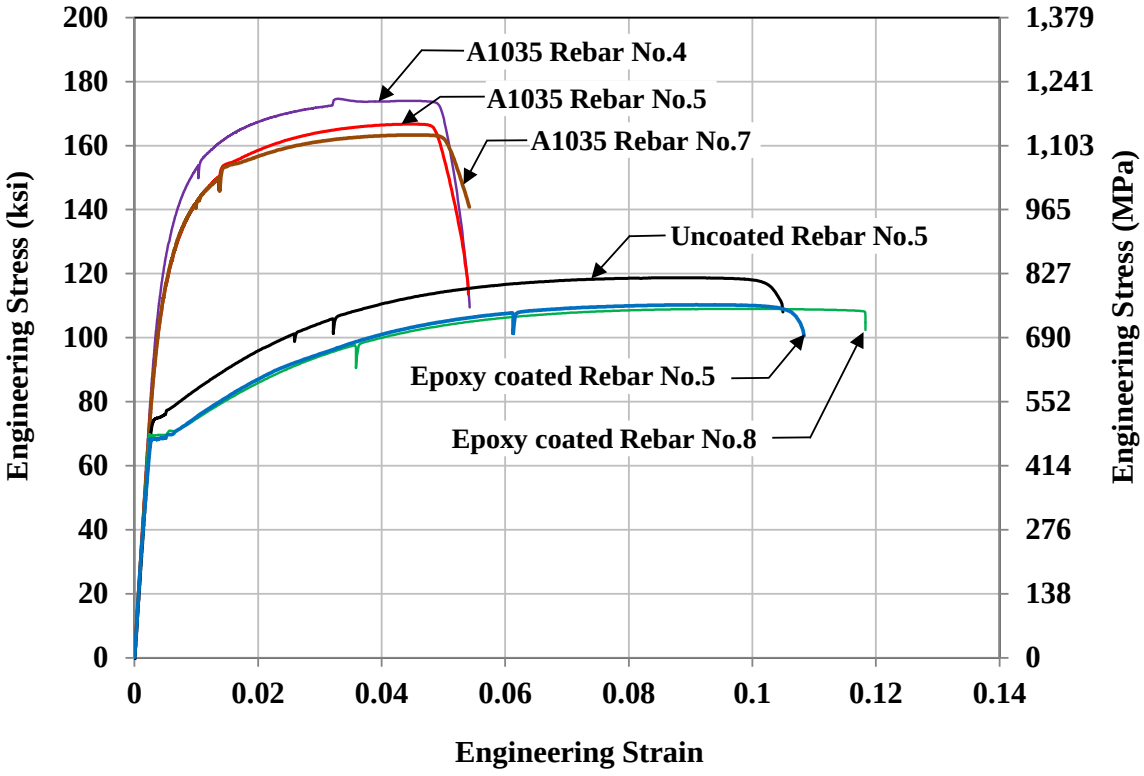

Figure 1. Graph. Tensile stress strain response of reinforcing bars.

Table 3. Properties of Reinforcing Steel

Bar Size	Bar Type	Yield Strength† (ksi)	Tensile Strength† (ksi)	Mean height* (in.)	Mean Spacing* (in.)	Relative rib area**
No. 4	A1035	134	172	0.024	0.330	0.074
No. 5	A1035	126	167	0.037	0.417	0.088
No. 7	A1035	126	162	0.056	0.561	0.099
No. 5	Epoxy	68	108	0.034	0.408	0.083
No. 8	Epoxy	70	109	0.053	0.615	0.086
No. 5	Uncoated	75	118	0.034	0.402	0.085

† Per ASTM A370.
*Per ASTM A615 and A1035.
**Per ACI 408R-03[17] and ACI 408.3R-09[18] for calculation of relative rib area.
Note: 1 in. = 2.54 cm, 1 ksi = 6.895 MPa.

The rib pattern for each type and size of the reinforcing bar used in the study is demonstrated in Figure 2. The A1035 high strength bar and the normal strength uncoated and epoxy coated bar were chosen to have similar rib patterns, as shown in Figure 2. The bar deformation, rib height and spacing, were measured following ASTM A615 and ASTM A1035. The height was determined from measurements made on three deformations. The spacing was determined by measuring the length of a minimum of ten spacings and dividing that length by the number of spaces included in the measurement; the average of two measurements was reported. The relative rib area, calculated as the ratio of the bearing area of bar deformations to the shear area between the deformations per ACI 408R-03[17], is also presented in Table 3. As shown in Table 3, they all had similar relative rib areas, mostly in a range of 0.083 to 0.088 with the exception of A1035 No.4 and No.7 bars having a relative rib area of 0.074 and 0.099, respectively.

Figure 2. Photo. Reinforcing bar rib pattern.

TEST SETUP AND PROCEDURES

Direct tension pullout tests, with a novel test specimen design and associated loading apparatus, were conducted in this study. The test setup was developed so as to mimic the tension-tension lap splice configuration that may be encountered in a field-deployed connection system.

The pullout tests speicmens were UHPC strips cast on top of precast concrete slabs, as shown in Figure 3. The No.8 bars extended 8 in. (20.3 cm) from the pre-cast concrete slab. UHPC strips were cast on top of the precast slab with the No. 8 bars in the center of the strips. Each tested bar was situated so as to be embedded into the UHPC strip and located between two of the No. 8 bars.

Each precast concrete slab has dimensions of 4 × 8 × 1 ft (1.2 × 2.4 × 0.3 m) (width × length × depth) and the spacing between the extended No.8 bars in the longitudinal direction (along the UHPC strip as shown in Figure 4) is either 8 or 12 in. (20.3 or 30.5 cm). More details of specimen layout on the precast slab are illustrated in Figure 4.

In Figure 3 and Figure 4, notations were assigned to represent dimension parameters, including c_{so} for the clear side cover, $2c_{si}$ for the clear spacing between the testing bar and the extended No.

8 bars, l_d for the embedment length of testing bar measured from the top surface of the UHPC strip to the end of the testing bar, and l_s for the lap splice length measured from the end of the testing bar to the end of extended No. 8 bars. These are also the main factors that will be investigated for their effect on bond strength in this study. The notations of c_{si}, c_{so}, l_d, and l_s are adopted from ACI 408 R-03 "Bond and Development of Staright Reinforcing Bars in Tension."[17]

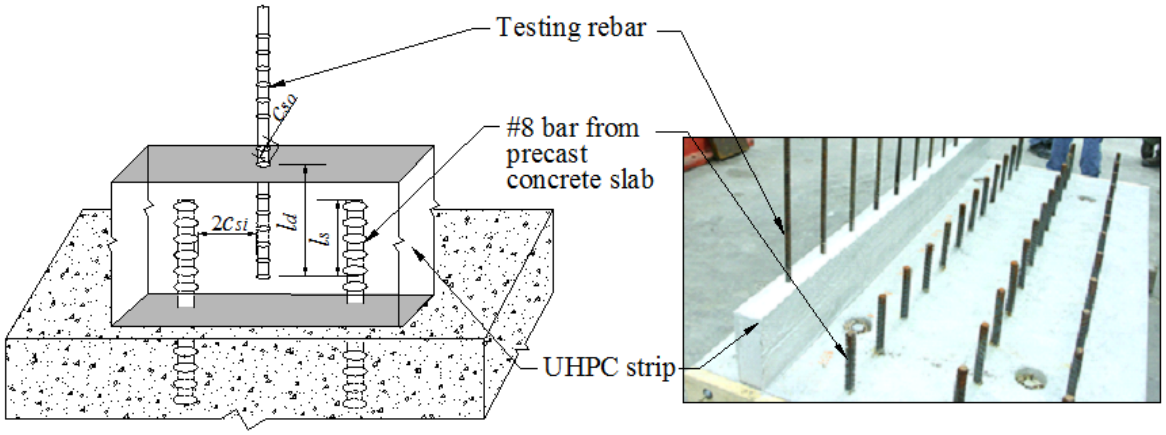

Figure 3. Illustration. Overall configuration of test specimens.

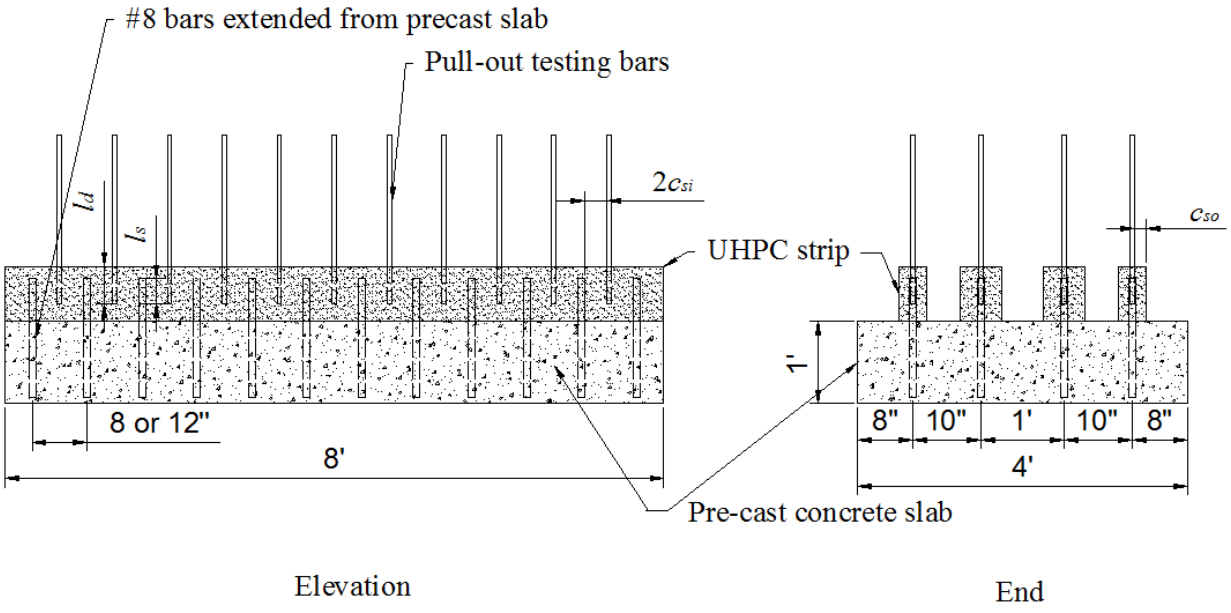

Figure 4. Illustration. Pullout test specimens layout.

The pullout tests were conducted using the fixture showing in Figure 5 and Figure 6. A hydraulic jack (Enerpac® Cylinder, Model RRH1508) was placed on a steel chair, and the steel chair stands on the precast slab. When a pullout force is applied, the fixture reacts against the precast slab. With such a setup, the reinforcing bars being tested as well as the extended No. 8 bars are both placed in tension. The UHPC surrounds these bars transfers the loads between them. This test setup simulates structural configurations wherein lap spliced reinforcement is loaded in tension.

Tests were conducted by applying a load to the free end of the embedded reinforcing bar. The load was applied under a closed-loop displacement control by adapting a servo valve into the system, which was attained with an MTS Flex Test GT controller uing a linear variable differential transformer (LVDT) for feedback. The jack was run at a constant displacment rate of 0.2 in./min (5 mm/min) as measured by the LVDT which captured the displacement at the bar chuck relative to the top of the jack. The top of the jack was approximately 30 in. (76 mm) above the precast slab and the bar chuck started approximately 36 in. (91 mm) above the top of the precast slab. A load cell located between the jack and the bar chuck measured the load applied to the bar. The bar displacement was measured at a location of approximately two inches (5.1 cm) above the top surface of UHPC strip, as shown in Figure 7. Three LVDTs were arranged in 120-degree angle and the average displacement of the three LVDTs were used to offset the possible bending of the loaded bar. The load cell and all LVDTs were calibrated to the MTS DUC conditioner. The load cell used in this study was Strainset® model FL100U(C)-2DGKT (S/N 08905-7) univeral flat load cell. The LVDTs used in this study were Omega® model LD300-150 (for displacement control) and Omega® model LD320-25 (for displacement measurement at the bottom).

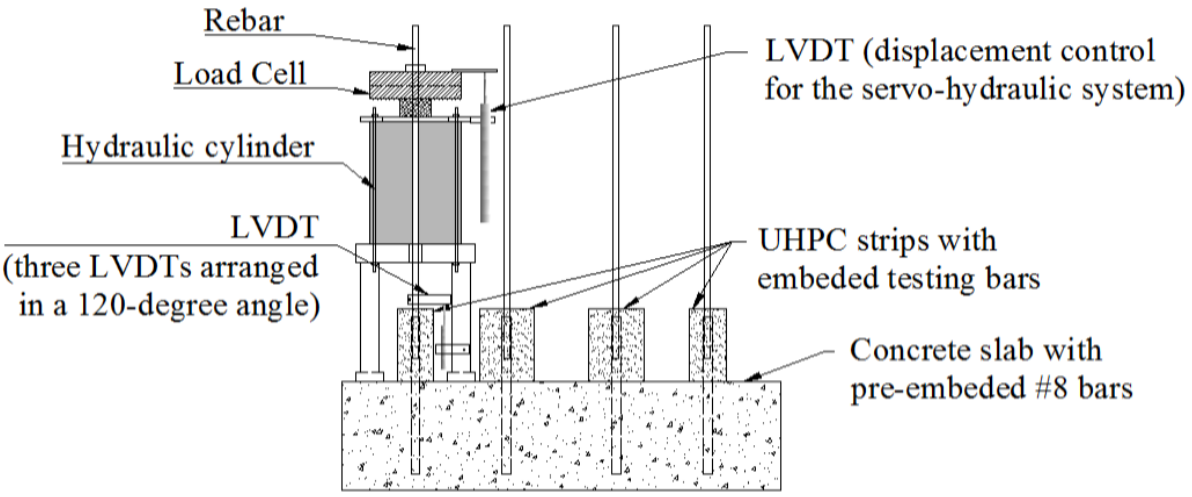

Figure 5. Illustration. Loading setup.

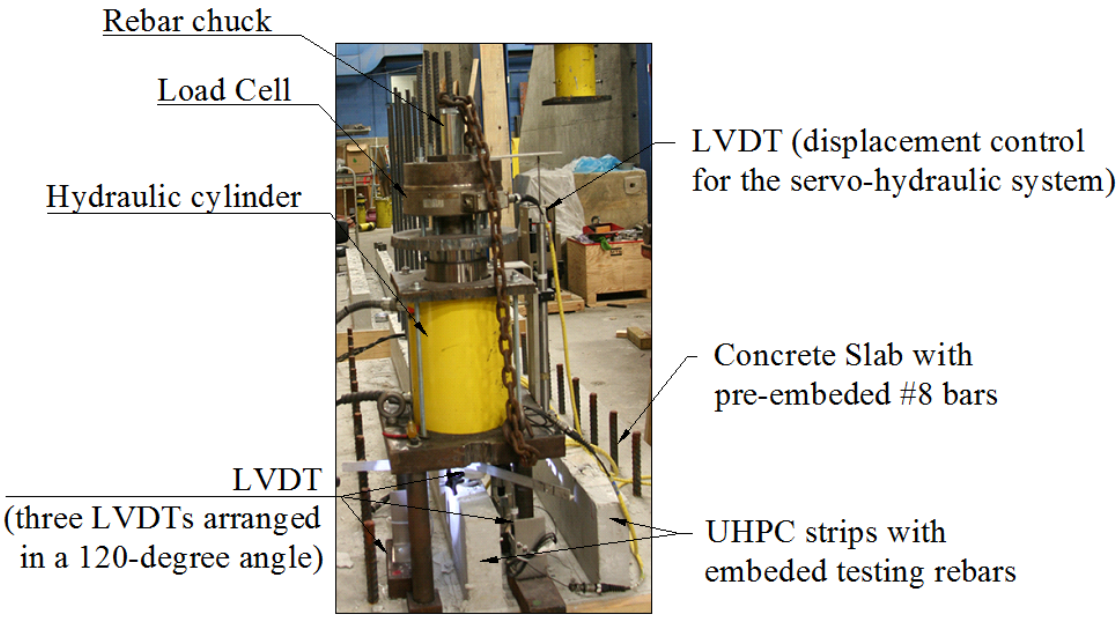

Figure 6. Photograph. Loading setup.

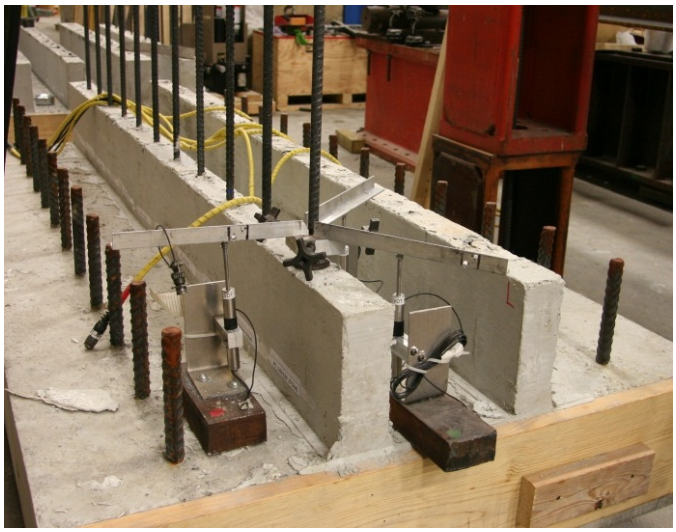

Figure 7. Photograph. Displacement measurement via three LVDTs.

SPECIMEN PREPARATION

The UHPC materials tested in this study contained 2% (by volume) steel fibers. Casting technique can influence the dispersion and orientation of the fiber reinforcement. In this study, the UHPC strips were prepared using plywood forms. Two cast orientations were compared, as

shown in Figure 8. The first orientation involved casting the specimen on its side as shown in Figure 8a and Figure 8b; the second orientation involved casting the specimen upright as shown in Figure 8c and Figure 8d, where the slab was placed with a small slope of approximately 1.5 degree to facilitate the flow of the UHPC. For both orientations, the UHPC was first poured in from one end and allowed to flow until the forms were mostly filled. Thereafter, the UHPC was poured in from the middle locations. The orientation of the casting was not observed to have a significant effect on bond behavior as will be discussed in Chapter 3. For the large majority of test specimens, the upright casting orientation was selected.

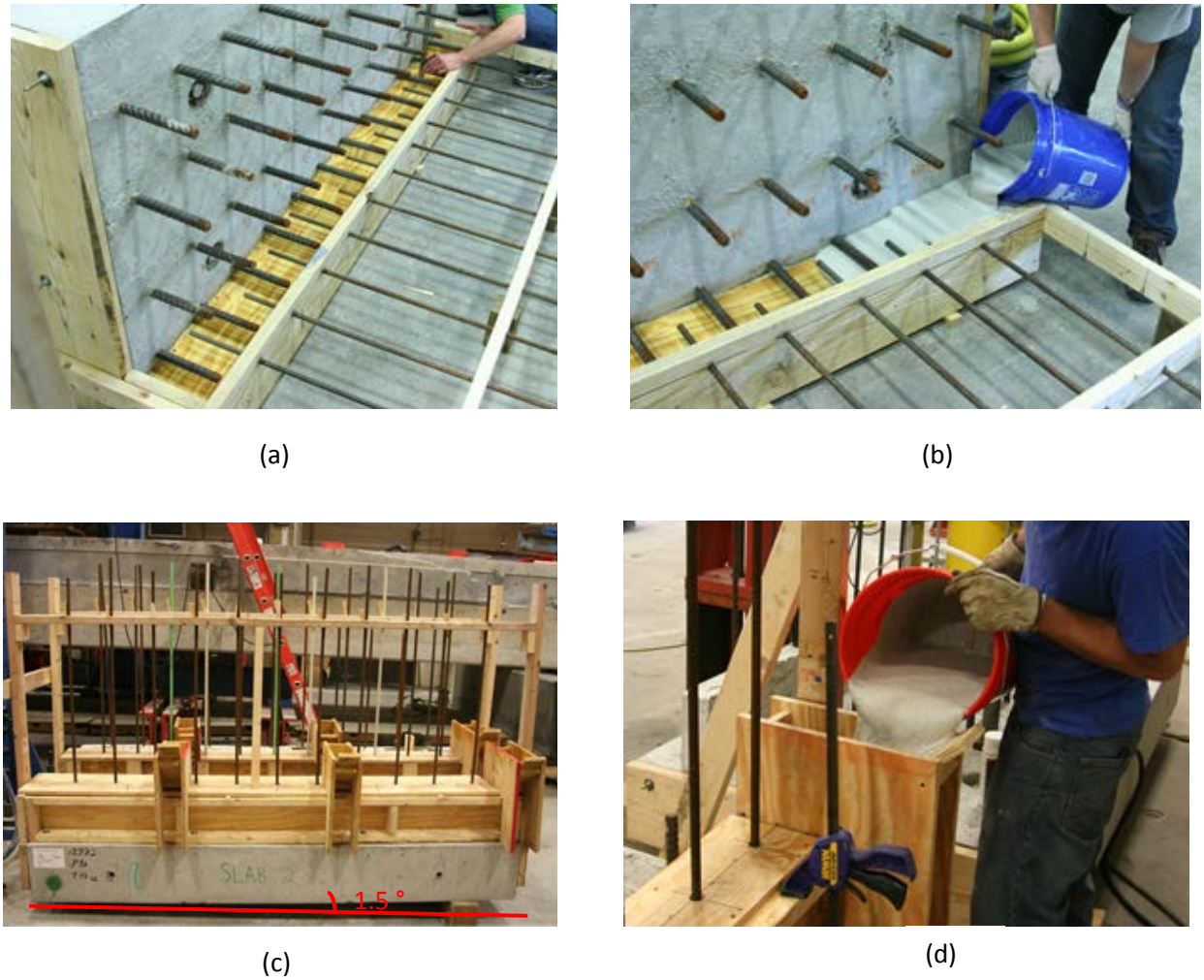

(a) (b)

(c) (d)

Figure 8. Photograph. UHPC strip casting setup and orientation: (a) side pour setup; (b) side pour casting; (c) upright pour setup; and (d) upright pour casting.

The actual dimension of c_{so}, $2c_{si}$, l_d, and l_s were measured. The side covers can be easily measured by taking the distance from the sides of the UHPC strip to the bar under consideration after forms are removed; the least side cover is reported as c_{so}. The clear spacing between the

testing bar and adjacent two No. 8 bars was determined by taking the difference between the spacing of the extended No. 8 bars before casting and the spacing of the testing bars after casting; the smaller value of the spacing to adjacent No.8 bars is used as $2c_{si}$. The actual embedment length (l_d) was determined by substracting the exposed length of the bar after casting from the original length of the bar and the spliced length (l_s) was calcuated as l_d – (strip height – 8 in.), where the 8 in. (203 mm) is the length of No. 8 bars that is extended outside the precast slab.

The forms were normally removed at 22 ± 1 hours after casting so the one-day testing can start at 23 ± 1 hours after casting.

TEST MATRIX

The objective of this study was to evaluate the bond behavior between the deformed reinforcing steel (lap spliced) and UHPC. The primary parameters investigated included the embedment length of reinforcing steel, concrete side cover, bar spacing, UHPC compressive strength, type of deformed bar, and size of deformed bar. Throughout the study, in order to better assess the influence of a particular variable, each individual parameter was varied while others remained constant. Each of the above mentioned variables will be evaluated and the results are presented in Chapter 3. The test matrix is provided in each section where the individual parameter is evaluated in Chapter 3.

CHAPTER 3. PULLOUT TESTS RESULTS

INTRODUCTION

The test results from the physical testing of the pullout specimens are presented in this chapter. The terminology and specimen notation used in this study are first introduced. Then the cracking and damage mechanisms in bond for the pullout specimens are presented. Following that, the parameters that could affect bond performance, including casting orientation, embedment length, side cover, bar spacing, UHPC compressive strength, reinforcing bar size, and reinforcing bar type are analyzed and discussed. The test matrix, including all the information of the specimen design, UHPC compressive strength, and bar stress at bond failure, is reported in each section.

TERMINOLOGY AND SPECIMEN NOTATION

Consistent terminology is used throughout this report in order to simplify the discussion of results. In terms of the bar stress versus bar slip response, the applied load and bar displacement were continuous recorded during the pullout test. The bar stress f_s was then calculated as the applied load divided by the cross section area of the reinforcing bar. The displacement was measured along a loaded portion of the reinforcing bar at about two inches (5.1 cm) above the top surface of UHPC strip (shown in Figure 7). This displacement is used as a measure of the bar slip, with the understanding that the displacement also included the stretching of the reinforcing bar under the pullout force. The bar stress is plotted versus slip to characterize the bond behavior and a typical bar stress versus slip curve for reinforcing bar in UHPC in this study is presented in Figure 9.

As shown in Figure 9, the point with the maximum bar stress was marked with ($f_{s,max}$, s_1), which refers to the bar stress and slip, respectively, at bond failure. During each test, the specimen surface was also continuously checked for signs of cracks and the bar stress at first observed crack was reported as $f_{s,crack}$. Due to safety considerations, visual inspection was stopped when the load was close the estimated maximum load. In some cases, visual inspection was stopped before the first crack was observed. The bar stress at first observed crack ($f_{s,crack}$), the maximum bar stress at bond failure ($f_{s,max}$), and the bar slip at bond failure (s_1) were reported for each specimen.

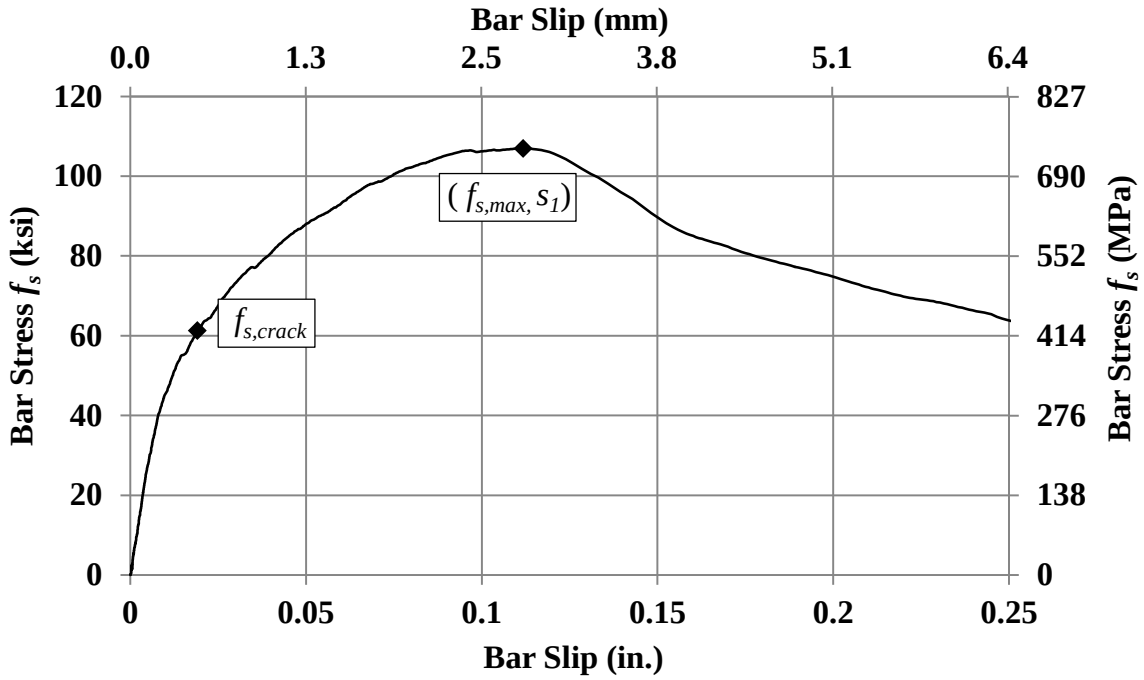

Figure 9. Illustration. Conceptual bar stress versus slip response.

Another term that has been often used in the report is the average bond strength at bond failure, μ_{TEST}. In general, the load transfer between the reinforcing bar and the surrounding concrete materials is assumed as following. At the beginning of the axial loading of the reinforcing bar, the outermost lug exerts a bearing force on the surrounding concrete materials and this bearing force at the outermost lug plus the friction force and chemical adhesion contribute to the bond strength at this stage. As load increases, this bearing force causes crushing of concrete materials in the vicinity of the outermost lug, the bar slips, and most of the friction force and chemical adhesion are lost. The slip causes the bearing reaction of next adjacent lugs, which contribute to the resisting the applied axial load. At ultimate load, it is assumed that all the lugs bear against concrete and help resist the axial load and that the bond stress distribution is uniform. The average bond strength can be calculated by dividing the bond force at failure by the overall contact area, using the equation in Figure 10.

$$\mu_{TEST} = \frac{f_{s,max}\,\pi d_b^2/4}{\pi d_b\, l_d} = \frac{f_{s,max}\, d_b}{4 l_d}$$

Figure 10. Equation. Average bond stress in reinforcing bar.

In this equation, $f_{s,max}$ is the bar stress at bond failure, d_b is the bar diameter, and l_d is the embedment length. The bond stress distribution for reinforcing bar in UHPC will be discussed in the later section where the effect of embedment length is investigated.

As mentioned in the introduction and also will be discussed in later sections, there are many factors that affect bond strength. The main parameters that this study investigated include the bar type and size, embedment length, side cover, bar spacing, and UHPC compressive strength. The specimens are named in a manner to be able illustrate all these variables. The specimen notation will be explained in an example in the following. Given an example specimen named B5-L6d-S2d-Sp4-1D-B2S1, the first term B5 represents the type and the size of the reinforcing bar, and the letter is for the bar type (B for uncoated black reinforcing bar, M for A1035 high strength reinforcing bar, E for epoxy coated reinforcing bar) and the number is for the bar size (for example, 5 for No. 5 bar); L6d represents a designed embedment length of six times of the testing bar diameter; S2d represents a designed side cover of two times of the testing bar diameter; Sp4 represents a designed center to center spacing of 4 in. (10.2 cm) between the testing bar and the nearest No.8 splice bar extending from the precast slab;1D represents the age (days) of the UHPC material at testing, which is one day in the example; B2S1 represents the Batch No. 2 of the UHPC casting and the specimens were cast on the precast Slab No. 1. The actual measurement of UHPC compressive strength at testing (f'_c), bar embedment length (l_d), bar spliced length (l_s), side cover (c_{so}), and clear spacing to nearest No. 8 bar ($2c_{si}$) are reported. The same notation will be used through the study.

It should be noted that the embedment length and side cover are defined in terms of bar diameter while the bar spacing is defined in terms of actual measurement in inches. The decision to define bar spacing in terms of a physical measurement results from the fact that the No. 8 bars extending from the precast slabs were spaced at either 8 or 12 in. (203 or 305 mm). In many cases, the testing bar was placed in the middle of the two No. 8 bars, therefore, the center-to-center spacing was either 4 or 6 in. (102 or 152 mm).

CRACKING AND DAMAGE MECHANISM

In general, the transfer of force from the reinforcing steel to the surrounding concrete is mainly through mechanical anchorage or bearing of the reinforcing bar ribs against the concrete surface, with chemical adhesion and frictional forces between the bar and the concrete playing a minimal role. For the pullout tests in this study, the reinforcing bar are lap spliced, as shown in Figure 11a, and the force on the testing bar is transferred to the concrete, which, in turn, transferred the force to adjacent No. 8 bars that extend from the precast concrete slab. The tensile forces due to this bearing effect could cause crack openings in a diagonal direction, as shown in Figure 11b. The wedging action of the deformations on the reinforcing bar could also cause hoop tensile stresses which can initiate splitting cracks as shown in Figure 11b.

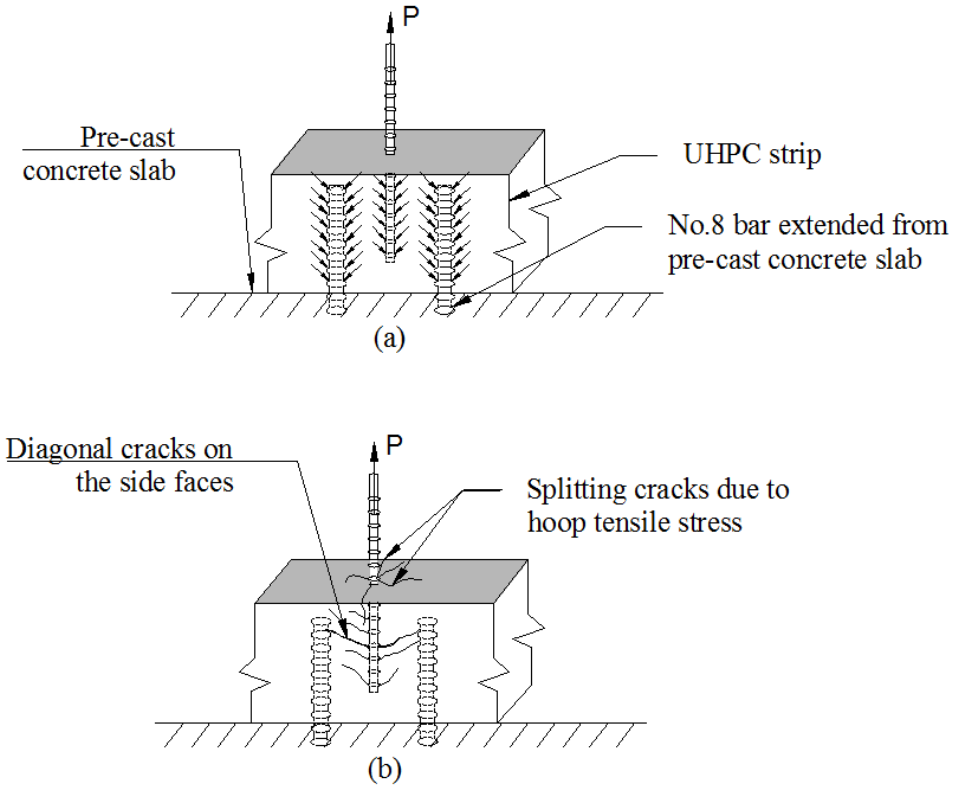

Figure 11. Illustration. Pullout tests: (a) forces on bars; and (b) crack patterns.

For tests in this study wherein the failure was not caused by reinforcing bar tensile rupture, the majority of the tests expressed a bond failure associated with splitting cracks, either split to the adjacent No.8 bars (Figure 12a), or to the side face (Figure 12b), or both (Figure 12c). In some cases, a UHPC tensile failure was observed wherein the tensile force separates a roughly planar region of concrete from the rest of the specimen, as shown in Figure 12d. In general, the specimens with UHPC tensile failures had smaller concrete side cover, demonstrating less bond strength than those with splitting failures. It should be noted that in cases with splitting failure, diagonal cracks would still form but would not be the control failure mode as shown in Figure 13. Figure 13a shows a few conical cracks observed with unaided vision; on this same specimen, when denatured alcohol was sprayed on the surface, more diagonal cracks appeared after the denatured alcohol evaporated from the surface, as shown in the Figure 13b. In almost all cases, the diagonal cracks like those in Figure 13 were observed. Conical surface failure around the reinforcing steel, as shown in Figure 14, was also observed in some cases.

In most structural applications, splitting failure is more common (ACI 408 R-03) [(17)] and the majority of the tests in this study failed with splitting cracks. When the effect of different parameters on bond strength is evaluated in later sections of this chapter, the analysis only includes those with splitting failures (Figure 12a, b, and c) and those failed with splitting cracks combined with small conical surfaces failures (Figure 14). In the section where the design

recommendations are developed, the specimens with UHPC tensile failures and the specimens with bar rupture are also included in the analysis.

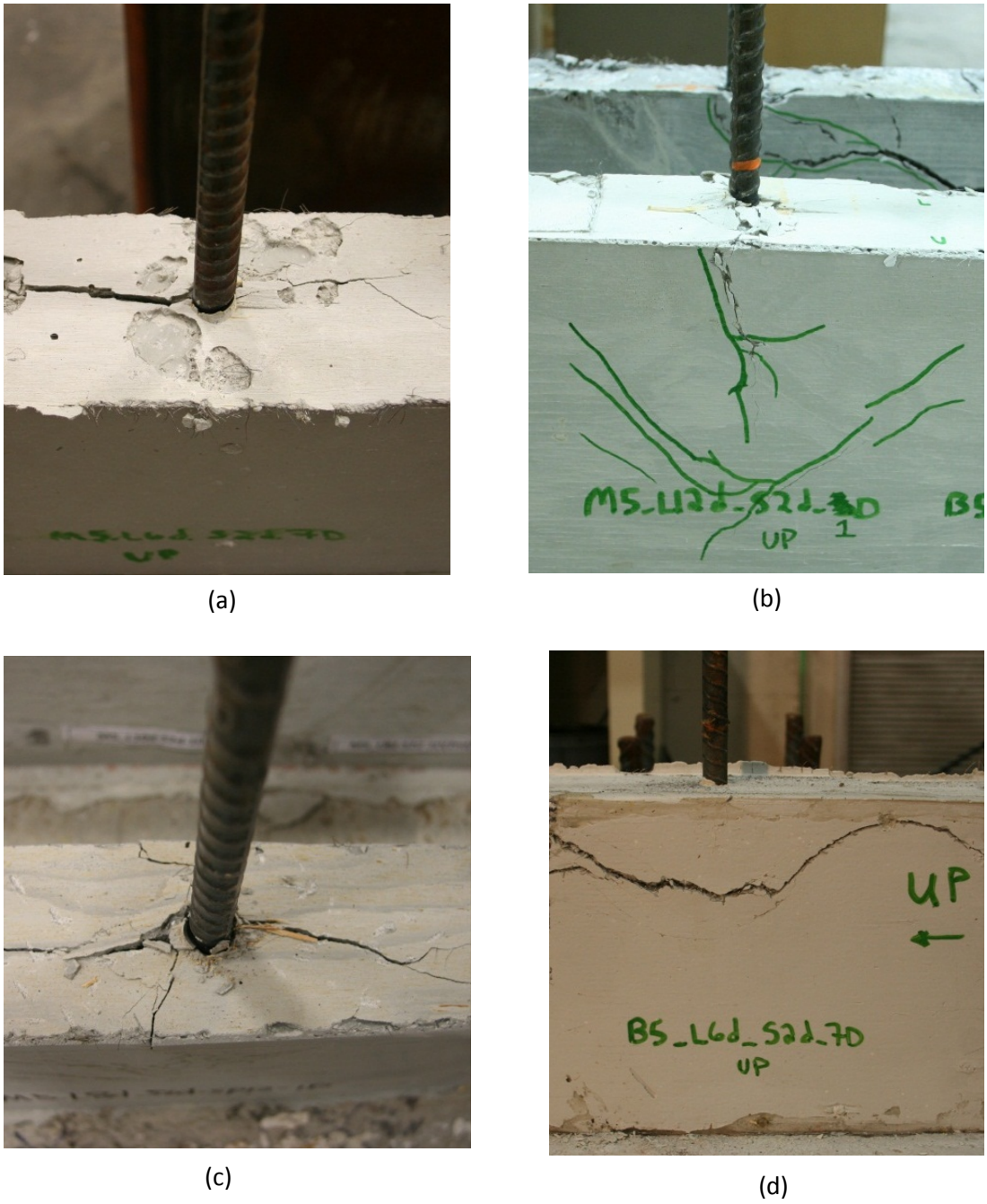

(a) (b)

(c) (d)

Figure 12. Photo. Crack patterns: (a) longitudinal splitting cracks to adjacent No. 8 bars; (b) splitting cracks to side face; (c) splitting cracks to side face and adjacent No. 8 bars; and (d) UHPC tensile failure with opened diagonal cracks.

(a) (b)

Figure 13. Photo. Diagonal crack observation: (a) visual inspection; and (b) crack inspection with denatured alcohol.

(a) (b)

Figure 14. Photo. Conical surface failure: (a) conical surface around the bar; and (b) conical surface extended to the side face.

FACTORS AFFECTING BOND

The factors affecting bond performance will be discussed in this section. The effect of casting orientation will be first presented. Then the parameters, including embedment length, concrete side cover, bar spacing, UHPC compressive strength, bar size, bar type, and bar yield strength, are evaluated.

Casting Orientation

Two casting orientations, either cast on side or cast upright (see Figure 8), were compared. It should be noted that, other than the casting orientation, each pair of the comparison specimens were identical specimens that were cast at the same time. A total of nine pairs of specimens were tested and the results are presented in Table 4.

As shown in Table 4, there was no appreciable difference between side-cast specimens and upright-cast specimens in eight of the nine pairs. In the one remaining pair, a difference of 19.7% was observed. For the purpose of easy construction and casting, the upright orientation was used in the rest of the study.

In this early stage of investigation, it was noted that with an embedment length of only $6d_b$ and side cover of $2d_b$ (specimens B5-L6d-S2d-Sp4-1D-B2S1 and B5-L6d-S2d-Sp4-1D-B2S2), the bond strength was already close to, or even beyond the yield strength of Grade 60 uncoated bar. To minimize the effect of bar yielding on bond strength when investigating other factors, the majority of the tests were conducted using A1035 high strength bar. The effect of reinforcing bar yielding before bond failure on bond strength will be discussed in the later section where the reinforcing bar type was evaluated.

During the investigation, it was also noted that the very end specimens that are close to the casting point (where the large majority of the UHPC is poured into the formwork) consistently displayed lower bond strength than specimens at the other positions. This is probably due to the variation of fiber distribution inside the UHPC. The results from the end specimens close to casting point are included in the section wherein the design recommendations are developed, but excluded from the sections of the report wherein the effect of different design parameters (l_d, c_{so}, c_{si}, f'_c, etc.) on bond strength is analyzed.

Table 4. Test Specimens – Effect of Casting Orientation.

Cast Orientation*	Batch ID†	f'_c, ksi	l_d, in.	l_s, in.	c_{so}, in.	c_{si}, in.	$f_{s,max}$, ksi	s, in.	$f_{s,crack}$, ksi	μ_{TEST}, ksi	Difference, %
Upright	B5-L6d-S2d-Sp4-1D-B2S1	13.4	3.8	2.8	1.1	1.5	82	0.091	NA	3368	-19.7
Side	B5-L6d-S2d-Sp4-1D-B2S2	13.4	3.9	2.9	1.2	1.3	67	0.061	20	2706	
Upright	B5-L8d-S2d-Sp4-1D-B2S1	13.4	5.3	4.3	1.2	1.5	96	0.205	24	2857	2.8
Side	B5-L8d-S2d-Sp4-1D-B2S2	13.4	5.1	4.1	1.4	1.5	95	0.215	NA	2936	
Upright	B5-L10d-S2d-Sp4-1D-B2S1	13.4	6.3	5.3	1.2	1.6	94	0.128	22	2335	-6.2
Side	B5-L10d-S2d-Sp4-1D-B2S2	13.4	6.3	5.3	1.4	1.5	88	0.167	NA	2189	
Upright	M5-L12d-S2d-Sp4-1D-B2S1	13.4	7.6	6.6	1.2	1.5	127	0.103	33	2603	1.6
Side	M5-L12d-S2d-Sp4-1D-B2S2	13.4	7.6	6.6	1.3	1.6	129	0.090	30	2645	
Upright	B5-L8d-S2d-Sp4-7D-B2S1	19.5	5.1	4.1	1.1	1.5	94	0.162	21	2913	0.7
Side	B5-L8d-S2d-Sp4-7D-B2S2	19.5	5.1	4.1	1.4	1.6	96	0.184	20	2933	
Upright	B5-L8d-S2d-Sp4-7D-B2S1	19.5	5.1	4.1	1.1	1.5	95	0.078	NA	2922	0.8
Side	B5-L8d-S2d-Sp4-7D-B2S2	19.5	5.1	4.1	1.4	1.6	97	0.075	NA	2947	
Upright	B5-L10d-S2d-Sp4-7D-B2S1	19.5	6.3	5.3	1.2	1.4	rupture‡	0.269	27	-	-
Side	B5-L10d-S2d-Sp4-7D-B2S2	19.5	6.3	5.3	1.3	1.6	rupture‡	0.262	NA	-	
Upright	B5-L10d-S2d-Sp4-7D-B2S1	19.5	5.9	4.9	1.2	1.4	rupture‡	0.161	21	-	-
Side	B5-L10d-S2d-Sp4-7D-B2S2	19.5	6.3	5.3	1.4	1.6	rupture‡	0.197	24	-	
Upright	M5-L12d-S2d-Sp4-7D-B2S1	19.5	7.6	6.6	1.2	1.4	rupture‡	0.135	27	-	-
Side	M5-L12d-S2d-Sp4-7D-B2S2	19.5	7.5	6.5	1.4	1.5	rupture‡	0.152	NA	-	

* Refer to Figure 8. ‡ Bar ruptured before bond failure. 1 ksi = 6.895 MPa; 1 in. = 2.54 cm

†The column headings are defined as follows:

- Batch ID notation example: B5-L6d-S2d-Sp4-1D-B2S1,the first term B5 represents the type and the size of the bar, and the letter is for the bar type (B for uncoated black bar, M for A1035 high strength bar, E for epoxy coated bar) and the number is for the bar size (for example, 5 for No. 5 bar); L6d represents a designed embedment length of six times of the testing bar diameter; S2d represents a designed side cover of two times of the testing bar diameter; Sp4 represents a designed center to center spacing of 4 in. (10.2 cm) between the testing bar and the nearest No.8 splice bar extending from the precast slab;1D represents the age (days) of the UHPC material at testing, which is one day in the example; B2S1 represents the batch No. 2 of the UHPC casting and the specimens were cast on the pre-cast slab No. 1.
- f'_c: UHPC compressive strength at testing;
- l_d, l_s, c_{so} and c_{si}: actual measurement of embedment length, spliced length, side cover, and half the clear spacing to nearest No. 8 bar (refer to Figure 3).
- $f_{s,max}$ and s_1 represent the bar stress and bar slip at bond failure, respectively.
- $f_{s,crack}$ represents the bar stress when the first crack was observed.
- μ_{TEST}, refer to the equation in Figure 10.
- Difference, the percentage difference between the specimen cast on side and the specimen cast upright.

Effect of Embedment Length

The effect of embedment length on bond strength is analyzed in this section. It was evaluated by varying the embedment length while keeping other factors constant, including side cover, bar spacing, and concrete compressive strength. The test matrix is presented in Table 5. A total of 37 tests (grouped into four sets) were included and all specimens used A1035 No. 5 bar. In the first set, the embedment lengths included $4d_b$, $6d_b$, $8d_b$, and $10d_b$; the side cover was designed to be constant at $2d_b$; the center-to-center spacing between the testing bar and the nearest No. 8 bar was kept constant at 4 in. (10 cm); and the tests were conducted at one day after casting when the UHPC compressive strength averaged 13.7 ksi (90 MPa). In Set 2, similar specimens as those in Set 1 were tested except that the specimens were tested at seven days after casting and the compressive strength averaged 19.4 ksi (133 MPa). In Sets 3 and 4, while the embedment length was varied, the side cover was increased to $3.5d_b$ and $3d_b$, respectively, compared with $2d_b$ in Sets 1 and 2. More details of the specimen design and actual measurement are presented in Table 5.

The bar stress at bond failure versus the embedment length for all the specimens is plotted in Figure 15. As shown in Figure 15, increasing the embedment length of a reinforcing bar increases the bond strength. The relationship between the bar stress at bond failure and the bonded length is nearly linear, similar to that observed in normal strength concrete (ACI 408 R-03) [(17)]. The linear relationship between bond force and the bonded length in normal strength concrete is often explained based on the assumption that all lugs bear against concrete at the ultimate stage and help in resisting the applied axial force, therefore at ultimate the bond stress distribution is nearly uniform. However, the bond stress distribution in high strength conventional concrete, with compressive strength over 13 ksi (90 MPa) and without fiber reinforcement, was found to be not uniform based on a study conducted by Azizinamini et al. [(19)]. Azizinamini et al. noted that for high strength concrete, the increase in bearing capacity is more than the increase in tensile strength, which in turn, would prevent crushing of the concrete in the vicinity of each lug to the extent that would otherwise take place in normal strength concrete. In other words, the high strength concrete would crack before crushing due to the less than proportional increase in tensile strength compared with bearing capacity. All lugs may not participate in resisting applied axial load before the concrete cracks, and the first few lugs contribute the most. The linear relationship observed in this study implies that the behavior attributed to conventional high strength concretes by Azizinamini et al.[(19)] may not be present in UHPC, potentially due to the enhanced pre- and post-cracking tensile response of the UHPC.

Table 5. Test specimens – effect of embedment length.

	Batch ID	f'_c, ksi	l_d, in.	l_s, in.	c_{so}, in.	c_{si}, in.	$f_{s,max}$, ksi	s_1, in.	$f_{s,crack}$, ksi
Set 1	M5-L4d-S2d-Sp4-1D-B5S2	13.9	2.56	1.56	1.19	1.53	43	0.033	NA
	M5-L4d-S2d-Sp4-1D-B5S2	13.9	2.69	1.69	1.20	1.56	49	0.020	NA
	M5-L6d-S2d-Sp4-1D-B3S1	13.2	3.69	3.44	1.16	1.56	77	0.042	45
	M5-L6d-S2d-Sp4-1D-B4S2	13.6	3.81	3.56	1.16	1.38	84	0.053	42
	M5-L6d-S2d-Sp4-1D-B4S2	13.6	3.81	2.81	1.29	1.38	82	0.053	58
	M5-L8d-S2d-Sp4-1D-B3S1	13.2	5.00	4.00	1.23	1.44	96	0.065	58
	M5-L8d-S2d-Sp4-1D-B6S3	13.9	4.60	3.60	1.25	1.47	108	0.057	68
	M5-L8d-S2d-Sp4-1D-B8S4	13.8	4.94	3.94	1.10	1.53	106	0.050	NA
	M5-L8d-S2d-Sp4-1D-B9S4	13.7	5.25	4.25	1.18	1.41	121	0.065	77
	M5-L10d-S2d-Sp4-1D-B6S3	13.9	6.25	5.25	1.18	1.47	144	0.082	77
	M5-L10d-S2d-Sp4-1D-B6S3	13.9	6.38	5.38	1.24	1.40	113	0.075	61
	M5-L10d-S2d-Sp4-1D-B9S4	13.7	6.31	5.31	1.17	1.53	132	0.076	65
Set 2	M5-L4d-S2d-Sp4-7D-B1S1	19.9	2.36	1.36	1.18	1.49	67	0.036	NA
	M5-L4d-S2d-Sp4-7D-B3S1	19.5	2.44	2.19	1.21	1.44	59	0.041	40
	M5-L6d-S2d-Sp4-7D-B1S1	19.9	3.29	2.29	1.37	1.65	91	0.072	NA
	M5-L6d-S2d-Sp4-7D-B3S1	19.5	3.75	3.50	1.25	1.56	91	0.068	52
	M5-L6d-S2d-Sp4-7D-B3S1	19.5	3.81	2.81	1.20	1.50	90	0.052	58
	M5-L6d-S2d-Sp4-7D-B4S2	19.2	3.88	2.88	1.14	1.44	83	0.047	65
	M5-L8d-S2d-Sp4-7D-B3S1	19.5	5.06	4.06	1.22	1.56	114	0.059	58
	M5-L8d-S2d-Sp4-7D-B9S4	18.8	5.00	4.00	1.12	1.50	127	0.070	NA
	M5-L10d-S2d-Sp4-7D-B9S4	18.8	6.12	5.12	1.11	1.56	154	0.100	NA
	M5-L10d-S2d-Sp4-7D-B9S4	18.8	6.06	5.06	1.15	1.47	153	0.115	NA
	M5-L10d-S2d-Sp4-7D-B3S1	19.5	6.19	5.19	1.17	1.50	145	0.091	74

Table 5(cont'd). Test specimens – effect of embedment length.

	Batch ID	f'_c, ksi	l_d, in.	l_s, in.	c_{so}, in.	c_{si}, in.	$f_{s,max}$, ksi	s_1, in.	$f_{s,crack}$, ksi
Set 3	M5-L6d-S3.5d-Sp4-1D-B4S2	13.6	3.88	3.63	2.24	1.63	96	0.043	NA
	M5-L6d-S3.5d-Sp4-1D-B4S2	13.6	3.81	2.81	2.25	1.56	90	0.045	79
	M5-L8d-S3.5d-Sp4-1D-B4S2	13.6	5.06	4.06	2.35	1.56	136	0.080	65
	M5-L8d-S3.5d-Sp4-1D-B7S3	13.5	5.13	4.13	2.08	1.56	137	0.068	97
	M5-L10d-S3.5d-Sp4-1D-B4S2	13.6	6.31	6.06	2.20	1.56	155	0.108	90
	M5-L10d-S3.5d-Sp4-1D-B4S2	13.6	6.31	5.31	2.24	1.63	166	0.161	68
	M5-L10d-S3.5d-Sp4-1D-B4S2	13.6	6.31	5.31	2.33	1.56	158	0.099	125
Set 4	M5-L6d-S3d-Sp4-1D-B10S4	13.9	3.44	2.44	1.82	1.50	85	0.037	NA
	M5-L6d-S3d-Sp4-1D-B10S4	13.9	3.75	2.75	1.83	1.53	84	0.051	NA
	M5-L6.7d-S3d-Sp4-1D-B10S4	13.9	4.22	3.22	1.87	1.59	103	0.045	NA
	M5-L6.7d-S3d-Sp4-1D-B10S4	13.9	4.13	3.13	1.85	1.50	115	0.060	NA
	M5-L8d-S3d-Sp4-1D-B10S4	13.9	5.44	4.44	1.92	1.50	138	0.072	NA
	M5-L8d-S3d-Sp4-1D-B10S4	13.9	5.25	4.25	1.86	1.59	134	0.080	NA
	M5-L10d-S3d-Sp4-1D-B10S4	13.9	6.13	5.13	1.83	1.50	141	0.053	NA

Note: For explanation of the specimen ID and each parameter, see note for Table 4. 1 ksi = 6.895 MPa; 1 in. = 2.54 cm.

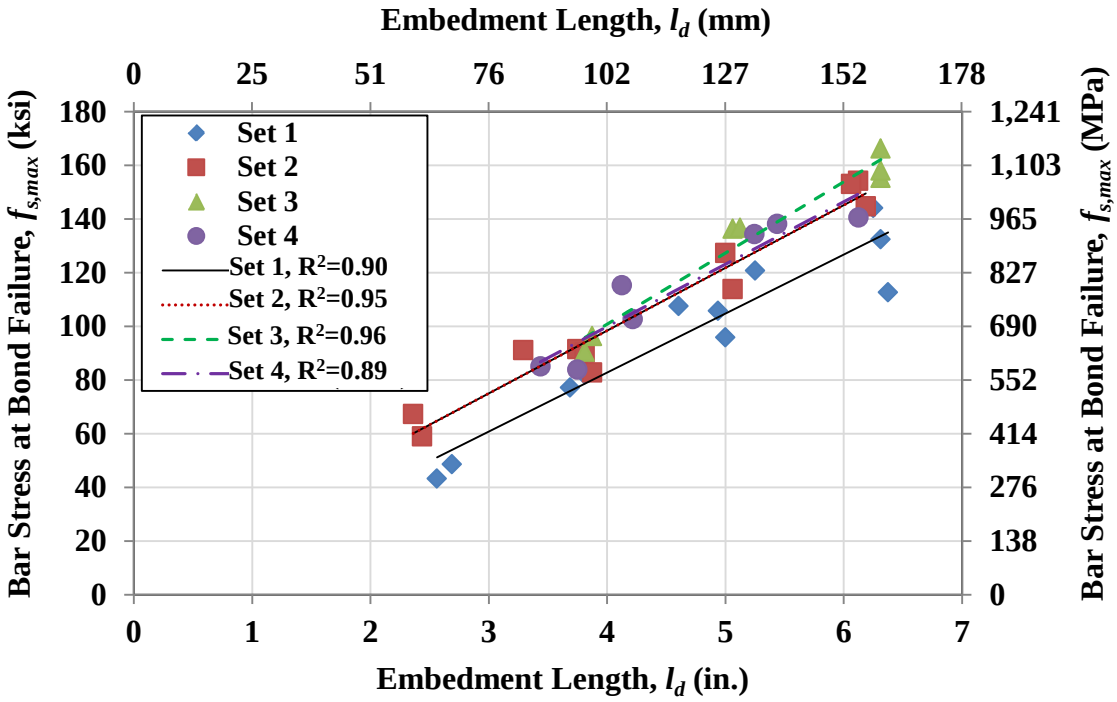

Figure 15. Graph. Effect of embedment length: $f_{s,max}$ versus embedment length l_d.

Side Cover

Concrete cover and bar spacing play important roles in bond strength. An understanding of the bond behavior in normal non-fiber reinforced concrete is necessary. As stated in ACI 408 R-03[17], for bond failure involving splitting of the concrete, the nature of the splitting failure depends on whether the concrete cover, $c_{so,}$ is smaller than c_{si}, which is 1/2 of the clear spacing to adjacent bar. The demonstration of c_{so} and c_{si} is presented in Figure 16 and also in Figure 3 in Chapter 2. When c_{so} is smaller than c_{si}, the splitting crack occurs through the cover to the free surface, as shown in Figure 16a. When c_{si} is smaller than c_{so}, the splitting crack forms between the reinforcing bars as shown in Figure 16b. In ACI 318 Building Code Requirements for Structural Concrete,[21] the actual values of c_{si} are used for development length calculations. In the Canadian requirements for reinforced concrete design (CSA standard A23.3-94),[21] a larger value defined as $[(4/3)c_{si} + (1/6)d_b]$ is used. Zuo and Darwin (1998) [22] suggested using either $1.6c_{si}$ when using a multiple of c_{si} or using c_{si} + 0.25 in. (c_{si} + 6.4 mm) when a constant value is added to c_{si}. Darwin et al. (1996a) [23] explained that the reason why a larger value than the actual value of c_{si} is used is most likely "due to the longer effective crack lengths that occur when concrete splits between bars." The presence of fiber reinforcement in UHPC can be expected to increase the resistance to splitting crack between bars and thus an even larger value than the actual value of c_{si} between bars may be necessary. In the present analysis, both the term c_{si} representing 1/2 of the clear spacing as well as the actual clear spacing, $2c_{si}$, are compared with side cover c_{so}.

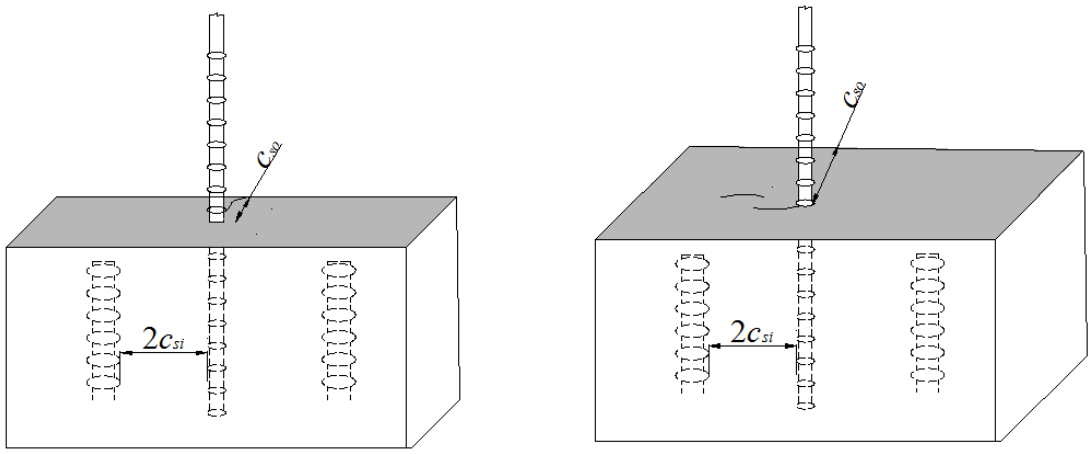

(a) (b)

Figure 16. Illustration. Bond splitting cracks: (a) $c_{si} > c_{so}$; and (b) $c_{si} < c_{so}$.

Within this study, a total of 37 specimens were tested in five sets and the results are presented in Table 6. Using the same philosophy that has been used in previous sections, the specimens were designed to have the same parameters except for side cover. A1035 No. 5 bars were used and all specimens were designed to have the same bar spacing to the nearest No. 8 bar. As shown in Table 6, for Set 1 an embedment length of $6d_b$ was used and the side cover included nominal values of $2d_b$, $2.7d_b$, $3d_b$, and $3.5d_b$ [corresponding to UHPC strip widths of 3 1/8, 4, 4 3/8, and 5 in. (7.9 to 10.2, 11.1 and 12.7 cm), respectively]. Set 2 had the same design as Set 1, except that the embedment length was increased to $8d_b$. In Set 3, specimens with a constant embedment length of $10d_b$ and a varied side cover of $2d_b$ and $3.5d_b$ were tested. All specimens in Sets 1, 2, and 3 were tested at one day after UHPC casting, with an average compressive strength of 13.7 ksi (94 MPa). Specimens in Sets 4 and 5 were tested at seven days after the UHPC casting, with an average compressive strength of 19.4 ksi (133 MPa). Specimens in Set 4 had an embedment length of $6d_b$ and side covers of $2d_b$, $3d_b$, and $3.5d_b$, while specimens in Set 5 had an embedment length of $8d_b$ and side covers of $2d_b$ and $3.5d_b$.

Based on the results shown in Table 6, it is clear that the maximum bar stress at bond failure increased as the side cover increased. For example, in Set 2 where a designed embedment length of $8d_b$ was used, the three specimens with a $2d_b$ side cover had bar stresses at bond failure of 108, 106, and 121 ksi (741, 729 and 833 MPa); when the side cover was increased to $3.5d_b$, the two specimens had bar stresses at bond failure of 136 and 137 ksi (940 and 943 MPa).

Table 6. Test specimens – effect of side cover.

	Batch ID	f'_c, ksi	l_d, in.	l_s, in.	c_{so}, in.	c_{si}, in.	$f_{s,max}$, ksi	s_1, in.	$f_{s,crack}$, ksi	μ_{TEST}, psi
Set 1	M5-L6d-S2d-Sp4-1D-B3S1	13.2	3.69	3.44	1.16	1.56	77	0.042	45	3269
	M5-L6d-S2d-Sp4-1D-B4S2	13.6	3.81	3.56	1.16	1.38	84	0.053	42	3430
	M5-L6d-S2d-Sp4-1D-B4S2	13.6	3.81	2.81	1.29	1.38	82	0.053	58	3363
	M5-L6d-S2.7d-Sp4-1D-B9S3	13.7	4.25	3.25	1.67	1.50	93	0.052	87	3420
	M5-L6d-S2.7d-Sp4-1D-B9S3	13.7	4.13	3.13	1.66	1.53	98	0.057	90	3725
	M5-L6d-S3d-Sp4-1D-B8S3	13.8	3.81	2.81	1.78	1.53	103	0.045	82	4211
	M5-L6d-S3d-Sp4-1D-B8S3	13.8	3.81	2.81	1.78	1.56	88	0.039	86	3608
	M5-L6d-S3d-Sp4-1D-B10S4	13.9	3.44	2.44	1.82	1.50	85	0.037	NA	3863
	M5-L6d-S3d-Sp4-1D-B10S4	13.9	3.75	2.75	1.83	1.53	84	0.051	NA	3494
	M5-L6d-S3.5d-Sp4-1D-B4S2	13.6	3.88	2.88	2.24	1.63	96	0.043	NA	3884
	M5-L6d-S3.5d-Sp4-1D-B4S2	13.6	3.81	2.81	2.25	1.56	90	0.045	79	3707
Set 2	M5-L8d-S2d-Sp4-1D-B6S3	13.9	4.60	3.60	1.25	1.47	108	0.057	68	3649
	M5-L8d-S2d-Sp4-1D-B8S4	13.8	4.94	3.94	1.10	1.53	106	0.050	0	3346
	M5-L8d-S2d-Sp4-1D-B9S4	13.7	5.25	4.25	1.18	1.41	121	0.065	77	3595
	M5-L8d-S2.7d-Sp4-1D-B9S3	13.7	5.31	4.31	1.55	1.47	129	0.074	87	3795
	M5-L8d-S2.7d-Sp4-1D-B9S3	13.7	5.13	4.13	1.67	1.47	128	0.065	0	3906
	M5-L8d-S3d-Sp4-1D-B8S3	13.8	5.13	4.13	1.49	1.47	134	0.073	95	4096
	M5-L8d-S3d-Sp4-1D-B8S3	13.8	4.94	3.94	1.80	1.56	126	0.060	84	3974
	M5-L8d-S3.5d-Sp4-1D-B4S2	13.6	5.06	4.06	2.35	1.56	136	0.080	65	4208
	M5-L8d-S3.5d-Sp4-1D-B7S3	13.5	5.13	4.13	2.08	1.56	137	0.068	97	4168

Table 6 (cont'd).Test specimens – effect of side cover.

	Batch ID	f'_c, ksi	l_d, in.	l_s, in.	c_{so}, in.	c_{si}, in.	$f_{s,max}$, ksi	s_1, in.	$f_{s,crack}$, ksi	μ_{TEST}, psi
Set 3	M5-L10d-S2d-Sp4-1D-B6S3	13.9	6.25	5.25	1.18	1.47	144	0.082	77	3602
	M5-L10d-S2d-Sp4-1D-B9S4	13.7	6.31	5.31	1.17	1.53	132	0.076	65	3276
	M5-L10d-S3.5d-Sp4-1D-B4S2	13.6	6.31	6.06	2.20	1.56	155	0.108	90	3843
	M5-L10d-S3.5d-Sp4-1D-B4S2	13.6	6.31	5.31	2.24	1.63	166	0.161	68	4116
	M5-L10d-S3.5d-Sp4-1D-B4S2	13.6	6.31	5.31	2.33	1.56	158	0.099	125	3911
Set 4	M5-L6d-S2d-Sp4-7D-B1S1	19.9	3.29	2.29	1.37	1.65	91	0.072	NA	4326
	M5-L6d-S2d-Sp4-7D-B3S1	19.5	3.75	3.50	1.25	1.56	91	0.068	52	3812
	M5-L6d-S2d-Sp4-7D-B3S1	19.5	3.81	2.81	1.20	1.50	90	0.052	58	3695
	M5-L6d-S2d-Sp4-7D-B4S2	19.2	3.88	2.88	1.14	1.44	83	0.047	65	3335
	M5-L6d-S3d-Sp4-7D-B10S4	19.6	3.94	2.94	1.85	1.66	118	0.058	NA	4673
	M5-L6d-S3d-Sp4-7D-B10S4	19.6	3.88	2.88	1.85	1.56	111	0.055	NA	4486
	M5-L6d-S3d-Sp4-7D-B10S4	19.6	4.19	3.19	1.89	1.53	117	0.050	NA	4359
	M5-L6d-S3.5d-Sp4-7D-B4S2	19.2	3.75	3.50	2.31	1.56	117	0.051	106	4876
	M5-L6d-S3.5d-Sp4-7D-B4S2	19.2	3.75	2.75	2.31	1.56	124	0.061	106	5148
Set 5	M5-L8d-S2d-Sp4-7D-B3S1	19.5	5.06	4.06	1.22	1.56	114	0.059	58	3515
	M5-L8d-S2d-Sp4-7D-B9S4	18.8	5.00	4.00	1.12	1.50	127	0.070	NA	3979
	M5-L8d-S3.5d-Sp4-7D-B4S2	19.2	5.00	4.00	2.27	1.56	145	0.096	87	4521

Note: For explanation of the specimen ID and each parameter, see note for Table 4. 1 ksi = 6.895 MPa; 1 in. = 2.54 cm.

Note that specimens in Sets 1, 2, and 3 had the same design except for embedment length and side cover. The same is true for specimens in Sets 4 and 5. To create a bigger data pool, specimens in Sets 1, 2, and 3 and the specimens in Sets 4 and 5 are combined by converting bar stress at bond failure to bond stress to offset the effect of different embedment lengths (refer to equation in Figure 10). The bond stress is plotted versus side cover for specimens in Sets 1, 2 and 3 and specimens in Sets 4 and 5 in Figure 17 and Figure 18, respectively. With constant bar spacing ($2c_{si}$) for all specimens, straight lines representing the point where the side cover c_{so} is equal to c_{si} and $2c_{si}$ are included in the figures.

As shown in Figure 17 and Figure 18, the bond strength increases as the side cover increases. It is noted that when the side cover (c_{so}) is bigger than half of the clear spacing (c_{si}), the bond strength still increases as the side cover increases, instead of being controlled by the constant value of c_{si}. This proves the early assumption that a greater bar spacing value than c_{si} should be used due to the presence of the fibers. All specimens had side covers (c_{so}) less than the clear bar spacing ($2c_{si}$). It is reasonable to predict that when the side cover is large enough, the bar spacing would become the controlling factor and the bond strength would reach a plateau.

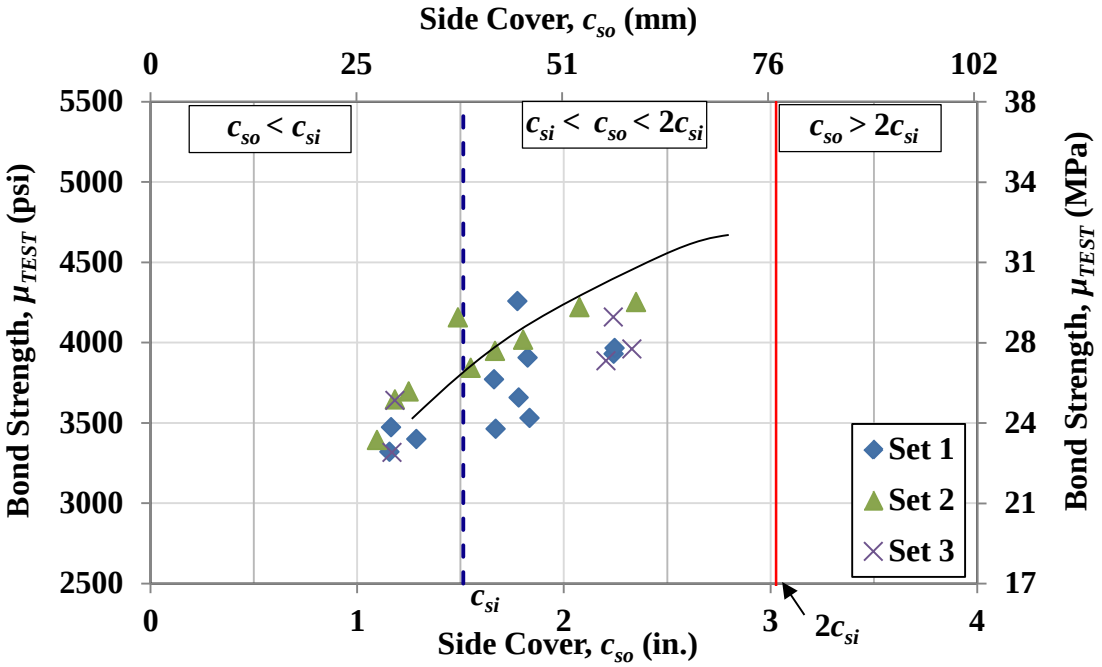

Figure 17. Graph. Effect of side cover: bond strength μ_{TEST} versus side cover for specimens in Sets 1, 2 and 3. The c_{si} is constant.

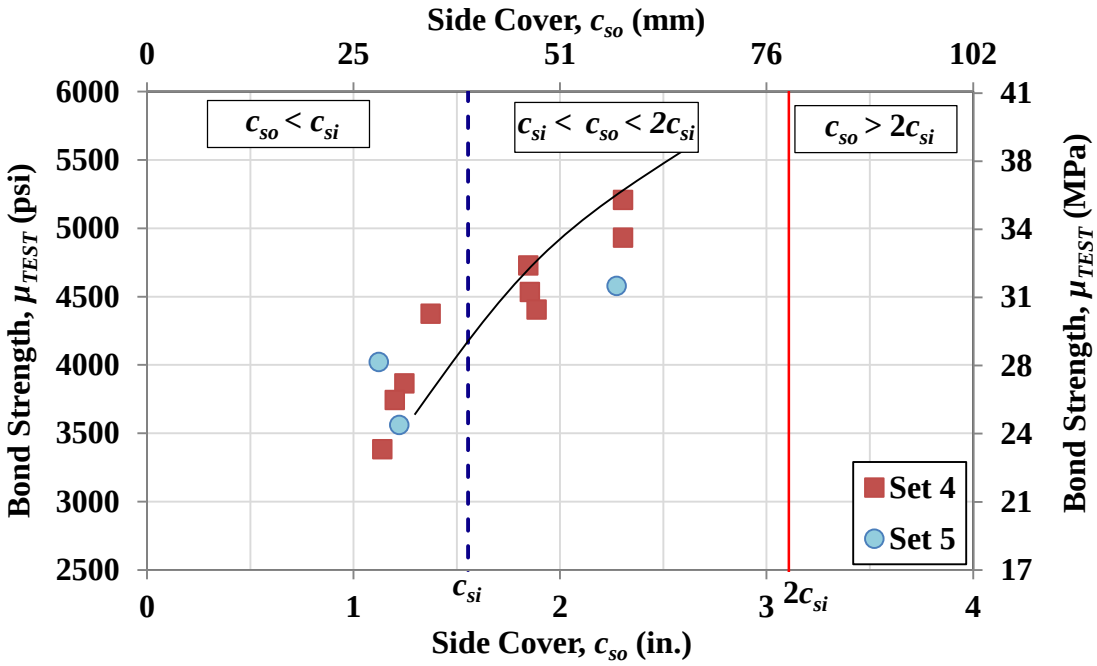

Figure 18. Graph. Effect of side cover: bond strength μ_{TEST} versus side cover for specimens in Sets 4 and 5. The c_{si} is constant.

Bar Spacing

The effect of bar spacing on bond performance is analyzed in this section. Details for the specimens are presented in Table 7. A1035 bars were used and a total of 46 specimens were included in four sets. In each set of tests, the side cover (c_{so}) and embedment length were designed to be constant while the bar spacing (c_{si}) varied. It should be noted that the bar spacing to the nearest adjacent No. 8 bars was designed in terms of actual length in inches instead of bar diameter. In Set 1, a constant embedment length of $8d_b$ (A1035 No. 5 bar) and a constant side cover of $2d_b$ were used; the bar spacing, c_{si}, varied from 0.1 to 5.7 in. (0.3 to 14.5 cm). All tests were conducted at one day after UHPC casting with an average compressive strength of 13.7 ksi (94.5 MPa). It should be pointed out that the specimens with a bar spacing of 0.1 in. (0.3 cm) were originally designed to have a contact lap splice, and the actual measurement indicated a bar spacing of 0.1 in. (0.3 cm). Given the small measured spacing value, these specimens were considered to have contact lap splices in the study.

All four sets specimens demonstrated similar trends and the results from Set 1 are discussed first here. As shown in Table 7, the bar stress at bond failure was only about 83 ksi (572 MPa) for a contact lap splice (the first two specimens in Set 1), and it increased to over 95 ksi (655 MPa) when c_{si} was increased from zero to the range of 0.5 to 2.6 in. (1.3 to 6.6 cm). When c_{si} was increased to over 3.5 in. (8.9 cm), the bar stress at bond failure dropped to as low as 70 ksi (483 MPa).

Table 7. Test specimens – effect of bar spacing

	Batch ID	f'_c, ksi	l_d, in.	l_s, in.	c_{so}, in.	c_{si}, in.	$f_{s,max}$, ksi	s_1, in.	$f_{s,crack}$, ksi	μ_{TEST}, psi
Set 1	M5-L8d-S2d-Sp0-1D-B6S7	13.9	5.0	4.0	1.3	0.1	82	0.037	NA	2576
	M5-L8d-S2d-Sp0-1D-B6S7	13.9	5.1	4.1	1.2	0.1	83	0.036	NA	2575
	M5-L8d-S2d-Sp2-1D-B11S4	13.6	5.1	4.1	1.2	0.5	119	0.050	77	3642
	M5-L8d-S2d-Sp2-1D-B11S4	13.6	4.8	3.8	1.3	0.6	109	0.065	71	3594
	M5-L8d-S2d-Sp4-1D-B3S1	13.2	5.0	4.0	1.2	1.4	96	0.065	58	2995
	M5-L8d-S2d-Sp4-1D-B6S3	13.9	4.6	3.6	1.2	1.5	108	0.057	68	3649
	M5-L8d-S2d-Sp4-1D-B8S4	13.8	4.9	3.9	1.1	1.5	106	0.050	NA	3346
	M5-L8d-S2d-Sp6-1D-B3S6	13.2	5.1	4.1	1.4	2.6	101	0.075	52	3075
	M5-L8d-S2d-Sp6-1D-B6S7	13.9	5.1	4.1	1.2	2.6	96	0.072	48	2965
	M5-L8d-S2d-Sp6-1D-B6S7	13.9	5.0	4.0	1.3	2.6	95	0.074	58	2968
	M5-L8d-S2d-Sp8-1D-B8S4	13.8	4.8	3.8	1.2	3.6	78	0.068	69	2545
	M5-L8d-S2d-Sp8-1D-B8S4	13.8	5.0	4.0	1.2	3.5	82	0.066	NA	2571
	M5-L8d-S2d-Sp8-1D-B11S4	13.6	5.0	4.0	1.2	3.5	86	0.076	57	2691
	M5-L8d-S2d-Sp8-1D-B11S4	13.6	5.1	4.1	1.2	3.6	94	0.120	54	2866
	M5-L8d-S2d-Sp12-1D-B6S7	13.9	5.0	4.0	1.3	5.6	70	0.081	45	2178
	M5-L8d-S2d-Sp12-1D-B11S4	13.6	5.0	4.0	1.2	5.7	85	0.124	55	2646
Set 2	M5-L8d-S3.5d-Sp0-1D-B7S7	13.5	4.9	3.9	2.1	0.1	105	0.000	NA	3372
	M5-L8d-S3.5d-Sp0-1D-B7S7	13.5	5.3	4.3	2.2	0.1	109	0.000	NA	3245
	M5-L8d-S3.5d-Sp2-1D-B11S6	13.6	5.1	4.1	2.2	0.6	159	0.059	58	4858
	M5-L8d-S3.5d-Sp2-1D-B11S6	13.6	5.1	4.1	2.2	0.7	149	0.084	68	4528
	M5-L8d-S3.5d-Sp4-1D-B4S2	13.6	5.1	4.1	2.4	1.6	136	0.000	NA	4208
	M5-L8d-S3.5d-Sp4-1D-B7S3	13.5	5.1	4.1	2.1	1.6	137	0.000	NA	4168

Table 7 (cont'd) Test specimens – effect of bar spacing

	Batch ID	f'_c, ksi	l_d, in.	l_s, in.	c_{so}, in.	c_{si}, in.	$f_{s,max}$, ksi	s_1, in.	$f_{s,crack}$, ksi	μ_{TEST}, psi
Set 2	M5-L8d-S3.5d-Sp6-1D-B7S7	13.5	5.1	4.1	2.2	2.5	137	0.032	90	4180
	M5-L8d-S3.5d-Sp6-1D-B7S7	13.5	5.3	4.3	2.1	2.4	145	0.048	NA	4314
	M5-L8d-S3.5d-Sp8-1D-B7S3	13.5	5.2	4.2	2.0	3.4	115	0.131	81	3452
	M5-L8d-S3.5d-Sp8-1D-B7S3	13.5	4.9	3.9	2.0	3.7	108	0.092	106	3434
	M5-L8d-S3.5d-Sp12-1D-B7S7	13.5	5.1	4.1	2.2	5.8	129	0.080	65	3925
	M5-L8d-S3.5d-Sp12-1D-B7S7	13.5	4.9	3.9	2.2	5.4	103	0.068	97	3288
	M5-L8d-S3.5d-Sp12-1D-B11S6	13.6	5.1	4.1	2.2	5.5	107	0.082	74	3260
Set 3	M5-L6d-S2d-Sp0-7D-B5S1	18.9	3.9	2.9	1.1	0.0	78	0.093	100	3142
	M5-L6d-S2d-Sp0-7D-B5S1	18.9	3.8	2.8	1.1	0.0	84	0.086	55	3506
	M5-L6d-S2d-Sp2-7D-B5S1	18.9	3.8	2.8	1.1	0.6	88	0.079	81	3589
	M5-L6d-S2d-Sp2-7D-B5S1	18.9	3.8	2.8	1.1	0.7	99	NA	81	4131
	M5-L6d-S2d-Sp4-7D-B1S1	19.9	3.3	2.3	1.4	1.6	91	0.085	87	4326
	M5-L6d-S2d-Sp4-7D-B3S1	19.5	3.8	2.8	1.2	1.6	91	0.112	61	3812
	M5-L6d-S2d-Sp4-7D-B3S1	19.5	3.8	2.8	1.2	1.5	90	NA	NA	3695
	M5-L6d-S2d-Sp4-7D-B4S2	19.2	3.9	2.9	1.1	1.4	83	0.131	NA	3335
	M5-L6d-S2d-Sp8-7D-B5S1	18.9	4.0	3.0	1.1	3.5	77	0.091	74	2999
Set 4	M4-L6d-S3.5d-Sp0-1D-B12S5	11.9	2.9	1.9	1.7	0.1	90	0.108	60	3894
	M4-L6d-S3.5d-Sp0-1D-B12S5	11.9	3.1	2.1	1.8	0.1	99	0.000	NA	4051
	M4-L6d-S3.5d-Sp2-1D-B12S5	11.9	3.1	2.1	1.7	0.5	111	0.000	NA	4516
	M4-L6d-S3.5d-Sp4-1D-B12S5	11.9	3.1	2.1	1.7	1.6	106	0.032	NA	4243
	M4-L6d-S3.5d-Sp4-1D-B12S5	11.9	3.1	2.1	1.6	1.4	97	0.036	NA	3867
	M4-L6d-S3.5d-Sp8-1D-B12S5	11.9	2.7	1.7	1.7	3.5	81	0.042	NA	3751
	M4-L6d-S3.5d-Sp8-1D-B12S5	11.9	3.1	2.1	1.7	3.6	85	0.041	NA	3483
	M4-L6d-S3.5d-Sp8-1D-B12S5	11.9	3.1	2.1	1.7	3.6	97	0.038	NA	3867

Note: For explanation of the specimen ID and each parameter, see note for Table 4. 1 ksi = 6.895 MPa; 1 in. = 2.54 cm.

The bond stress (μ_{TEST}) is plotted versus bar clear spacing ($2c_{si}$) for specimens in Set 1 in Figure 19. The bond stress (μ_{TEST}) is used in Figure 19 to account for the different embedment length of the compared specimens. It should be noted that the specimens in Set 1 were designed to have the same nominal embedment length, though the actual embedment length varied slightly between 4.8 and 5.1 in. (12.2 and 13.0 cm) with one having 4.6 in. (11.7 cm). The bar clear spacing ($2c_{si}$) was chosen for the reason stated in previous section that a greater bar spacing value than c_{si} should be used due to the presence of the fibers. The actual clear spacing $2c_{si}$ was used in current study. Figure 19 also includes two straight lines, representing the points of $2c_{si} = c_{so}$ and $2c_{si} = l_s tan(\theta)$, respectively. The meaning of $2c_{si}$ and $l_s tan(\theta)$ are demonstrated in Figure 20. The $2c_{si}$ represents the clear spacing to the nearest bar; l_s is the lap splice length (instead of embedded length l_d); and θ is the angle between the diagonal cracks and testing bar. The angle θ for the A1035 No.5 bar tested in this study was measured to be approximately 55 degrees. The hypothesis of adding the two straight lines is as follows: when $2c_{si} \leq c_{so}$, where c_{so} has constant values in each set of comparison, the bond strength is controlled by the bar spacing $2c_{si}$, with larger bar spacing resulting in higher bond strength; when $c_{so} < 2c_{si} \leq l_s tan(\theta)$, the bond strength is controlled by constant side cover c_{so}; and when $2c_{si} > l_s tan(\theta)$, the diagonal cracks would not intersect with the near No. 8 bars. In this last situation, the adjacent No.8 bars would not help to stop the propagation of the diagonal cracks and the bond strength would likely be primarily dependent on the mechanical performance of the UHPC.

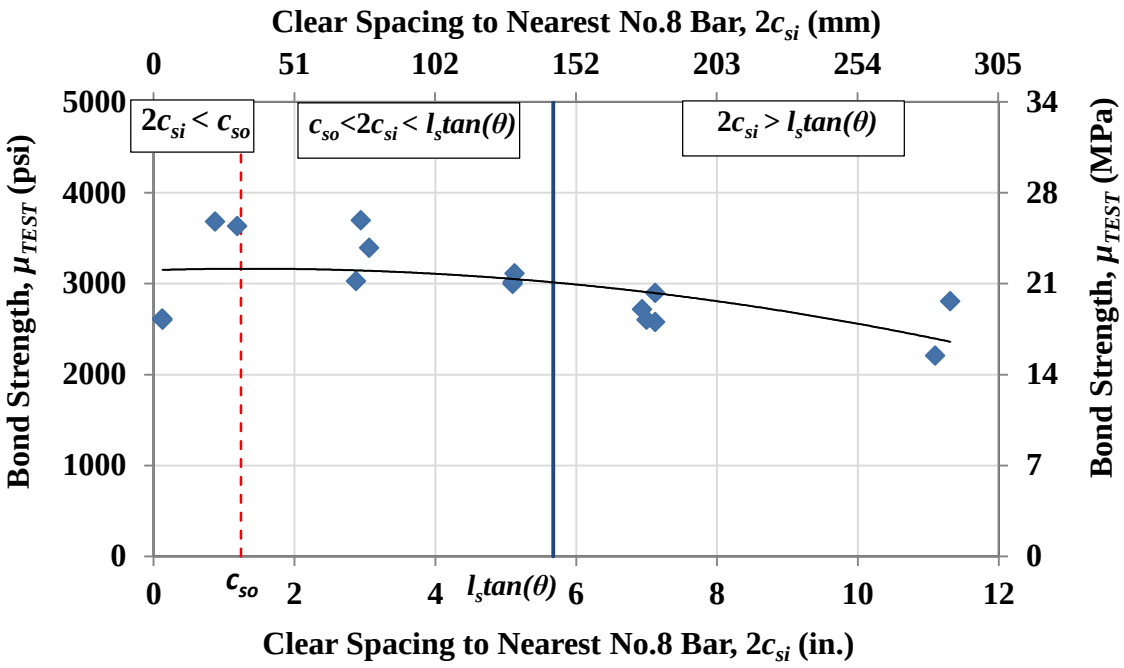

Figure 19. Graph. Effect of bar spacing: bond strength μ_{TEST} versus $2c_{si}$ for specimens in Set 1. The c_{so} is constant.

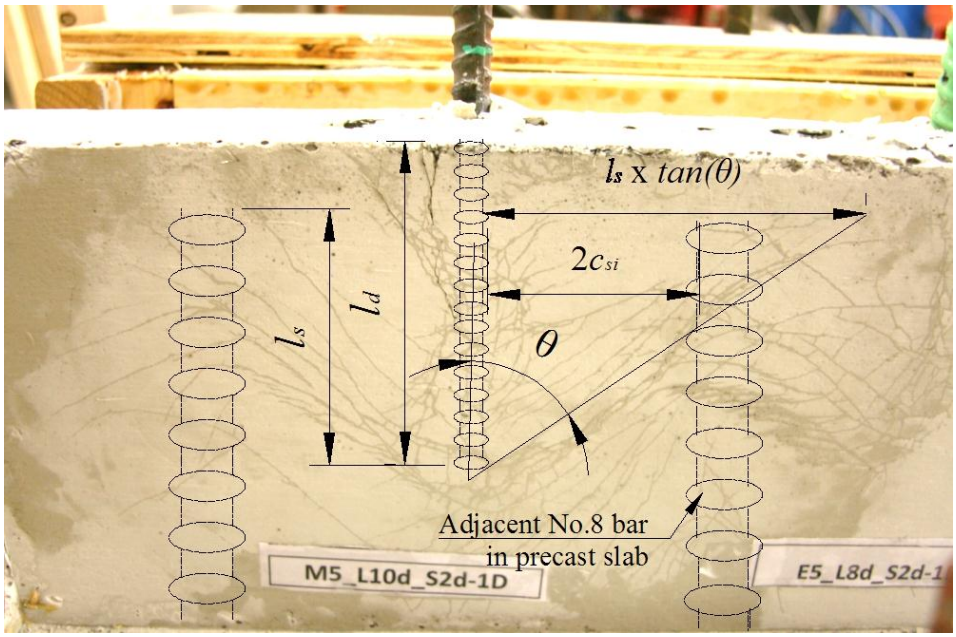

Figure 20. Illustration. Geometrical demonstration of $l_s tan(\theta)$ and $2c_{si}$.

The bond strength is plotted versus $2c_{si}$ in Figure 19, and as shown, only a very limited number of specimens fell in the range of $2c_{si} < c_{so}$. When the testing bar was in contact with extended No.8 bars ($2c_{si}$ near to zero), it expressed less bond strength than those with larger spacing. The bond strength for the two contact lap splice specimens was 2575 and 2576 psi (17.8 and 17.8 MPa), respectively. For the specimens with bar spacing greater than zero but less than $l_s tan(\theta)$, the observed bond strength was about the same, close to or greater than 3000 psi (20.7 MPa). Note that, other than the contact lap splice, the least bar spacing (center-to-center) that was tested in the study was 2 in. (5.1 cm), which is approximately $2d_b$ bar clear spacing. When the testing bar was placed further than $l_s tan(\theta)$ away from the adjacent No. 8 bars, the bond strength decreased, with an average bond stress of 2583 psi (17.8 MPa) for the six specimens in Set 1.

The similar trend was also observed in the other three sets of specimens. The bond strength versus bar clear spacing curve for specimens in Sets 2, 3, and 4 are presented in Figure 21, Figure 22, and Figure 23, respectively. The specimens in Set 2 had similar design as those in Set 1, except that the side cover was increased from $2d_b$ to $3.5d_b$. The specimens in Set 3 had a nominal embedment length of $6d_b$ and side cover of $2d_b$ and all tests were conducted at 7 days after UHPC casting, with an average compressive strength of 19.2 ksi (132 MPa). While A1035 No. 5 bars were used in Sets 1, 2 and 3, A1035 No. 4 bars were used in Set 4, with an embedment length of $6d_b$ and side cover of $3.5d_b$. The bar spacing for specimens in Sets 2, 3, and 4 was varied. The trend that can be noted from these series of tests is that specimens with the bar spacing between $2d_b$ and $l_s tan(\theta)$ have higher bond strength than those with a contact lap splice and those with bar spacing bigger than $l_s tan(\theta)$. The bar spacing of $2d_b$ is the least clear spacing, other than contact lap splice, investigated in this study.

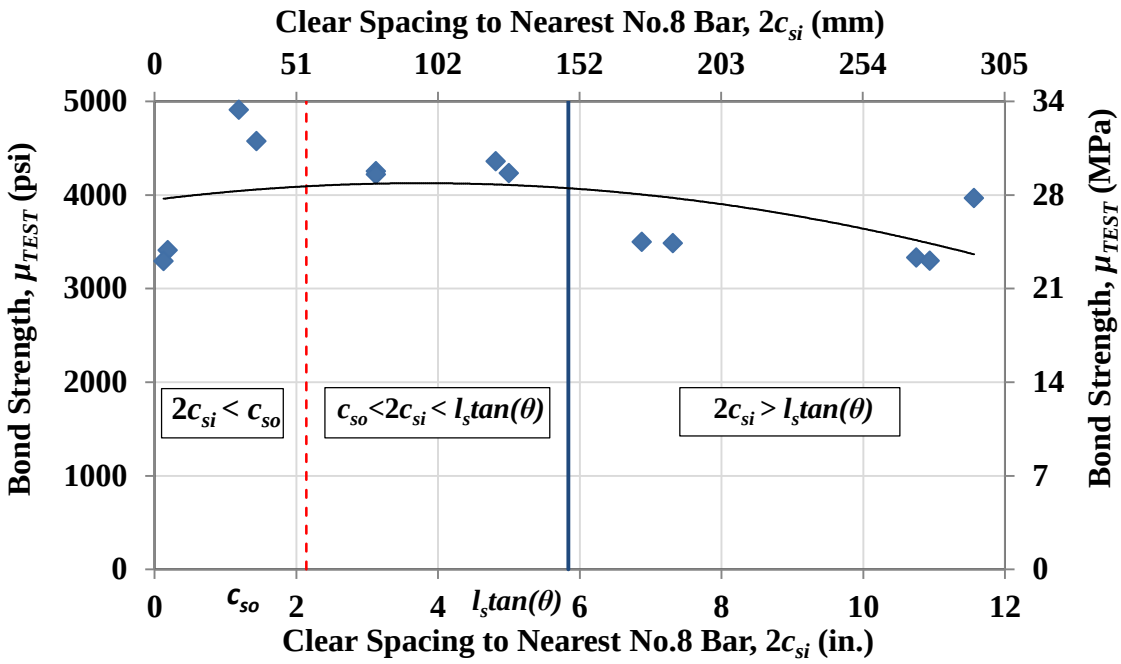

Figure 21. Graph. Effect of bar spacing: bond strength μ_{TEST} versus $2c_{si}$ for specimens in Set 2. The c_{so} is constant.

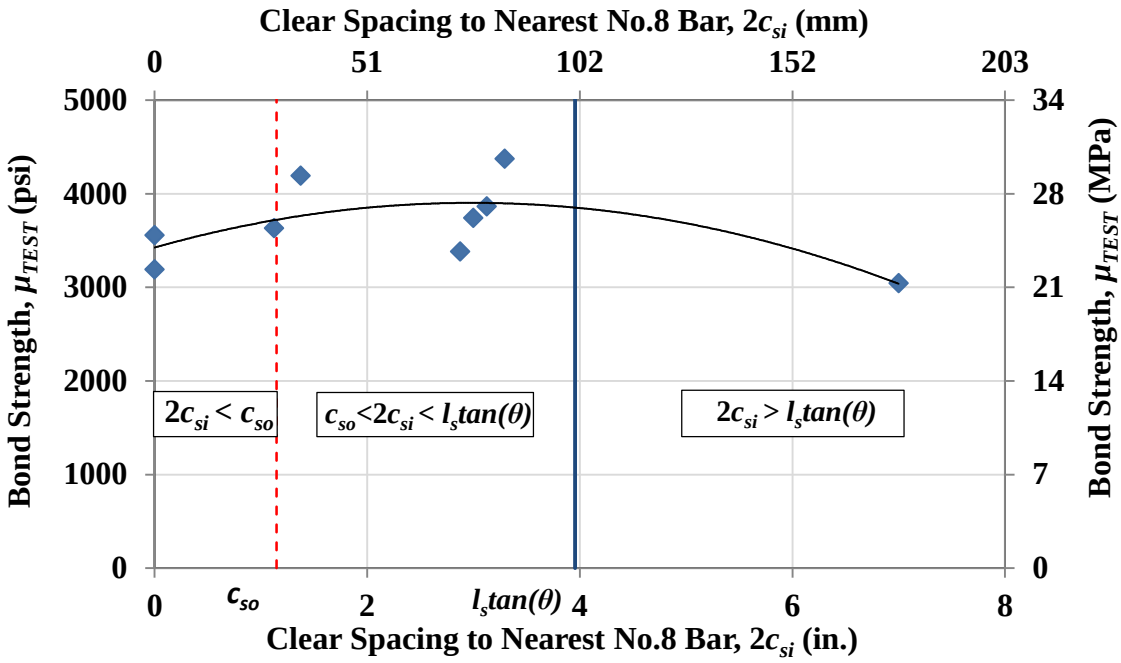

Figure 22. Graph. Effect of bar spacing: bond strength μ_{TEST} versus $2c_{si}$ for specimens in Set 3. The c_{so} is constant.

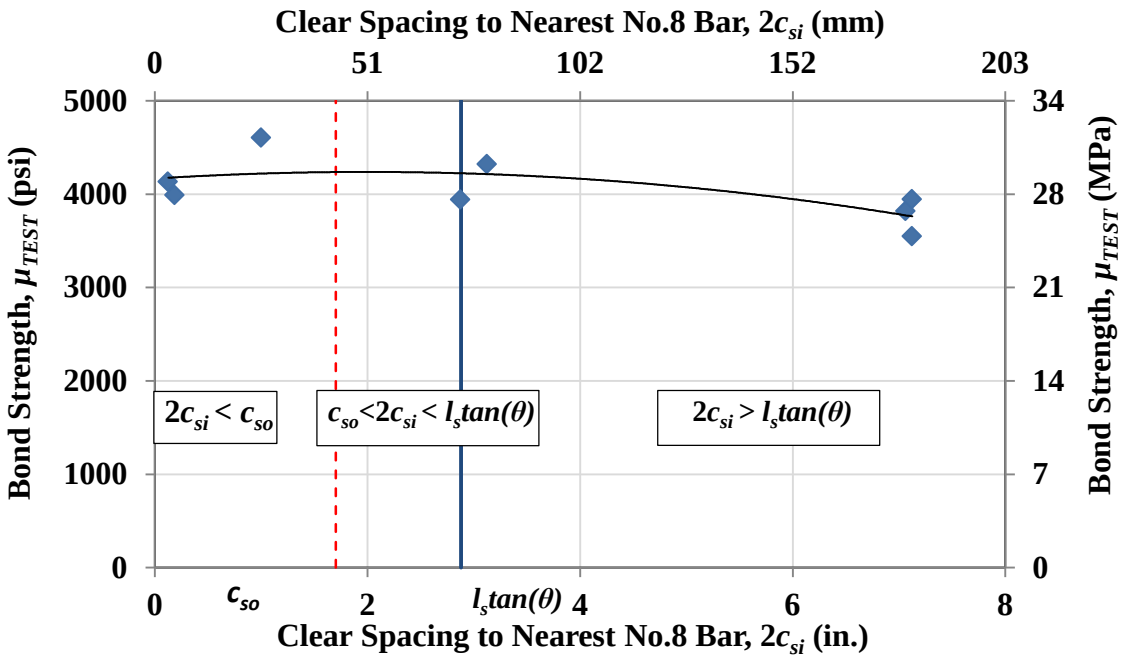

Figure 23. Graph. Effect of bar spacing: bond strength μ_{TEST} versus $2c_{si}$ for specimens in Set 4. The c_{so} is constant.

The average bond strength for specimens with bar spacing between $2d_b$ and $l_s tan(\theta)$ was compared with those with bar spacing out of the range and the results are presented in Table 8. As shown in Table 8, the reduction of bond strength is over twenty percent in most cases. The decrease on bond stress for contacted lap splice specimens is probably due to decreased contact area between the reinforcing bar and UHPC materials, especially considering the dispersion of the fiber reinforcement into the spaces near closely spaced bars, which is needed to locally enhance the mechanical resistance of the UHPC. This is contrary to early studies in normal non-fiber reinforced concrete [23,24,25], where it was concluded that tied spliced (zero spacing) bars had similar or even better bond strength than non-contact lap splices. When the bar clear spacing is larger than $l_s tan(\theta)$, the induced diagonal cracks from the pullout force will not intersect with the adjacent bar and the bond strength is primarily dependent on the performance of the individual bar in the UHPC.

Table 8. Bond strength reduction for bar clear spacing out of the range of $2d_b < 2c_{si} < l_s tan(\theta)$.

Bar clear spacing	$2d_b < 2c_{si} < l_s tan(\theta)$	Contact lap splice		$2c_{si} > l_s tan(\theta)$	
	Avg. μ_{TEST}, psi	Avg. μ_{TEST}, psi	Reduction, %	Avg. μ_{TEST}, psi	Reduction, %
Set 1	3279	2575	21	2583	21
Set 2	4376	3309	24	3472	21
Set 3	3815	3324	13	2999	21
Set 4	NA	4154	NA	3842	NA

UHPC Compressive Strength

The effect of UHPC compressive strength on bond strength is analyzed in this section. For the UHPC materials tested in this study, the average compressive strength was 13.5 ksi (93 MPa) at one day, 17.0 ksi (117 MPa) at three days, 19.4 ksi (133 MPa) at seven days, and 21.3 ksi (147 MPa) at 14 days.

A total of 41 specimens were included and all specimens were tested with A1035 No.5 bars. The details of all specimens are presented in Table 9. The specimens were grouped into three sets based on side cover, and specimens with different embedment lengths were included in the same set. The specimens were grouped so that the specimens in each set can be either directly compared to those with the same embedment length or indirectly compared by comparing the bond strength μ_{TEST} for all specimens. As shown in Table 9, in Set 1 a side cover of $2d_b$ with a constant bar spacing [center to center 4 in. (10 cm)] was used; specimens with embedment length of $4d_b$, $6d_b$, $8d_b$, $10d_b$, and $12d_b$ were tested at either 1, 3, or 7 days after casting. Set 2 specimens had a side cover of $3d_b$ with embedment length of either $6d_b$ or $6.7d_b$ and they were tested at either 1 or 7 days. Similarly, Set 3 specimens had a side cover of $3.5d_b$ and embedment length of either $6d_b$ or $8d_b$; they were tested at either 1 or 7 days.

As expected, an increase in the compressive strength increases the bond strength, as shown in Table 9. For example, for specimens with embedment length of $6d_b$ and side cover of $2d_b$ in Set 1, the average bar stress at bond failure increased from 81 to 89 ksi (558 to 613 MPa) when the compressive strength increased from 13.5 to 19.5 ksi (93 to 135 MPa). In a separate comparison, when the embedment length was $12d_b$ with the UHPC compressive strength at 13.4 ksi (92 MPa), the average bar stress at bond failure was 128 ksi (883 MPa); increasing the UHPC compressive strength to 19.5 ksi (135 MPa) resulted in bar rupture, with bar stress over 160 ksi (1103 MPa) before bond failure.

The relationship between the bond strength and UHPC compressive strength was also assessed. Traditionally, the effect of concrete properties on bond strength is represented by the square root of the compressive strength $f'_c{}^{1/2}$, which is related to tensile strength of the concrete. This representation is normally limited to a maximum concrete strength of 8000 psi (55 MPa) (ACI 408 R-03) [17]. The relationship between the bond strength and the UHPC compressive strength is evaluated here. The bond strength μ_{TEST} is plotted versus f'_c and $f'_c{}^{1/2}$ for specimens in Sets 1, 2, and 3 in Figure 24, Figure 25, and Figure 26, respectively. As shown in the figures, the correlation coefficient (R^2) values for all three sets of tests are low, no matter it is between μ_{TEST} and f'_c or between μ_{TEST} and $f'_c{}^{1/2}$. Since the UHPC material investigated is both high strength and fiber reinforced, other material properties besides compressive strength should be involved in the evaluating of bond strength.

Table 9. Test specimens – effect of UHPC compressive strength.

	Batch ID	f'_c, ksi	l_d, in.	l_s, in.	c_{so}, in.	c_{si}, in.	$f_{s,max}$, ksi	s_1, in.	$f_{s,crack}$, ksi	μ_{TEST}, psi
Set 1	M5-L4d-S2d-Sp4-1D-B5S2	13.9	2.6	1.6	1.2	1.5	43	0.033	NA	2640
	M5-L4d-S2d-Sp4-1D-B5S2	13.9	2.7	1.7	1.2	1.6	49	0.020	NA	2828
	M5-L4d-S2d-Sp4-7D-B1S1	19.9	2.4	1.4	1.2	1.5	67	0.036	NA	4449
	M5-L4d-S2d-Sp4-7D-B3S1	19.5	2.4	2.2	1.2	1.4	59	0.041	40	3781
	M5-L6d-S2d-Sp4-1D-B3S1	13.2	3.7	3.4	1.2	1.6	77	0.042	45	3269
	M5-L6d-S2d-Sp4-1D-B4S2	13.6	3.8	3.6	1.2	1.4	84	0.053	42	3430
	M5-L6d-S2d-Sp4-1D-B4S2	13.6	3.8	2.8	1.3	1.4	82	0.053	58	3363
	M5-L6d-S2d-Sp4-7D-B1S1	19.9	3.3	2.3	1.4	1.6	91	0.072	NA	4326
	M5-L6d-S2d-Sp4-7D-B3S1	19.5	3.8	3.5	1.2	1.6	91	0.068	52	3812
	M5-L6d-S2d-Sp4-7D-B3S1	19.5	3.8	2.8	1.2	1.5	90	0.052	58	3695
	M5-L6d-S2d-Sp4-7D-B4S2	19.2	3.9	2.9	1.1	1.4	83	0.047	65	3335
	M5-L8d-S2d-Sp4-1D-B3S1	13.2	5.0	4.0	1.2	1.4	96	0.065	58	2995
	M5-L8d-S2d-Sp4-1D-B6S3	13.9	4.6	3.6	1.2	1.5	108	0.057	68	3649
	M5-L8d-S2d-Sp4-1D-B8S4	13.8	4.9	3.9	1.1	1.5	106	0.050	NA	3346
	M5-L8d-S2d-Sp4-3D-B1S1	17.3	4.8	3.8	1.4	1.3	108	0.075	NA	3506
	M5-L8d-S2d-Sp4-3D-B9S4	16.6	5.2	4.2	1.3	1.4	111	0.066	NA	3330
	M5-L8d-S2d-Sp4-7D-B3S1	19.5	5.1	4.1	1.2	1.6	114	0.059	58	3515
	M5-L8d-S2d-Sp4-7D-B9S4	18.8	5.0	4.0	1.1	1.5	127	0.070	NA	3979
	M5-L10d-S2d-Sp4-1D-B6S3	13.9	6.3	5.3	1.2	1.5	144	0.082	77	3602
	M5-L10d-S2d-Sp4-1D-B9S4	13.7	6.3	5.3	1.2	1.5	132	0.076	65	3276
	M5-L10d-S2d-Sp4-7D-B3S1	19.5	6.2	5.2	1.2	1.5	145	0.091	74	3653
	M5-L10d-S2d-Sp4-7D-B9S4	18.8	6.1	5.1	1.1	1.6	154	0.100	NA	3935
	M5-L10d-S2d-Sp4-7D-B9S4	18.8	6.1	5.1	1.2	1.5	153	0.115	NA	3944

Table 9 (cont'd). Test specimens – effect of UHPC compressive strength.

	Batch ID	f'_c, ksi	l_d, in.	l_s, in.	c_{so}, in.	c_{si}, in.	$f_{s,max}$, ksi	s_1, in.	$f_{s,crack}$, ksi	μ_{TEST}, psi
Set 1	M5-L12d-S2d-Sp4-1D-B2S1	13.4	7.6	6.6	1.2	1.5	127	0.103	106	2603
	M5-L12d-S2d-Sp4-1D-B2S2	13.4	7.6	6.6	1.3	1.6	129	0.090	97	2645
	M5-L12d-S2d-Sp4-7D-B2S1	19.5	7.6	6.6	1.2	1.4	bar rupture (>160 ksi)	0.135	87	NA
	M5-L12d-S2d-Sp4-7D-B2S2	19.5	7.5	6.5	1.4	1.5	bar rupture (>160 ksi)	0.152	NA	NA
Set 2	M5-L6d-S3d-Sp4-1D-B10S4	13.9	3.4	2.4	1.8	1.5	85	0.037	NA	3863
	M5-L6d-S3d-Sp4-1D-B10S4	13.9	3.8	2.8	1.8	1.5	84	0.051	NA	3494
	M5-L6d-S3d-Sp4-7D-B10S4	19.6	3.9	2.9	1.8	1.7	118	0.058	NA	4673
	M5-L6d-S3d-Sp4-7D-B10S4	19.6	3.9	2.9	1.9	1.6	111	0.055	NA	4486
	M5-L6.7d-S3d-Sp4-1D-B10S4	13.9	4.2	3.2	1.9	1.6	103	0.045	NA	3800
	M5-L6.7d-S3d-Sp4-1D-B10S4	13.9	4.1	3.1	1.8	1.5	115	0.060	NA	4365
	M5-L6.7d-S3d-Sp4-7D-B10S4	19.6	4.3	3.3	1.9	1.6	130	0.061	NA	4775
	M5-L6.7d-S3d-Sp4-7D-B10S4	19.6	4.2	3.2	1.9	1.5	117	0.050	NA	4359
Set 3	M5-L6d-S3.5d-Sp4-1D-B4S2	13.6	3.9	3.6	2.2	1.6	96	0.043	NA	3884
	M5-L6d-S3.5d-Sp4-1D-B4S2	13.6	3.8	2.8	2.2	1.6	90	0.045	79	3707
	M5-L6d-S3.5d-Sp4-7D-B4S2	19.2	3.8	3.5	2.3	1.6	117	0.051	106	4876
	M5-L6d-S3.5d-Sp4-7D-B4S2	19.2	3.8	2.8	2.3	1.6	124	0.061	106	5148
	M5-L8d-S3.5d-Sp4-1D-B4S2	13.6	5.1	4.1	2.4	1.6	136	0.080	65	4208
	M5-L8d-S3.5d-Sp4-1D-B7S3	13.5	5.1	4.1	2.1	1.6	137	0.068	97	4168
	M5-L8d-S3.5d-Sp4-1D-B7S3	13.5	5.1	4.1	1.8	1.5	113	0.054	100	3477
	M5-L8d-S3.5d-Sp4-7D-B4S2	19.2	5.0	4.0	2.3	1.6	145	0.096	87	4521

Note: For explanation of the specimen ID and each parameter, see note for Table 4. 1 ksi = 6.895 MPa; 1 in. = 2.54 cm.

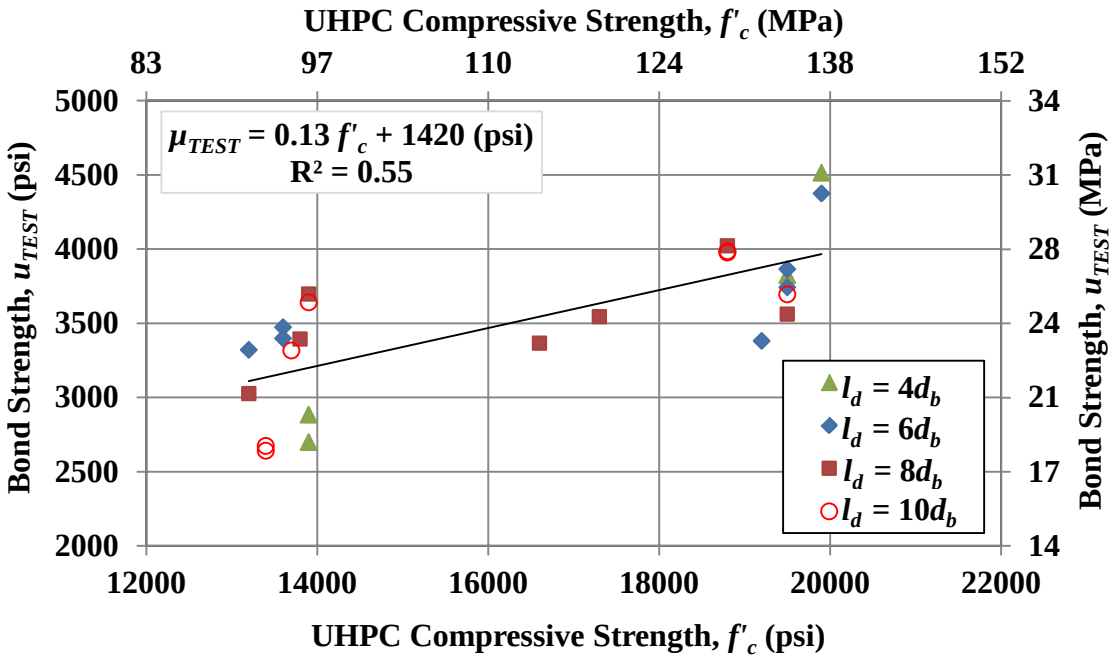

(a)

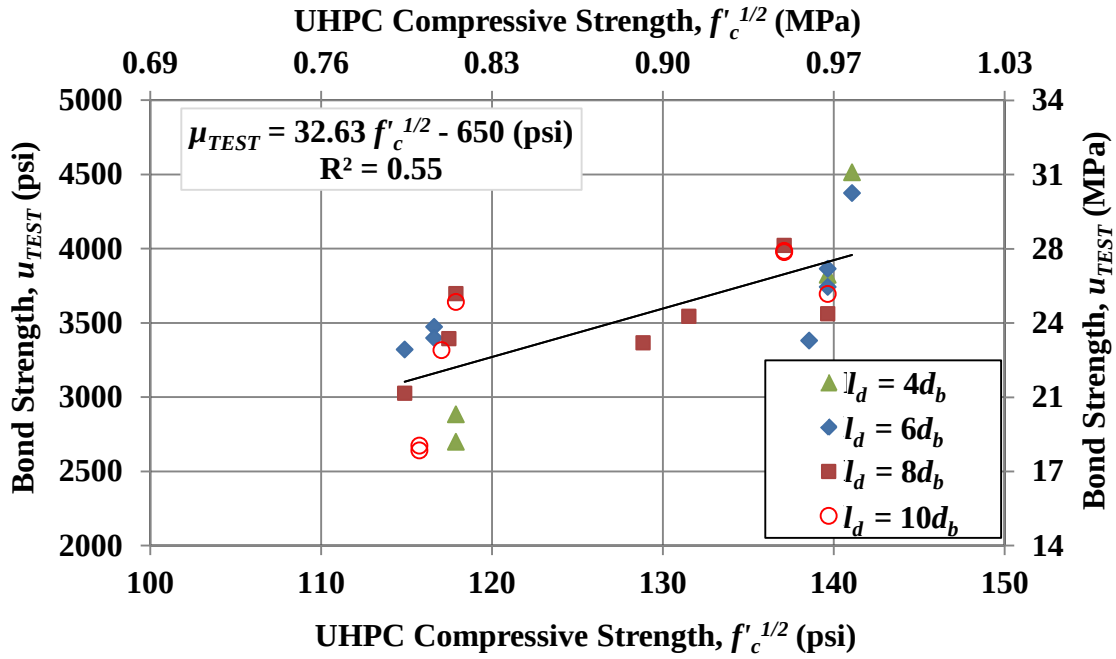

(b)

Figure 24. Graph. Effect of UHPC compressive strength: bond (a) u_{TEST} versus f'_c and (b) u_{TEST} versus $f'_c{}^{1/2}$ for specimens in Set 1.

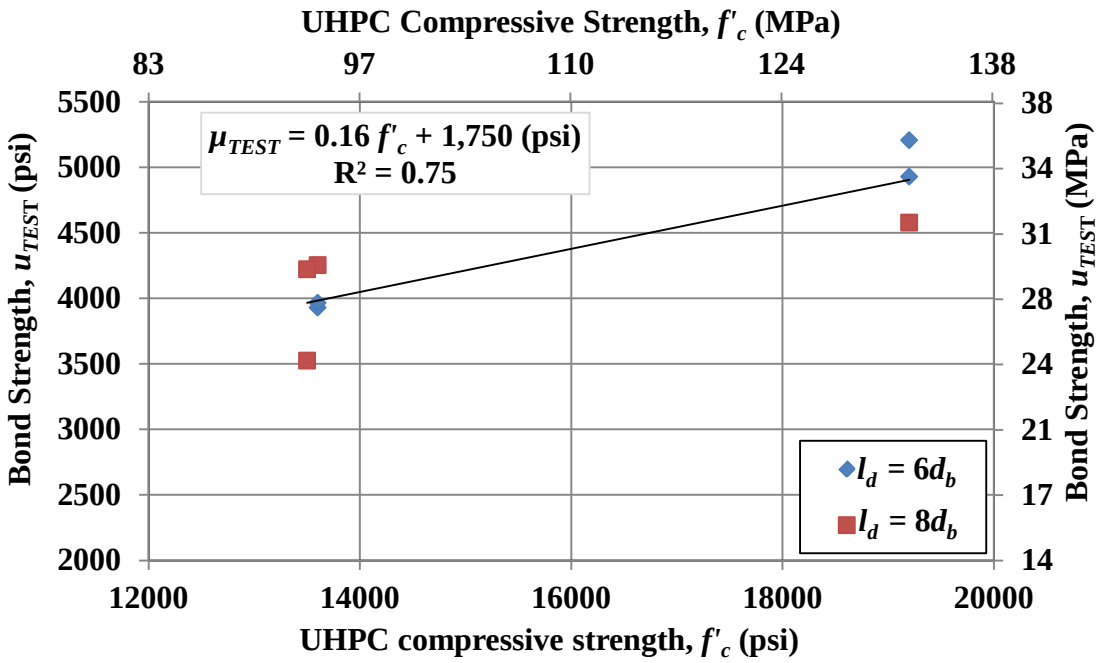

(a)

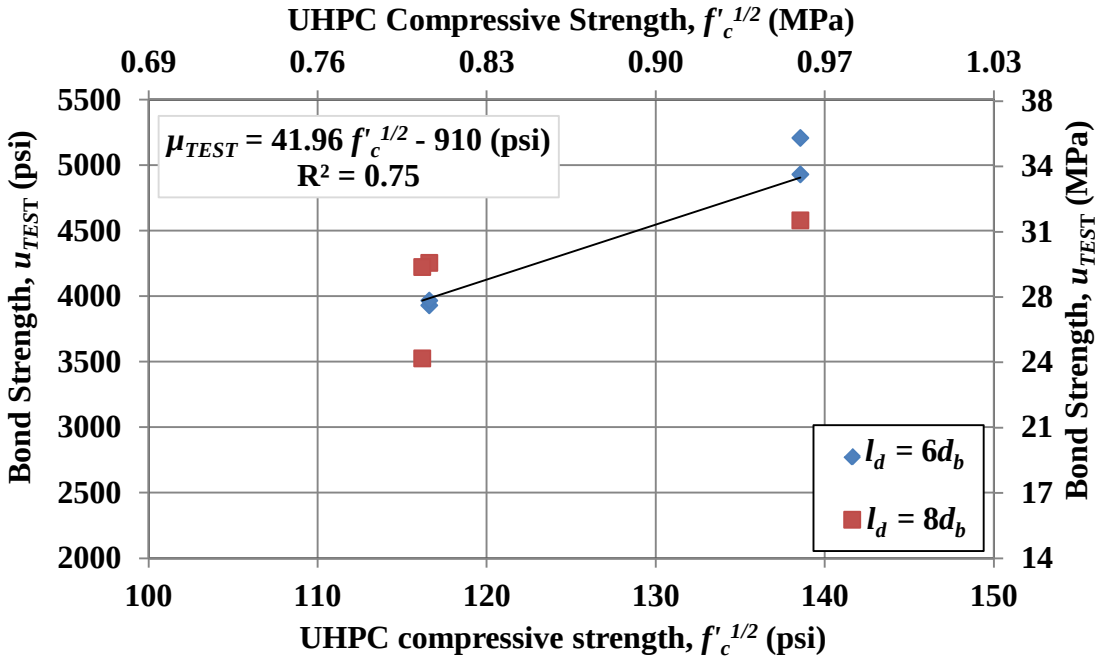

(b)

Figure 25. Graph. Effect of UHPC compressive strength: *(a)* u_{TEST} versus f'_c and (b) u_{TEST} versus $f'_c{}^{1/2}$ for specimens in Set 2.

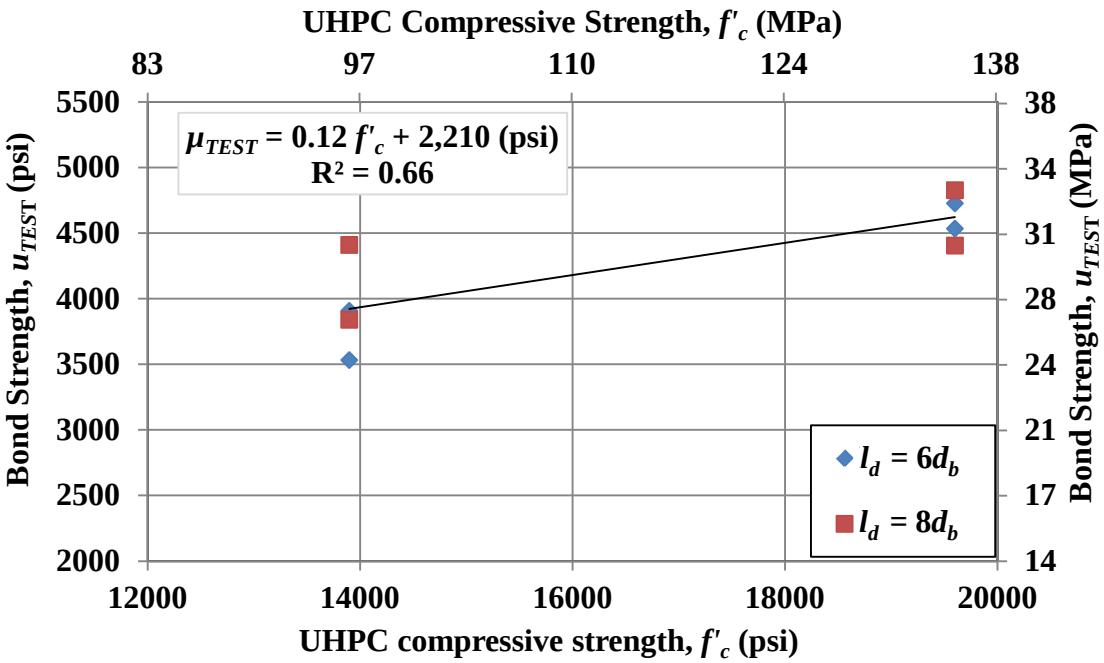

(a)

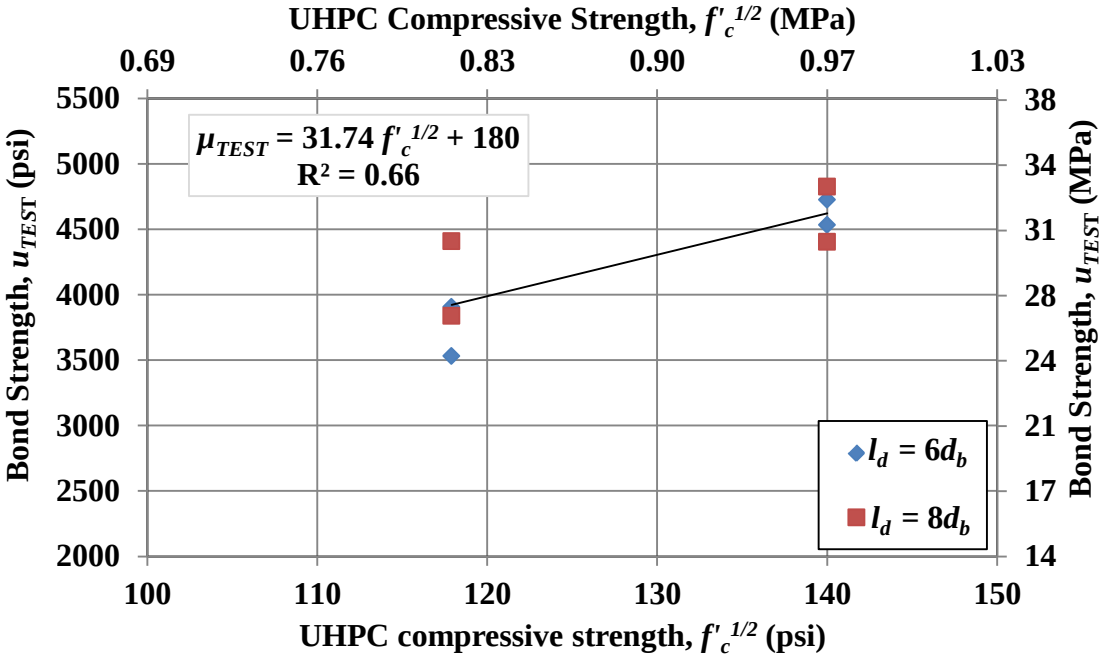

(b)

Figure 26. Graph. Effect of UHPC compressive strength: *(a)* u_{TEST} versus f'_c and (b) u_{TEST} versus $f'_c{}^{1/2}$ for specimens in Set 3.

Reinforcing Bar Size

The majority of the tests in the study were conducted with A1035 No. 5 bar to serve as the baseline. In this section, the effect of bar size on bond strength is evaluated. Tests on A1035 No. 4, No. 5 and No. 7 bar were used in this analysis.

With the consideration that the design (development length, concrete cover, and bar spacing) is often defined in terms of bar diameter (d_b) in design codes, the embedment length and confinement used for different size bar will also be based on individual bar diameter in this section. For example, No. 4 bar with $2d_b$ side cover, which is 1 in. (2.5 cm), will be compared with the No. 5 bar with $2d_b$ side cover, which is 1.25 in. (3.2 cm), and they are considered to have the same side cover. Also as discussed previously, specimens with the bar spacing between $2d_b$ and $l_s tan(\theta)$ are recognized as demonstrating similar performance. All specimens in this section had bar spacing in this range and the effect of bar spacing is assumed to be minimal and will be neglected in this analysis.

A total of 27 tests were included in this section, divided into two sets as shown in Table 10. Set 1 included specimens with No. 5 and No. 4 bars and Set 2 included specimens with No. 5 and No. 7 bars. Specimens in each set had the same design for side cover and had varied embedment lengths. Specimens in each set can be either directly compared among those with the same design of embedment length or compared as a whole by comparing the bond strength u_{TEST}, which included the embedment length in the calculation. All specimens were tested at one day after UHPC casting to ensure a similar compressive strength.

A direct comparison between the specimens with the same design reveals that, in general, higher bar stress was developed for smaller bars at bond failure. For example, for the specimen with No. 4 bar embedded $8d_b$ (specimen ID M4-L8d-S3.5d-Sp4-1D-B9S3) in Set 1, the bar stress at bond failure was 147 ksi (1014 MPa), higher than the 136 and 137 ksi (938 and 945 MPa) for the two specimens with No. 5 bars (specimen ID M5-L8d-S3.5d-Sp4-1D-B4S2 and M5-L8d-S3.5d-Sp4-1D-B7S3). Similarly, for the five specimens with No.7 bars embedded $8d_b$ in Set 2, the bar stress at bond failure ranged from 81 to 109 ksi (558 to 752 MPa) with an average of 99 ksi (686 MPa), compared with 96 to 121 ksi (662 to 834 MPa) with an average of 107 ksi (741 MPa) for the corresponding specimens with No. 5 bars.

Table 10. Test specimens – effect of bar size.

	Batch ID	f'_c, ksi	l_d, in.	l_s, in.	c_{so}, in.	c_{si}, in.	$f_{s,max}$, ksi	s_1, in.	$f_{s,crack}$, ksi	μ_{TEST}, psi
Set 1	M4-L8d-S3.5d-Sp4-1D-B9S3	13.7	4.1	3.1	1.7	1.5	147	0.073	NA	4460
	M5-L8d-S3.5d-Sp4-1D-B4S2	**13.6**	**5.1**	**4.1**	**2.4**	**1.6**	**136**	**0.080**	**65**	**4208**
	M5-L8d-S3.5d-Sp4-1D-B7S3	**13.5**	**5.1**	**4.1**	**2.1**	**1.6**	**137**	**0.068**	**97**	**4168**
	M4-L6d-S3.5d-Sp4-1D-B12S5	11.9	3.1	2.1	1.7	1.6	106	0.041	NA	4243
	M4-L6d-S3.5d-Sp4-1D-B12S5	11.9	3.1	2.1	1.6	1.4	97	0.038	NA	3867
	M5-L6d-S3.5d-Sp4-1D-B4S2	**13.6**	**3.9**	**2.9**	**2.2**	**1.6**	**96**	**0.043**	**NA**	**3884**
	M5-L6d-S3.5d-Sp4-1D-B4S2	**13.6**	**3.8**	**2.8**	**2.2**	**1.6**	**90**	**0.045**	**79**	**3707**
	M4-L10d-S3.5d-Sp4-1D-B9S3	13.7	5.2	4.2	1.7	1.6	156	0.105	NA	3757
	M4-L10d-S3.5d-Sp4-1D-B9S3	13.7	5.2	4.2	1.7	1.6	165	0.144	NA	3978
	M5-L10d-S3.5d-Sp4-1D-B4S2	**13.6**	**6.3**	**5.3**	**2.2**	**1.6**	**155**	**0.108**	**90**	**3843**
	M5-L10d-S3.5d-Sp4-1D-B4S2	**13.6**	**6.3**	**5.3**	**2.2**	**1.6**	**166**	**0.161**	**68**	**4116**
	M5-L10d-S3.5d-Sp4-1D-B4S2	**13.6**	**6.3**	**5.3**	**2.3**	**1.6**	**158**	**0.099**	**125**	**3911**
Set 2	M7-L8d-S2d-Sp2-1D-B12S5	11.9	6.9	5.9	2.0	0.6	109	0.058	NA	3462
	M7-L8d-S2d-Sp6-1D-B12S5	11.9	6.8	5.8	1.9	2.4	81	0.068	NA	2609
	M7-L8d-S2d-Sp6-1D-B12S5	11.9	7.0	6.0	1.9	2.1	122	0.111	NA	3824
	M7-L8d-S2d-Sp6-1D-B12S5	11.9	7.0	6.0	1.9	2.5	92	0.080	NA	2875
	M7-L8d-S2d-Sp4-1D-B8S3	13.8	7.2	6.2	1.7	1.5	93	0.036	NA	2823
	M5-L8d-S2d-Sp4-1D-B3S1	**13.2**	**5.0**	**4.0**	**1.2**	**1.4**	**96**	**0.065**	**58**	**2995**
	M5-L8d-S2d-Sp4-1D-B6S3	**13.9**	**4.6**	**3.6**	**1.2**	**1.5**	**108**	**0.057**	**68**	**3649**
	M5-L8d-S2d-Sp4-1D-B8S4	**13.8**	**4.9**	**3.9**	**1.1**	**1.5**	**106**	**0.050**	**NA**	**3346**
	M5-L8d-S2d-Sp4-1D-B9S4	**13.7**	**5.3**	**4.3**	**1.2**	**1.4**	**121**	**0.065**	**77**	**3595**
	M7-L6d-S2d-Sp4-1D-B8S3	13.8	5.3	4.3	1.6	1.3	60	0.021	NA	2510
	M7-L6d-S2d-Sp4-1D-B8S3	13.8	5.0	4.0	1.6	1.4	61	0.042	NA	2657
	M5-L6d-S2d-Sp4-1D-B3S1	**13.2**	**3.7**	**3.4**	**1.2**	**1.6**	**77**	**0.042**	**45**	**3269**
	M5-L6d-S2d-Sp4-1D-B3S1	**13.2**	**3.8**	**2.8**	**1.3**	**1.6**	**70**	**0.058**	**55**	**2876**
	M5-L6d-S2d-Sp4-1D-B4S2	**13.6**	**3.8**	**3.6**	**1.2**	**1.4**	**84**	**0.053**	**42**	**3430**
	M5-L6d-S2d-Sp4-1D-B4S2	**13.6**	**3.8**	**2.8**	**1.3**	**1.4**	**82**	**0.053**	**58**	**3363**

Note: For explanation of the specimen ID and each parameter, see note for Table 4. 1 ksi = 6.895 MPa; 1 in. = 2.54 cm.

The bond stress at bond failure was also calculated for each specimen and is presented in Table 10. The average bond stress for all No. 4 and No. 5 bars in Set 1 and for all No. 7 and No. 5 bars in Set 2 were compared in Figure 27. In addition to the average values of bond strength, the figure also shows the maximum and minimum values for the included specimens and the number of tests conducted. As shown in Figure 27, No. 4 bars had slightly higher average bond strength than the No. 5 bars in Set 1, and No. 5 bars had higher average bond strength than the No. 7 bars in Set 2. Note that all the comparisons are made between specimens with a similar design which is based on the individual bar diameter. With these conditions, the tests results indicated that for bars with larger diameter, the bond strength decreased and a longer embedment length should considered.

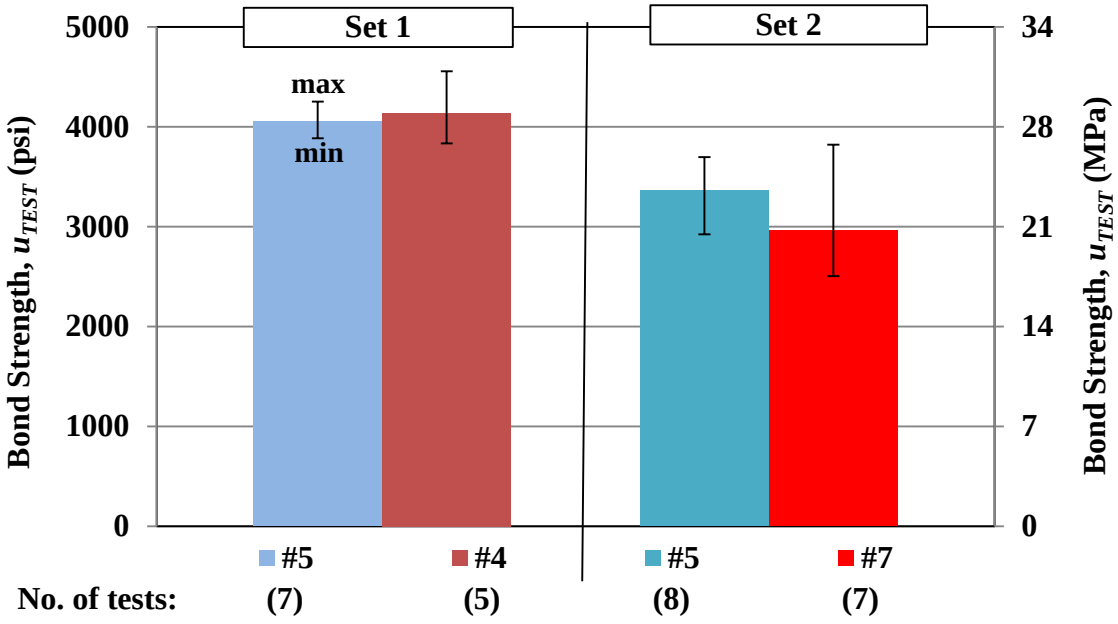

Figure 27. Chart. Bond strength versus bar size.

Reinforcing Bar Type and Yielding Strength

As demonstrated in previous sections, a reinforcing bar embedded only $6d_b$ in UHPC (with appropriate cover) can achieve a bar stress over 70 ksi (483 MPa) before bond failure. To minimize the effect of reinforcing bar yielding on bond strength when other factors were evaluated, the majority of the tests in the study were conducted using A1035 Grade 120 bar. The effect of bar type and the effect of bar yielding prior to bond failure are evaluated in this section.

A total of 46 tests are included in this section and the tests were grouped into six sets based on embedment length as shown in Table 11. Each set had three types of reinforcing bar, uncoated, epoxy coated, and A1035, except for Set 6 having only uncoated and A1035 bar. The six sets are presented in an order from low bond strength to high bond strength. In each set, the bond strength of different types of bar can be compared directly with the fact they had the same

design. The reinforcing bar properties, including yield and tensile strengths and relative rib area, can be found in Table 2 and the rib pattern can be found in Figure 2. As the relative rib area is one of the main factors when looking at different types reinforcing bar, it should be noted that the No.5 uncoated, epoxy coated, and A1035 bar used in this study had similar relative rib areas, with values of 0.085, 0.083 and 0.088, respectively.

The average bar stress at bond failure for each type of bar in each set is presented in Figure 28. The maximum and minimum values for included specimens in each group are also presented. As shown in Figure 28, for specimens with ultimate bar stress at bond failure below or close to the yield strength of the uncoated bar (Sets 1 and 2), the A1035 and uncoated bar had similar bond strength. When the bar stress at bond failure was greater than the yield strength of the uncoated bar, the A1035 bar had higher ultimate bar stress than the corresponding uncoated bar. In all cases, the epoxy coated bar had lower ultimate bar stress than the corresponding uncoated and A1035 bar. It is reasonable to predict the bond performance of the Grade 60 uncoated bar based on the tests of A1035 bar, up to at least the yield strength of the Grade 60 uncoated bar; beyond the yield, it is important to realize the fact that bars that yielded before bond failures produced average bond stress lower than A1035 bars in similar test specimens. The epoxy coated bar had lower bond strength than uncoated bar.

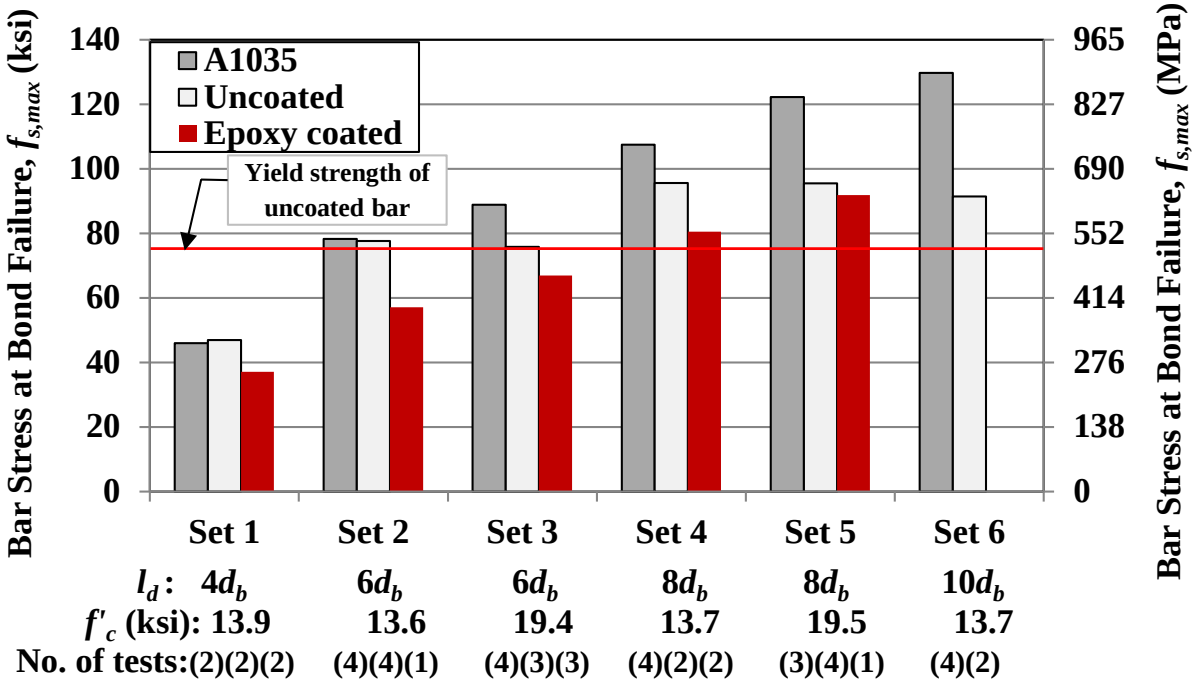

Figure 28. Chart. Average bar stress at bond failure for different types of reinforcing bar.

Table 11. Test specimens – effect of bar type.

	Batch ID	f'_c, ksi	l_d, in.	l_s, in.	c_{so}, in.	c_{si}, in.	$f_{s,max}$, ksi	s_1, in.	$f_{s,crack}$, ksi	μ_{TEST}, psi
Set 1	**B5-L4d-S2d-Sp4-1D-B5S2**	**13.9**	**2.6**	**1.6**	**1.1**	**1.6**	**46**	**0.032**	**NA**	**2719**
	B5-L4d-S2d-Sp4-1D-B5S2	**13.9**	**2.5**	**1.5**	**1.2**	**1.5**	**48**	**0.033**	**NA**	**3014**
	E5-L4d-S2d-Sp4-1D-B5S2	13.9	2.6	1.6	1.0	1.5	38	0.051	NA	2233
	E5-L4d-S2d-Sp4-1D-B5S2	13.9	2.6	1.6	1.2	1.5	37	0.045	NA	2177
	M5-L4d-S2d-Sp4-1D-B5S2	13.9	2.6	1.6	1.2	1.5	43	0.033	NA	2640
	M5-L4d-S2d-Sp4-1D-B5S2	13.9	2.7	1.7	1.2	1.6	49	0.020	NA	2828
Set 2	**B5-L6d-S2d-Sp4-1D-B2S1**	**13.4**	**3.8**	**2.8**	**1.1**	**1.5**	**82**	**0.091**	**NA**	**3368**
	B5-L6d-S2d-Sp4-1D-B4S2	**13.6**	**3.8**	**2.8**	**1.3**	**1.4**	**76**	**0.087**	**44**	**3156**
	B5-L6d-S2d-Sp4-1D-B6S3	**13.9**	**3.4**	**2.4**	**1.2**	**1.3**	**70**	**0.055**	**65**	**3222**
	B5-L6d-S2d-Sp4-1D-B6S3	**13.9**	**3.8**	**2.8**	**1.1**	**1.4**	**83**	**0.090**	**55**	**3393**
	E5-L6d-S2d-Sp4-1D-B4S2	13.6	3.8	2.8	1.2	1.4	57	0.055	42	2378
	M5-L6d-S2d-Sp4-1D-B3S1	13.2	3.7	3.4	1.2	1.6	77	0.042	45	3269
	M5-L6d-S2d-Sp4-1D-B3S1	13.2	3.8	2.8	1.3	1.6	70	0.058	55	2876
	M5-L6d-S2d-Sp4-1D-B4S2	13.6	3.8	3.6	1.2	1.4	84	0.053	42	3430
	M5-L6d-S2d-Sp4-1D-B4S2	13.6	3.8	2.8	1.3	1.4	82	0.053	58	3363
Set 3	**B5-L6d-S2d-Sp4-7D-B2S2**	**19.5**	**3.9**	**2.9**	**1.3**	**1.6**	**73**	**0.067**	**65**	**2901**
	B5-L6d-S2d-Sp4-7D-B4S2	**19.2**	**3.8**	**2.8**	**1.3**	**1.4**	**81**	**0.101**	**47**	**3337**
	B5-L6d-S2d-Sp4-7D-B5S2	**18.9**	**3.8**	**2.8**	**1.2**	**1.5**	**73**	**0.066**	**52**	**3037**
	E5-L6d-S2d-Sp4-7D-B1S1	19.9	3.6	2.6	1.3	1.5	71	0.059	NA	3112
	E5-L6d-S2d-Sp4-7D-B4S2	19.2	3.8	2.8	1.3	1.4	64	0.031	NA	2651
	E5-L6d-S2d-Sp4-7D-B5S2	18.9	3.8	2.8	1.1	1.6	66	0.063	58	2742
	M5-L6d-S2d-Sp4-7D-B1S1	19.9	3.3	2.3	1.4	1.6	91	0.072	NA	4326
	M5-L6d-S2d-Sp4-7D-B3S1	19.5	3.8	3.5	1.2	1.6	91	0.068	52	3812
	M5-L6d-S2d-Sp4-7D-B3S1	19.5	3.8	2.8	1.2	1.5	90	0.052	58	3695
	M5-L6d-S2d-Sp4-7D-B4S2	19.2	3.9	2.9	1.1	1.4	83	0.047	65	3335

Table 11 (cont'd). Test specimens – effect of bar type.

	Batch ID	f'_c, ksi	l_d, in.	l_s, in.	c_{so}, in.	c_{si}, in.	$f_{s,max}$, ksi	s_1, in.	$f_{s,crack}$, ksi	μ_{TEST}, psi
Set 4	**B5-L8d-S2d-Sp4-1D-B2S1**	**13.4**	**5.3**	**4.3**	**1.2**	**1.5**	**96**	**0.205**	**77**	**2857**
	B5-L8d-S2d-Sp4-1D-B2S2	**13.4**	**5.1**	**4.1**	**1.4**	**1.5**	**95**	**0.215**	**NA**	**2936**
	E5-L8d-S2d-Sp4-1D-B6S3	13.9	4.7	3.7	1.2	1.4	78	0.090	58	2612
	E5-L8d-S2d-Sp4-1D-B6S3	13.9	5.1	4.1	1.2	1.3	83	0.106	55	2553
	M5-L8d-S2d-Sp4-1D-B3S1	13.2	5.0	4.0	1.2	1.4	96	0.065	58	2995
	M5-L8d-S2d-Sp4-1D-B6S3	13.9	4.6	3.6	1.2	1.5	108	0.057	68	3649
	M5-L8d-S2d-Sp4-1D-B8S4	13.8	4.9	3.9	1.1	1.5	106	0.050	NA	3346
	M5-L8d-S2d-Sp4-1D-B9S4	13.7	5.3	4.3	1.2	1.4	121	0.065	77	3595
Set 5	**B5-L8d-S2d-Sp4-7D-B2S1**	**19.5**	**5.1**	**4.1**	**1.1**	**1.5**	**94**	**0.162**	**68**	**2913**
	B5-L8d-S2d-Sp4-7D-B2S1	**19.5**	**5.1**	**4.1**	**1.1**	**1.5**	**95**	**0.078**	**NA**	**2922**
	B5-L8d-S2d-Sp4-7D-B2S2	**19.5**	**5.1**	**4.1**	**1.4**	**1.6**	**96**	**0.184**	**65**	**2933**
	B5-L8d-S2d-Sp4-7D-B2S2	**19.5**	**5.1**	**4.1**	**1.4**	**1.6**	**97**	**0.075**	**NA**	**2947**
	E5-L8d-S2d-Sp4-7D-B1S1	19.9	4.9	3.9	1.5	1.6	92	0.167	NA	2935
	M5-L8d-S2d-Sp4-7D-B1S1	19.9	4.8	3.8	1.1	1.4	125	0.087	NA	4069
	M5-L8d-S2d-Sp4-7D-B3S1	19.5	5.1	4.1	1.2	1.6	114	0.059	58	3515
	M5-L8d-S2d-Sp4-7D-B9S4	18.8	5.0	4.0	1.1	1.5	127	0.070	NA	3979
Set 6	**B5-L10d-S2d-Sp4-1D-B2S1**	**13.4**	**6.3**	**5.3**	**1.2**	**1.6**	**94**	**0.128**	**71**	**2335**
	B5-L10d-S2d-Sp4-1D-B2S2	**13.4**	**6.3**	**5.3**	**1.4**	**1.5**	**88**	**0.167**	**NA**	**2189**
	M5-L10d-S2d-Sp4-1D-B6S3	13.9	6.3	5.3	1.2	1.5	144	0.082	77	3602
	M5-L10d-S2d-Sp4-1D-B6S3	13.9	6.4	5.4	1.2	1.4	113	0.075	61	2760
	M5-L10d-S2d-Sp4-1D-B9S4	13.7	6.3	5.3	1.2	1.5	132	0.076	65	3276

Note: For explanation of the specimen ID and each parameter, see note for Table 4. 1 ksi = 6.895 MPa; 1 in. = 2.54 cm

The average bond stress μ_{TEST} for each type of reinforcing bar in each set is calculated and presented in Table 12, as well as the bond stress reduction between different reinforcing bar. As shown in Table 12, the uncoated bars in Sets 1 and 2 had about the same bond stress as A1035 bars, with a slight difference of 4.9% and 1.6%, respectively; when the maximum bar stress at bond failure exceeded the yield strength of the uncoated bar, as those in Sets 3, 4, 5, and 6, the A1035 bars had much higher ultimate bond stress than that of uncoated bars, ranging from 14.7% to 29.6% with an average of 21.7% higher. Another noted trend is that the reduction on bond strength due to the yielding of uncoated bar is amplified as the ultimate bar stress at bond failure increases. The reduction on bond stress were 18.5%, 14.7%, 24.0%, and 29.6% following the order of Sets 3, 4, 5, and 6, which are grouped in the order of increasing ultimate bar stress at bond failure.

The bond stress reduction of epoxy coated bar compared with uncoated bar is also presented in Table 12. The reductions were 23.1% and 27.6% in Sets 1 and 2 where the ultimate bar stress at bond failure is below or close to yield strength of the uncoated bar. The difference seemed to be minimized when there is a sufficient embedment length that the bar yielded before bond failure, with 8.3% and 10.8% reduction in Sets 3 and 4 and almost no reductions in Set 5.

Table 12. Bond stress reduction between different types of reinforcing bar.

	Average μ_{TEST}, psi			Reduction, %	
	A1035	**Uncoated**	**Epoxy**	**(A1035-Uncoated)/A1035**	**(Uncoated-Epoxy)/Uncoated**
Set 1	2734	2867	2205	-4.9	23.1
Set 2	3235	3285	2378	-1.6	27.6
Set 3	3792	3092	2835	18.5	8.3
Set 4	3396	2896	2583	14.7	10.8
Set 5	3854	2929	2935	24.0	-0.2
Set 6	3213	2262	-	29.6	-

CHAPTER 4. DESIGN RECOMMENDATIONS FOR REINFORCING BAR EMBEDDED IN UHPC

One of the main goals of the research is to develop design details for reinforcing bar embedded in UHPC, which would provide guidance for engineers using reinforced UHPC in innovative applications. In this report, the focus has been on a widely available UHPC product containing 2% steel fiber (by volume). Reinforcing bar sizes ranging from No. 4 to No. 8 and bar type including A615 Grade 60 uncoated and epoxy coated bar and A1035 Grade 120 bar were included in the study.

One design detail that would reach at least the lesser of the bar yield stress or 75 ksi (517 MPa) at bond failure for different bar type and size tested in this study is first presented. Other design details that would also attain a similar stress level are then presented. Finally, details relevant to an alternative design concept wherein the bar stress reaches a significantly higher stress level alongside an ensured ductility prior to bond failure is presented.

MINIMUM BAR STRESS OF LESSER OF YIELD OR 75 ksi (517 MPa)

The fundamental design concept embedded into the reinforcing steel development and splice length provisions of the AASHTO LRFD Bridge Design Specification and the ACI 318 Building Code is to allow for the attainment of the yield strength of the mild steel reinforcement. The research studies on which these provisions are based were primarily conducted on structural components wherein the stress in the reinforcement at failure was below the yield stress of the bar. These results allowed for extrapolation of the observed bar stress at failure up to the yield strength of the bar. Aside from special provisions that ensure ductility by limiting the locations of splices or anchorages, these design specifications do not specifically ensure ductility of spliced or embedded reinforcing bars beyond the initial yielding of the bar.

Given this construct, the results obtained in this study were analyzed so as to create design guidance that parallels the existing provisions in these design specifications. Specifically, test results were analyzed to ensure that the bar could attain the lesser of its yield stress or 75 ksi (517 MPa).

As mentioned earlier in the report, there were specimens that were intentionally excluded from previously discussed analyses, including those end specimens close to the casting point and those specimens that failed with UHPC tensile failures. In this present section wherein design guidance is developed, all test specimens were included in the analysis.

First, the bar stress at bond failure is plotted versus embedment length in Figure 29 for all the A1035 No. 5 bars tested in study, with those end specimens close to casting point and those with UHPC tensile failures included. The specimens had a variety of side cover and bar spacing. For the side cover, values of $2d_b$, $2.7d_b$, $3d_b$,and $3.5d_b$ were included; for the bar spacing to the nearest No. 8 bars, values of 0, 2, 4, 6, 8, and 12 in. (0, 5.1, 10.2, 15.2, 20.3 and 30.5 cm) were used. The specimens were grouped into two base categories, one with side over equal to $2d_b$ and the other one with side

cover greater than or equal to 2.7d_b, as shown in Figure 29. Then, the specimens with those specific conditions, including the zero bar spacing, bar spacing greater than $l_s tan(\theta)$, end specimens close to casting point, and specimens with UHPC tensile failures were marked on top of the base categories, as explained in the note of Figure 29. For those without any mark on top, they all had bar spacing between 2d_b and $l_s tan(\theta)$. It is also important to note that all the tests included were conducted at one day after casting with a UHPC compressive strength of approximately 13.5 ksi (93.1 MPa).

As shown in Figure 29, in general, the bar stress at bond failure increases as the embedment length increases. The large majority of the specimens had a bar stress at bond failure over 80 ksi (552 MPa); the ones with bar stress at bond failure below 80 ksi (552 MPa) were those with a side cover of 2d_b, combined with either a short embedment length of 4d_b and 6d_b or disadvantageous spacing (bar spacing = 0 or bar spacing > $l_s tan(\theta)$). It is also important to note that for the specimens with a side cover of 2d_b, combined with sufficient embedment length (≥8d_b) and appropriate bar spacing (between 2d_b and $l_s tan(\theta)$ in this study), they all have reached a bar stress of at least 80 ksi (552 MPa).

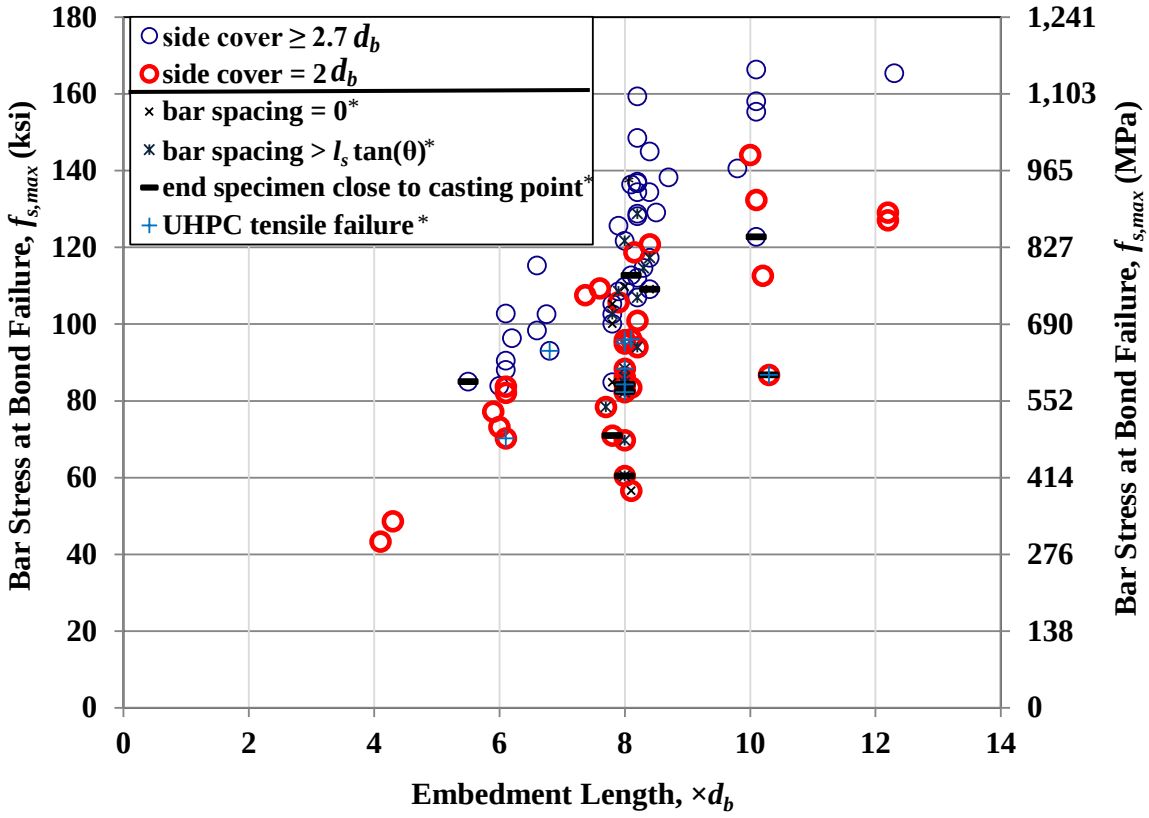

Note: * Specimens were grouped into two base categories based in side cover, one with side cover equal to 2d_b and the other one with side cover greater than or equal to 2.7d_b. The specimens with specific conditions, including bar spacing equal to zero, bar spacing greater than $l_s tan(\theta)$, end specimens close to casting point, and specimens with UHPC tensile failures were marked on top of that. For example, ⊖ refers to a specimen with side cover of 2d_b and with a specific condition of end specimen close to the casting point; ⊗ refers to a specimen with side cover ≥ 2.7d_b, and with specific conditions of zero bar spacing to nearest bar and end specimen close to the casting point. For those without any mark on top, they had bar spacing between 2d_b and $l_s tan(\theta)$.

Figure 29. Graph. Bar stress at bond failure versus embedment length for all tests with A1035 No. 5 bars.

Based on Figure 29, the plot of bar stress at bond failure versus embedment length is modified by excluding the specimens with a side cover of $2d_b$, and the results are shown in Figure 30. As shown in Figure 30, all specimens exhibited a bar stress higher than 80 ksi (552 MPa), with the specimens with bar spacing equal to zero or greater than $l_s tan(\theta)$ and/or end specimens close to casting point generally exhibiting lesser bar stresses at bond failure. It should be noted that there is only one specimen that failed with UHPC tensile failure in this group while the majority of the specimens failed with UHPC tensile failure were those with a side cover only $2d_b$, as shown in Figure 29. The specimens with an embedment length of $8d_b$ and a side cover of $3d_b$ are identified in Figure 30 with a red diamond; all of them have reached a bar stress over 100 ksi (690 MPa) at bond failure; those with appropriate bar spacing [between $2d_b$ and $l_s tan(\theta)$] reached a bar stress over 120 ksi (827 MPa).

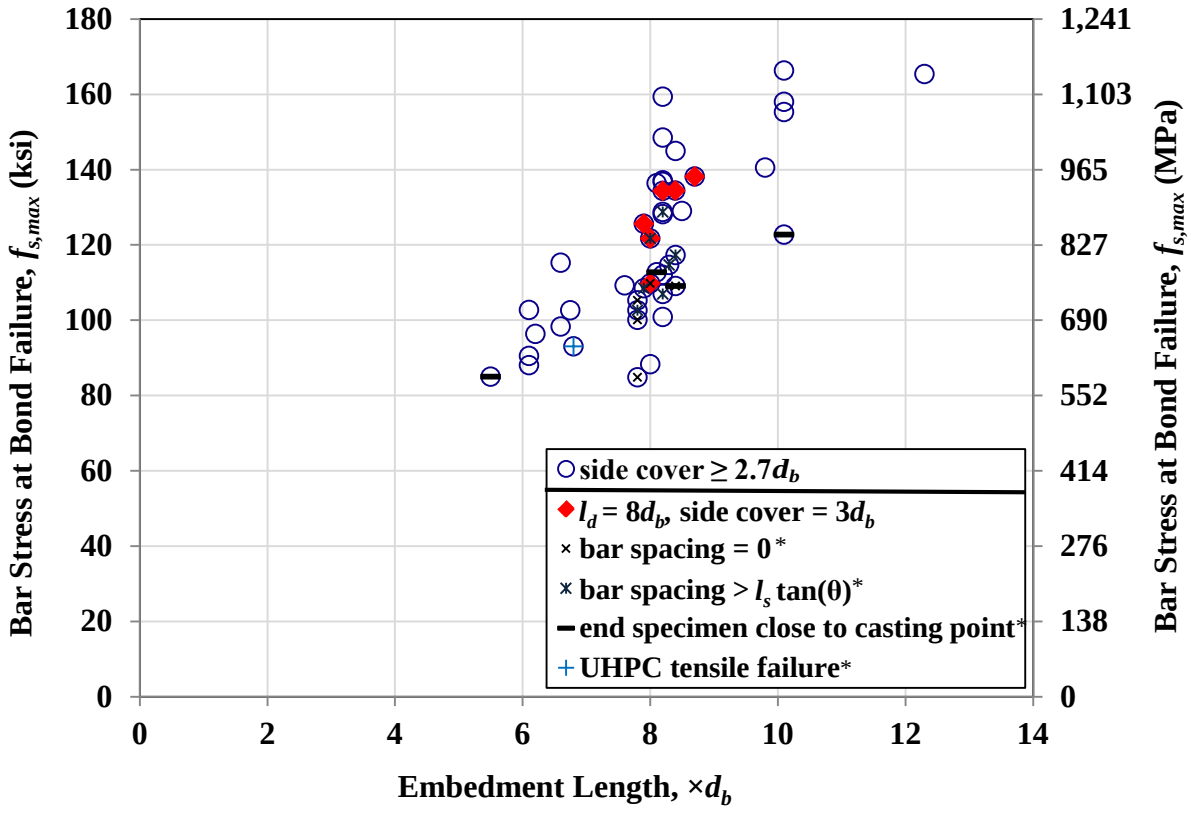

*** refer to the note for Figure 29.**

Figure 30. Graph. Bar stress at bond failure versus embedment length for all tests with A1035 No. 5 bars and with a side cover ≥ 2.7d_b.

Based on Figure 29 and Figure 30, a design detail that will allow for the attainment of the lesser of the bar yield strength or 75 ksi (517 MPa) before bond failure in this UHPC material for all the bar types and bar sizes tested in this study is developed and verified in the following. A review of some of the findings presented in previous sections is necessary here. As discussed earlier, for bars with larger diameter, the bond strength decreased and a longer embedment length should be used. Uncoated bar that yielded before bond failure tends to have lower ultimate bond

strength than corresponding high strength reinforcing bar that does not yield. Epoxy coated reinforcing bar, in general, has less bond strength than uncoated bar. Given these considerations, the design with a minimum embedment length of $8d_b$, minimum side cover of $3d_b$, bar spacing between $2d_b$ and $l_s tan(\theta)$, and minimum UHPC compressive strength of 13.5 ksi (93 MPa) is recommended. The crack angle θ for the bar tested in this study is about 55 degrees. In general, the angle of inclination can vary from 45° to 80° and depends on whether the reinforcing bar ribs are lateral, diagonal, or wavy with respect to the axis of the bar.[27] To simplify the design and also to be conservative, the angle of 45° is used and the bar spacing is then recommended to be between $2d_b$ and l_s. For all the A1035 No.5 bars tested in this study, when the recommended design condition were met, they all had a bar stress at bond failure over 120 ksi (827 MPa), as shown in Figure 30. For different type and size bars, it will be discussed in the following.

For situations where the above design recommendation is problematic, alternate recommendations can be developed. Addressing the effect of bar type first, the previous analysis has indicated that the yielding of reinforcing bar would reduce the ultimate bar stress at bond failure as compared to a similar bar with a higher yield strength. The research also indicated that the performance of A1035 can be used to well predict the performance of normal strength uncoated bar up to at least the yield strength of the uncoated bar. It would be conservative to predict that the uncoated bar would yield if the corresponding A1035 high strength reinforcing bar reached an ultimate bar stress well over the yield strength of the uncoated bar. For epoxy coated bar, the research indicated minimal reduction compared with uncoated bar when there was a sufficient embedment length that the bar yielded before bond failure. In fact, there were two epoxy coated bar specimens with an embedment length of $8d_b$ and side cover of only $2d_b$ in this study (Table 11 Set 4), and they had bar stress at bond failure of 78 and 83 ksi (538 and 572 MPa), which is above the yield strength; if the side cover was increased to $3d_b$ as recommended, a higher bar stress at bond failure would be expected.

The analysis in previous sections indicated that larger size bar tends to have lower bar stress at bond failure compared with smaller bars with the same design in terms of individual bar diameter. However, the reduction is minimal. To verify the selected design having sufficient bond strength for larger bars, the tests with A1035 No.7 bar and epoxy coated No. 8 bar were examined and the results are presented in Figure 31. Most of the tests were conducted using A1035 No.7 bar, with a side cover of either $2d_b$ or $2.35d_b$, corresponding to a UHPC strip width of 4-3/8 and 5 in. (11.1 and 12.7 cm), respectively. One specimen with epoxy coated No.8 bar was tested as the possible weakest case in this study. As shown in Figure 31, for the A1035 No.7 bar with a $6d_b$ embedment length, the bar stress at bond failure was only about 60 ksi (414 MPa) for specimens with $2d_b$ side cover; it increased to about 77 ksi (531 MPa) when the side cover was increased to $2.35d_b$. With a $8d_b$ embedment length and $2d_b$ side cover, all A1035 No.7 bars have reached a bar stress of 80 ksi (552 MPa) or more, except for the two end specimens close to the casting point having bar stress of 68 and 76 ksi (469 and 524 MPa). For the specimen cast with No. 8 epoxy coated bar, it had an embedment length of $8d_b$ and a side cover of $2d_b$, and it reached a bar stress of 91 ksi (627 MPa) at bond failure. Therefore, for larger bars, up to No. 8 in this study, it would be

conservative to expect bar stress at bond failure to be at least the lesser of 75 ksi (517 MPa) or the bar yield strength with an embedment length of $8d_b$ and side cover of $3d_b$.

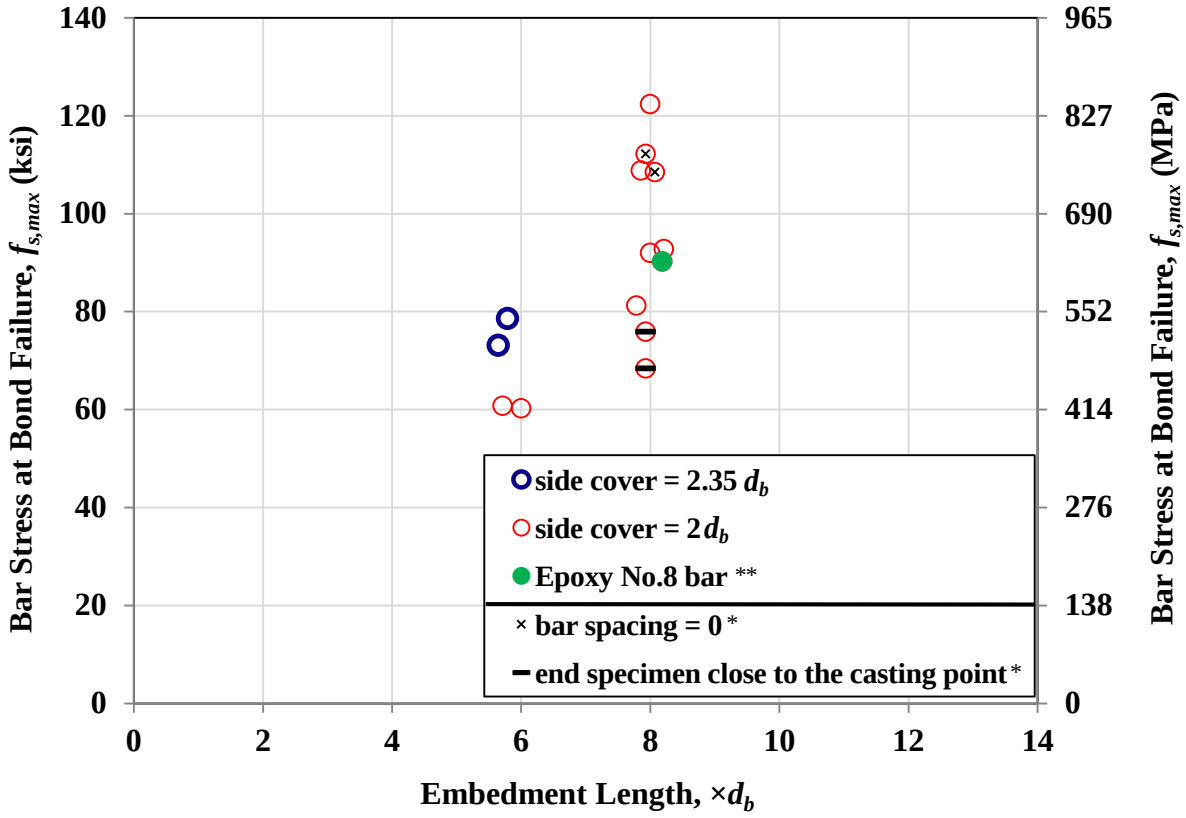

*refer to the note for Figure 29. ** Test with epoxy coated No.8 bar, all other tests were with A1035 No.7 bar.

Figure 31. Graph. Bar stress at bond failure versus embedment length for tests with A1035 No. 7 bars and epoxy coated No.8 bars.

MINIMUM BAR STRESS OF LESSER OF YIELD OR 75 ksi (517 MPa) – ALTERNATIVE

The design with a minimum embedment length of $8d_b$, a minimum side cover of $3d_b$, a bar clear spacing between $2d_b$ and l_s, and a minimum UHPC compressive strength of 13.5 ksi (93.1 MPa) is recommended for general application of deformed bar to reach the lesser of the bar yield strength or 75 ksi (517 MPa) at bond failure. In some cases, reinforcing bar would reach a much higher bar stress at bond failure with this design detail. For example, the A1035 No. 5 bars tested in the study reached a bar stress over 120 ksi (827 MPa) at bond failure. For specific applications with different bar type, bar size, and UHPC compressive strength, designers may want to consider refinements of these recommendations based on the test results. For example, if a larger side cover is provided or/and UHPC with a higher compressive strength is used, the embedment length can be reduced. For this purpose, the following three figures were developed for reference when modification of the recommended design is needed.

The average bar stress at bond failure for different design details is presented in Figure 32 through Figure 34. Figure 32 included the tests with A1035 high strength No. 5 bars, Figure 33 presented the specimens with normal strength epoxy coated and uncoated No.5 bars, and Figure 34 had the specimens with A1035 No. 4 and No. 7 bars and epoxy coated No. 8 bars. For each design detail, the average bar stress at bond failure and the maximum and minimum values for involved specimens are presented in the bar chart. Below each bar chart, the design detail, including embedment length, concrete cover, UHPC compressive strength, and number of tests conducted are presented. For general information, the specimens were tested either at 1, 7, or 14 days after casting, corresponding to compressive strength of approximately of 13, 19, and 21 ksi (90, 131, and 145 MPa), respectively.

All specimens in the three figures have a bar clear spacing between $2d_b$ and $l_s tan(\theta)$. It is important to consider this, because, as demonstrated in an earlier section, the specimens with bar clear spacing that is too small or too large tend to exhibit lower bond strengths, with the potential for a twenty percent or more reduction. It should also be noted that the specimens with UHPC tensile failure and the end specimens close to casting point are all included in the three figures; in fact, these specimens were the main reason why some of the results have a large range (the range between the maximum and minimum values showing in each figure). The UHPC tensile failure is attributable to insufficient UHPC cross sectional area to carry applied force and thus can generally be minimized by providing sufficient concrete side cover ($\geq 3d_b$). The specimens that failed with bar rupture before bond failure are outlined in red.

With the design of a minimum embedment length of $8d_b$, a minimum side cover of $3d_b$, a bar clear spacing between $2d_b$ and l_s, and a minimum UHPC compressive strength of 13.5 ksi (93.1 MPa) as the baseline, minor adjustment can be made based the limited test results shown in Figure 32 through Figure 34 per practical need. For example, for situations where the above conditions are met except that the minimum side cover is between $2d_b$ and $3d_b$, the minimum embedment length can be increased to $10d_b$. Based on Figure 32, for A1035 No. 5 bars, both the design with an embedment length of $6d_b$ accompanied with a side cover of $3d_b$ and the design with an embedment length of $8d_b$ accompanied with a side cover of $2d_b$ could reach a bar stress of at least 75 ksi (517 MPa) before bond failure at one day after casting with UHPC compressive strength of 13.8 ksi (95 MPa). If sufficient UHPC compressive strength was gained, for example at 14 days after casting, the uncoated No.5 bar with an embedment length of $6d_b$ and a side cover of $2d_b$ could also reach a bar stress equal to the lesser of the yield strength or 75 ksi (517 MPa) before bond failure (see Figure 33).

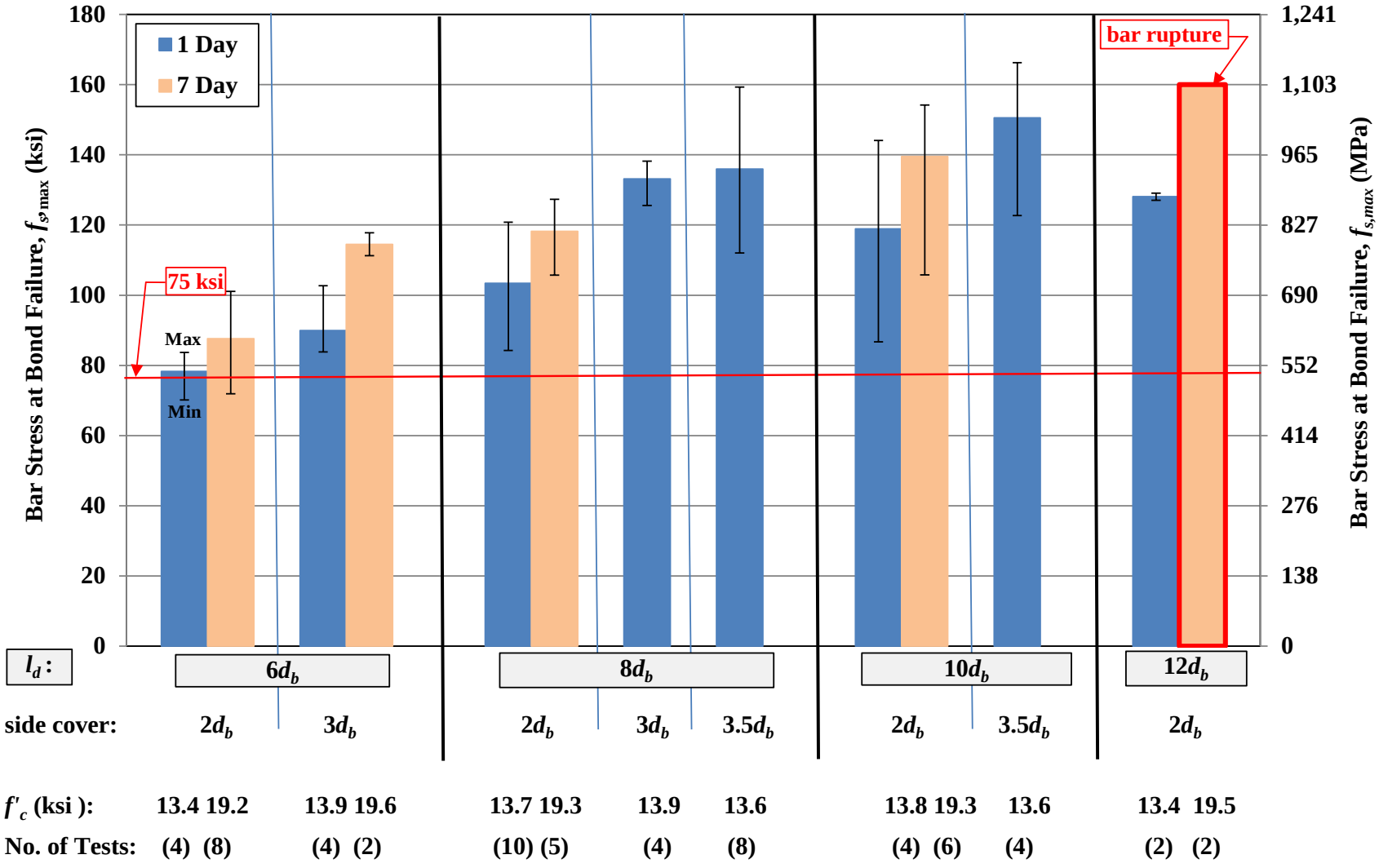

Figure 32. Chart. Bar stress at bond failure for all A1035 No.5 bars with different design details. All specimens had a bar clear spacing between $2d_b$ and $l_s tan(\theta)$.

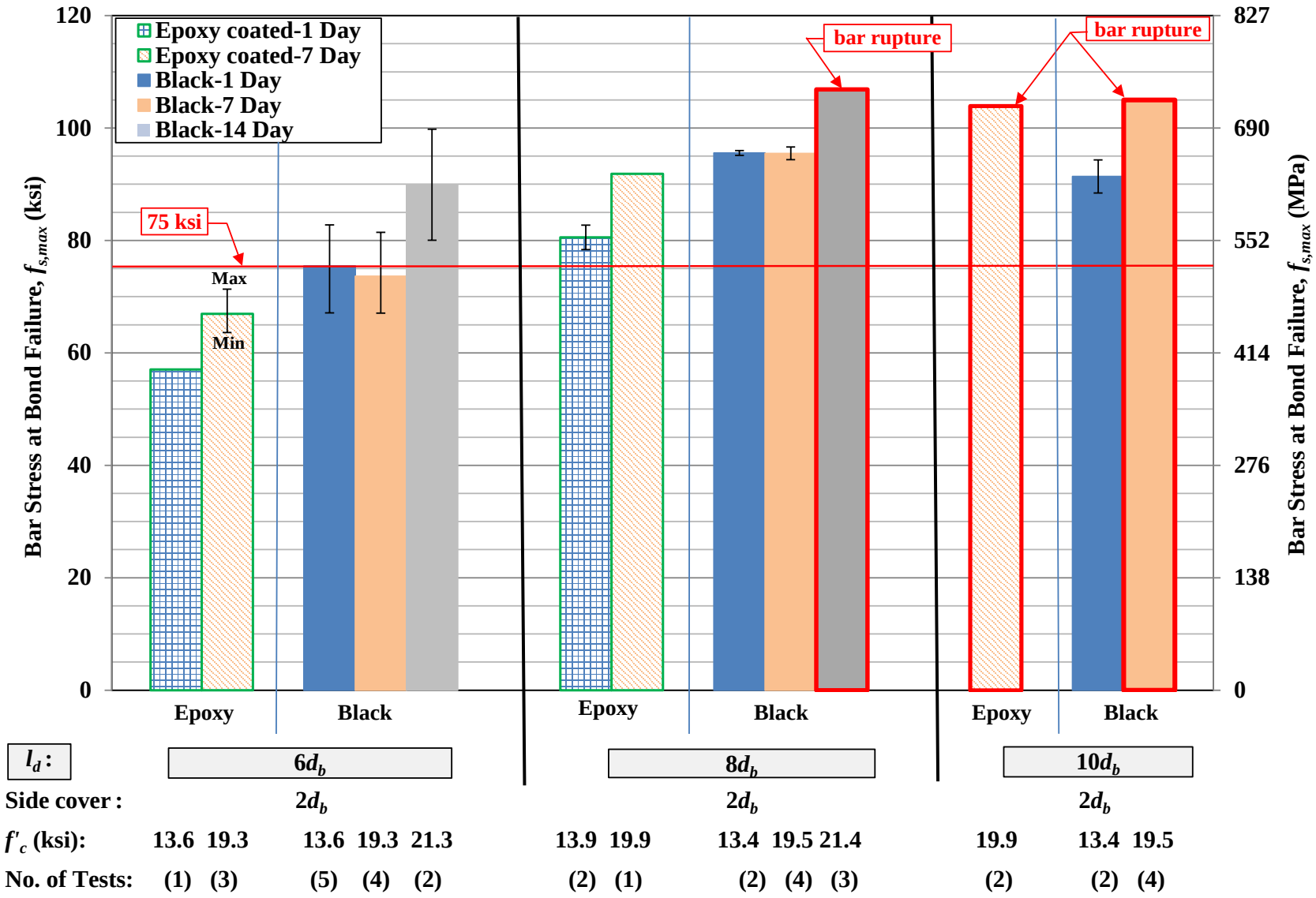

Figure 33. Chart. Bar stress at bond failure for all epoxy coated and uncoated No.5 bars with different design details. All specimens had a bar clear spacing between $2d_b$ and $l_s tan(\theta)$.

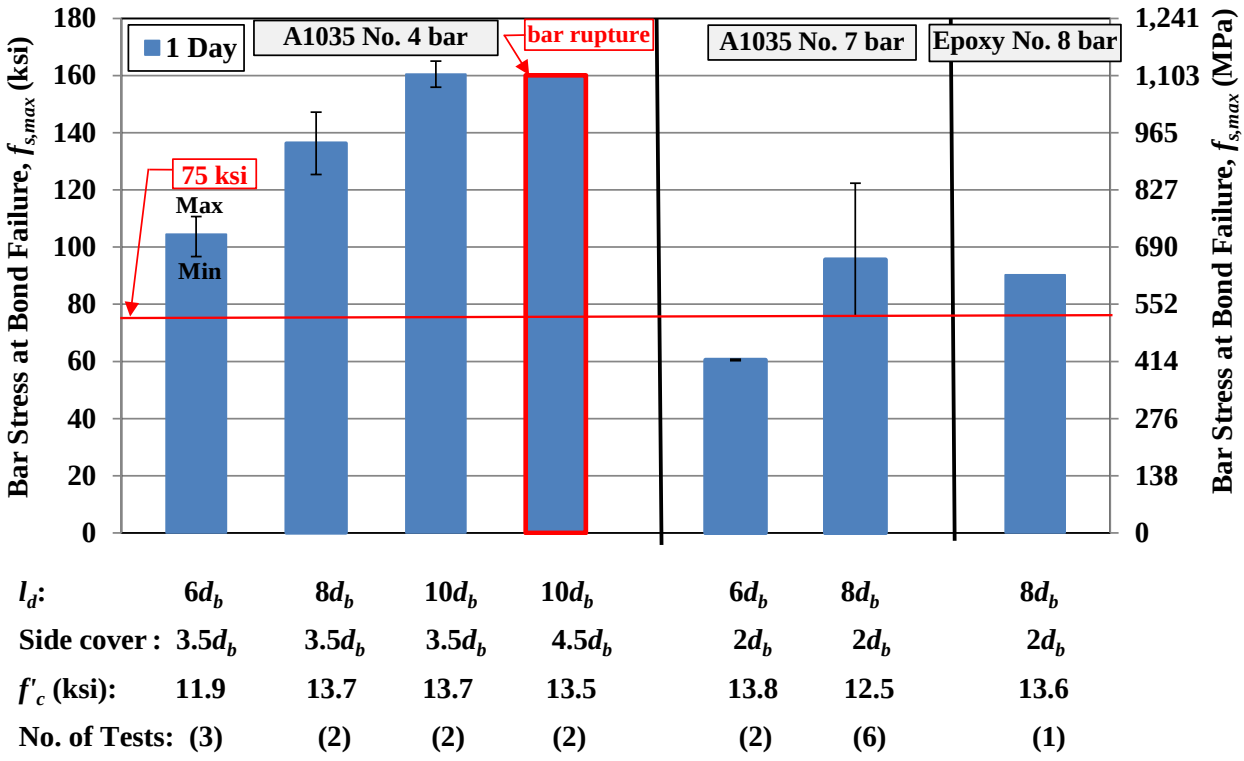

Figure 34. Chart. Bar stress at bond failure for all A1035 No. 4 and No.7 bars and epoxy coated No. 8 bar with different design details. All specimens had a bar clear spacing between $2d_b$ and $l_s tan(\theta)$.

BAR STRESS ABOVE 75 ksi (517 MPa) OR BAR RUPTURE BEFORE BOND FAILURE

In some design cases, such as seismic design, the ductility of reinforcing steel beyond the yield point is also considered. For this purpose, a few embedment configurations relevant to attainment of a bar stress beyond 75 ksi (517 MPa), or even allowing for bar rupture before bond failure, are discussed in this section based on the limited tests in this study.

For details engaging high strength reinforcing bars that do not exhibit a defined yield plateau, the results presented in Figure 32 are quite instructive. For example, for A1035 No.5 bars, the results indicate that when there is a minimum side cover of $3d_b$ and a minimum UHPC compressive strength of 19.5 ksi (134 MPa), specimens with embedment length of at least $6d_b$ reached a bar stress greater than 100 ksi (690 MPa).

For details engaging normal strength reinforcing bars, a limited set of test configurations resulted in sufficient bar stress and ductility that the rupture of the reinforcing bar occurred before bond failure. The relevant test configurations that achieved bar rupture for both normal and high strength reinforcing bar are as follows:

- A615 Grade 60 No. 5 uncoated bar with an embedment length of $8d_b$, side cover of $2d_b$, and UHPC compressive strength of 21.4 ksi (148 MPa).
- A615 Grade 60 No. 5 uncoated bar with an embedment length of $10d_b$, side cover of $2d_b$, and UHPC compressive strength of 19.5 ksi (134 MPa).
- A615 Grade 60 No. 5 epoxy coated bar with an embedment length of $10d_b$, side cover of $2d_b$, and UHPC compressive strength of 19.9 ksi (137 MPa).
- A1035 Grade 120 No. 5 uncoated bar with an embedment length of $12d_b$, side cover of $2d_b$, and UHPC compressive strength of 19.5 ksi (134 MPa).
- A1035 Grade 120 No. 4 uncoated bar with an embedment length of $10d_b$, side cover of $4.5d_b$, and UHPC compressive strength of 13.5 ksi (93 MPa).

CHAPTER 5. CONCLUSIONS

INTRODUCTION

The research discussed herein focused on assessing the bond strength of deformed reinforcing steel in UHPC. Deformed reinforcing steel, including ASTM A615 Grade 60 uncoated No. 5 bar and epoxy coated No. 5 and No.8 bars and ASTM A1035 Grade 120 No.4, No.5, and No.7 bars, were tested. The specific UHPC material used in this study had a steel fiber content of two percent by volume and an average compressive strength of 13.5 ksi (93 MPa) at one day, 17.0 ksi (117 MPa) at three days, 19.4 ksi (133 MPa) at seven days, and 21.3 ksi (147 MPa) at 14 days.

The main factors affecting bond performance, including the structural characteristics like the embedment length, concrete side cover, bar spacing, bar size, and bar type, and materials properties such as UHPC compressive strength and bar yield strength are investigated. The summary of the findings are presented in this chapter. Design details for using deformed reinforcing steel in UHPC are then recommended. At the end, the proposed future research on this topic is included.

CONCLUSIONS

The following conclusions are based on the research presented in this report for deformed reinforcing steel embedded in UHPC.

- Increasing the embedment length of the bar increases bond strength.
- The relationship between the bond strength and the bonded length for reinforcing bar embedded in UHPC is nearly linear, indicating that UHPC exhibits enhanced performance as compared to conventional high strength concrete.
- Bond strength increases as the side cover increases.
- Non-contact lap splice specimens, where the bar spacing is less than $l_s tan(\theta)$ [†], exhibit higher bond strength than contact lap splice specimens; when the bar clear spacing is bigger than $l_s tan(\theta)$, the bond strength decreases as compared to those having lesser spacing.
- The decrease in bond stress for contact lap splice specimens is probably due to decreased contact area between the reinforcing bar and UHPC materials. Tight spacing between bars limits the ability of the fiber reinforcement to locally enhance the mechanical resistance of the UHPC.
- When the bar clear spacing is bigger than $l_s tan(\theta)$, the induced diagonal cracks from the pullout force will not intersect with the adjacent bar. The adjacent bar will not help stop the propagation of the diagonal cracks. The bond strength becomes a function of the mechanical properties of the UHPC.

[†] $l_s tan(\theta)$: refer to Figure 20.

- Models that use bar spacing and bar cover to predict bond stress may need to be reevaluated in consideration of the added crack propagation resistance provided by fiber reinforcement in UHPC.
- An increase on the compressive strength of the UHPC results in an increased bond strength.
- The effect of UHPC properties on bond strength cannot be effectively represented by the compressive strength f'_c, or the square root of its compressive strength $f'^{1/2}_c$. Other UHPC mechanical properties, particularly those relevant to the post-cracking tensile behavior of UHPC, may be more appropriate for evaluating the bond strength of reinforcing bar in UHPC.
- For bars with larger diameter, the bond strength decreases.
- Bars that yield before bond failure have less ultimate bond strength than high strength bars that do not yield before bond failure; the reduction in bond strength is amplified as the ultimate bond strength increases.
- The epoxy coated bar had lower bond strength than uncoated bar; the reduction was minimized when there is a sufficient embedment length that the bar yields before bond failure.

RECOMMENDED DESIGN

One of the main goals of the research is to develop design recommendations for reinforcing bar embedded in UHPC, thus providing guidance for designers using reinforced UHPC in innovative applications. This study focused on a widely available UHPC product containing 2% steel fiber (by volume). Reinforcing bar sizes ranging from No. 4 to No. 8 and bar type including A615 Grade 60 uncoated and epoxy coated bar and A1035 Grade 120 bar were included in the study.

Deformed reinforcing bar embedded in UHPC can attain the lesser of the bar yield strength or 75 ksi (517 MPa) at bond failure when the following conditions are met:

- Bar size from No. 4 to No. 8,
- Uncoated or epoxy coated bar,
- Minimum embedment length of $8d_b$,
- Minimum side cover of $3d_b$,
- Bar clear spacing between $2d_b$ and l_s, and
- Minimum UHPC compressive strength of 13.5 ksi (93 MPa).

For lap splice reinforcement configurations, a minimum lap splice length of 75 percent of the embedment length is suggested, which is the range into which most of tests in this study fell. Note that d_b is the bar diameter and l_s is the lap splice length.

For situations wherein the above conditions are met except that the minimum side cover is between $2d_b$ and $3d_b$, the minimum embedment length should be increased to $10d_b$.

Refinements of the recommended design can be made for specific applications. For example, if a larger side cover is provided or/and UHPC has gained higher compressive strength, an embedment length reduction may be possible; if a longer embedment length is provided, the side cover can be correspondingly reduced with caution. Figure 32, Figure 33, and Figure 34 provide supporting information.

FUTURE RESEARCH

The research in this study mainly focuses on one specific UHPC material. Future research in this topic area may also consider the following:

- Bond performance in other UHPC materials and other grout materials, such as traditional non-shrinkage grout and epoxy grout.
- Investigation of the mechanical properties that are predictive of the bond performance of UHPC materials.
- Development of a general expression to estimate the bond strength of deformed steel reinforcing bars in UHPC materials with different fiber content.

ACKNOWLEDGMENTS

The research which is the subject of this document was funded by the U.S. Federal Highway Administration. This support is gratefully acknowledged.

This research project could not have been completed were it not for the dedicated support of the federal and contract staff associated with the FHWA Structural Concrete Research Program. Recognition also goes to the technical staff who assisted with specimen fabrication and testing. PSI, Inc. provided laboratory support to FHWA under contract DTFH61-10-D-00017 through the duration of this research project.

REFERENCES

1. Graybeal, B., "Splice Length of Prestressing Strand in Field-Cast UHPC Connections," U.S. Department of Transportation, Federal Highway Administration, FHWA-HRT-14-047, February 2014, 46 pp.

2. Ultra-High Performance Concrete, U.S. Department of Transportation, Federal Highway Administration. *https://www.fhwa.dot.gov/research/resources/uhpc/.*

3. Graybeal, B. (2010). Behavior of Field-Cast Ultra-High Performance Concrete Bridge Deck Connections Under Cyclic and Static Structural Loading, Report No. PB2011-101995, National Technical Information Service, Springfield, VA.

4. Graybeal, B. (2012). Development of a Field-Cast Ultra-High Performance Concrete Composite Connection Detail for Precast Concrete Bridge Decks, Report No. PB2012-107569, National Technical Information Service, Springfield, VA.

5. Graybeal, B., "Ultra-High Performance Concrete," U.S. Department of Transportation, Federal Highway Administration, FHWA-HRT-11-038, March 2011, 8 pp.

6. Graybeal, B., "Material Property Characterization of Ultra-High Performance Concrete," Federal Highway Administration, Report No. FHWA-HRT-06-103, August 2006, 186 pp.

7. Fehling, E., Lorenz, P., and Leutbecher, T., "Experimental Investigations on Anchorage of Rebars in UHPC," *Proceedings of Hipermat 2012 3rd International Symposium on UHPC and Nanotechnology for High Performance Construction Materials*, Ed., Schmidt, M.,Fehling, E., Glotzbach, C., Fröhlich, S., and Piotrowski, S., Kassel University Press, Kassel,Germany, 2012, pp. 533–540.

8. Swenty, M. and Graybeal, B., "Influence of Differential Deflection on Staged Construction Deck-Level Connections," FHWA, U.S. Department of Transportation, Report No. FHWAHRT-12-057, National Technical Information Service Accession No. PB2012-111528, 2012.

9. Holschemacher, K., Weiβe, D., and Klotz, S., "Bond of Reinforcement in Ultra High Strength Concrete," *Proceedings of the International Symposium on Ultra High Performance Concrete*, Ed., Schmidt, M., Fehling, E., and Geisenhanslüke, C., Kassel University Press, Kassel, Germany, 2004, pp. 375–387.

10. Holschemacher, K., Weiße, D., and Klotz, S., "Bond of Reinforcement in Ultra High-Strength Concrete," *Seventh International Symposium on the Utilization of High-Strength/High-Performance Concrete*, Vol. I, Publication No. SP-228, Ed., Russell, H.G., American Concrete Institute, Farmington Hills, MI, 2005, pp. 513–528.

11. ASTM C39-11, "Standard Test Method for Compressive Strength of Cylindrical Concrete Specimens," *ASTM Book of Standards Volume 04.02*, ASTM International, West Conshohocken, PA, 2011.

12. Graybeal, B.A., 2007, "Compressive Behavior of Ultra-High Performance Fiber-Reinforced Concrete," *ACI Materials Journal*, V. 104, No. 2, Mar.-Apr., pp. 146-152.

13. Graybeal, B., and B. Stone, "Compression Response of a Rapid-Strengthening Ultra-High Performance Concrete Formulation," Federal Highway Administration, National Technical Information Service Accession No. PB2012-112545, September 2012, 66 pp.

14. ASTM A615/A615M-13, "Standard Specification for Deformed and Plain Carbon-Steel Bars for Concrete Reinforcement," *ASTM Book of Standards Volume 01.04*, ASTM International, West Conshohocken, PA, 2013.

15. ASTM A1035/A1035M-13b, "Standard Specification for Deformed and Plain, Low-Carbon, Chromium, Steel Bars for Concrete Reinforcement," *ASTM Book of Standards Volume 01.04*, ASTM International, West Conshohocken, PA, 2013.

16. ASTM A370 -12a, "Standard Test Methods and Definitions for Mechanical Testing of Steel Products," *ASTM Book of Standards Volume 01.04*, ASTM International, West Conshohocken, PA, 2012

17. ACI Committee 408. (2003). Bond and Development of Reinforcement, *Bond and Development of Straight Reinforcing Bars in Tension* (ACI 408R-03), American Concrete Institute, Farmington Hills, MI, 49 pp.

18. ACI Committee 408. (2009). Guide for Lap Splice and Development Length of High Relative Rib Area Reinforcing Bars in Tension and Commentary (ACI 408.3R-09), American Concrete Institute, Farmington Hills, MI, 12 pp.

19. Azizinamini, A., Stark, M., Toller, J.J., and Ghosh, S.K., 1993, "Bond Performance of Reinforcing Bars Embedded in High-Strength Concrete," *ACI Structural Journal*, V. 90, No. 5, Sep.-Cot., pp. 554-561.

20. ACI Committee 318 (2011), "Building Code Requirements for Structural Concrete and Commentary (318-11),"American Concrete Institute, Farmington Hills, Mich., 503 pp.

21. CSA Standard A23.3-94, 1994, "Design of Concrete Structures," Canadian Standards Association, Ontario, Canada.

22. Darwin, D.; Idun, E. K.; Zuo, J.; and Tholen, M. L., 1998, "Reliability-Based Strength Reduction Factor for Bond," *ACI Structural Journal*, V. 95, No. 4, July-Aug., pp. 434-443.

23. Darwin, D.; Tholen, M. L.; Idun, E. K.; and Zuo, J., 1996a, "Splice Strength of High Relative Rib Area Reinforcing Bars," *ACI Structural Journal*, V. 93, No. 1, Jan.-Feb., pp. 95-107.

24. Walker, W. T., 1951, "Laboratory Tests of Spaced and Tied Reinforcing Bars," ACI JOURNAL, *Proceedings* V. 47, No. 5, Jan., pp. 365-372.

25. Chamberlin, S. J., 1952, "Spacing of Spliced Bars in Tension Pullout Specimens," ACI JOURNAL, *Proceedings*, V. 49, No. 3, Nov., pp. 261-274.

26. Chinn, J.; Ferguson, P. M.; and Thompson, J. N., 1955, "Lapped Splices in Reinforced Concrete Beams," ACI JOURNAL, *Proceedings* V. 52, No. 2, Oct., pp. 201-213.

27. Orangun, C.O., Jirsa, J. O., and Breen, J. E., “The Strength of Anchor Bars : A Reevaluation of Test Data on Development Length and Splices,” *Research Report* No. 154-3F, Center for Transportation Research, The University of Texas at Austin, Texas, 1975, 194 pp.